SP-1224

June 1999

Envisat

The Altimetry Report: Science and Applications

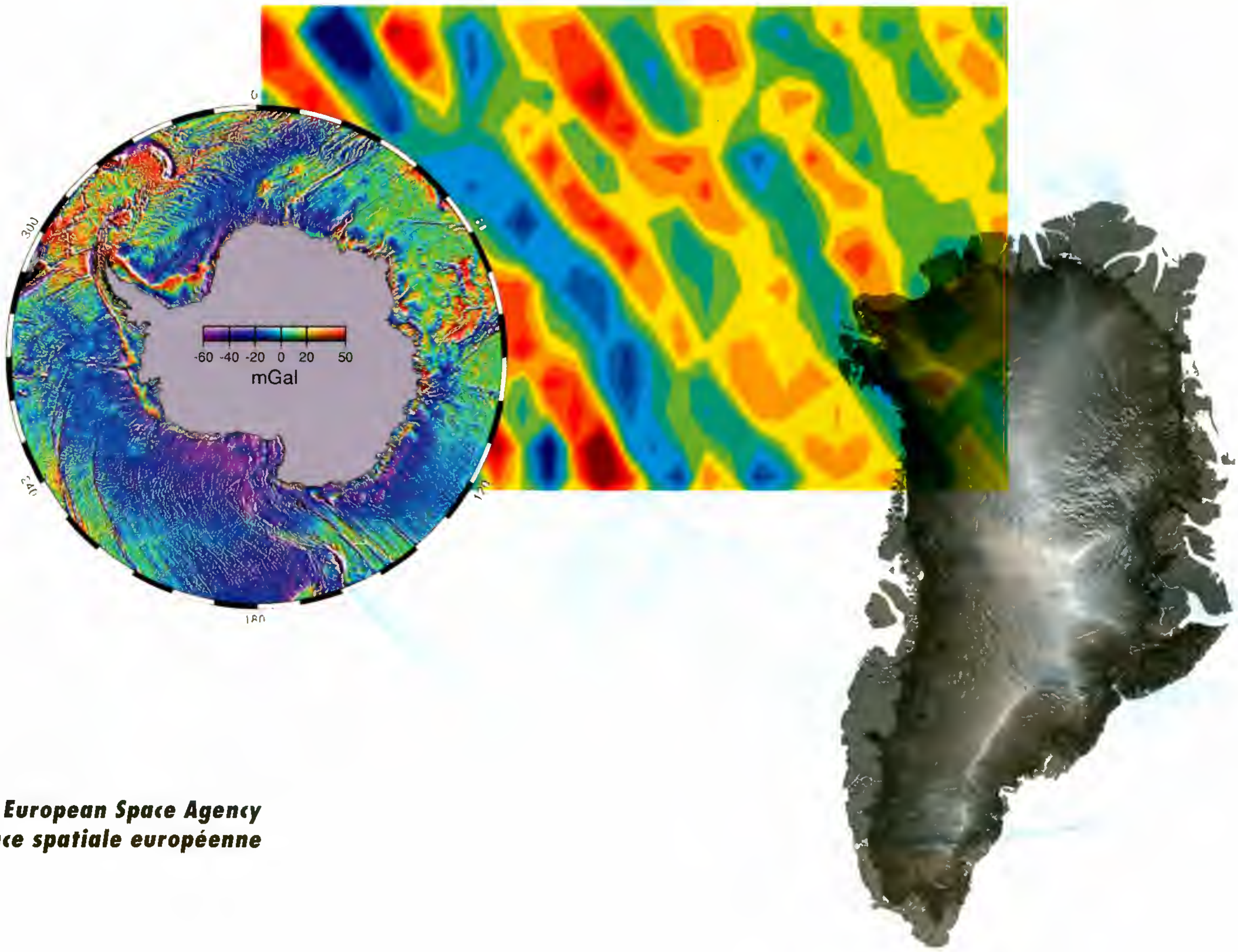

European Space Agency
Agence spatiale européenne

SP-1224
May 1999

RA-2/MWR SCIENCE AND APPLICATIONS

European Space Agency
Agence spatiale européenne

RA-2/MWR-2 Science Advisory Group

Wolfgang Bosch	DGFI, Germany
Luigi Cavaleri	ISDGM, Italy
Peter Janssen	ECMWF, UK
Laurence Eymard	CRPE, France
Seymour Laxon	MSSL, UK
Pierre-Yves Le Traon	CLS, Argos, France
John Lillibridge	NOAA, USA
Jean-François Minster	INSU, France
Remko Scharroo	Delft University of Technology, The Netherlands
Christian Tscherning	University of Copenhagen, Denmark
Patrick Vincent	CNES, France
Duncan Wingham	MSSL, UK

Executive

Jerome Benveniste	ESA-ESRIN, Italy
Richard Francis	ESA-ESTEC, The Netherlands
Pierre Femenias	ESA-ESRIN, Italy
Johnny Johannessen	ESA-ESTEC, The Netherlands
Guido Levrini	ESA-ESTEC, The Netherlands
Monica Roca	ESA-ESTEC, The Netherlands

Title: **SP-1224 – RA-2/MWR Science & Applications**

Published by: ESA Publications Division
ESTEC, P.O. Box 299
2200 AG Noordwijk
The Netherlands
Tel: +31 71 565 3400
Fax: +31 71 565 5433

Prepared by: RA-2/MWR Science Advisory Group
Technical Coordinator: J. Johannesen, Earth Sciences Division, ESA
Editor: R.A. Harris

Price: 50 DFl
ISBN No: 92-9092-492-6
Printed in: The Netherlands

Foreword

This report is being published to help promote the European Space Agency's environmental research satellite Envisat and to support the Earth Observation user community in the use of the dual frequency Radar Altimeter (RA-2) which forms an important part of the Envisat payload. It addresses the RA-2's technical characteristics and reviews the current state-of-the-art regarding the scientific and operational utilisation of altimeter data.

The report contains four sections: a) a description of the RA-2 system and mission elements; b) a review of main altimeter errors, their correction and corresponding measurement accuracies; c) the foundations for the multidisciplinary scientific objectives; and d) descriptions of operational applications. The last two of these sections build on experience with current operating radar altimeter systems such as those on ERS, TOPEX/POSEIDON and Geosat Follow-On, with a projection towards the future utilisation of the dual frequency RA-2 on Envisat.

The principal authors of the report are W. Bosch, L. Cavaleri, L. Eymard, P. Janssen, S. Laxon, P.-Y. Le Traon, J. Lillibridge, J.-F. Minster, R. Scharroo, C. Tscherning, P. Vincent, and D. Wingham supported by members of the Executive (see Page ii).

The Agency would like to thank the principal authors and members of the RA-2 Science Advisory Group for their endeavours in producing this report. Much effort has gone into its production and it is expected to form an important reference document for the Envisat RA-2 mission.

Contents

Acronyms & Abbreviations

AATSR	Advanced Along Track Scanning Radiometer
ACSYS	Arctic Climate SYstems Study
AGC	Automatic Gain Control
ASAR	(Envisat) Advanced SAR
AVHRR	Advanced Very High Resolution Radiometer
BAHC	Biological Aspects of the Hydrological Cycle
BMRC	Bureau of Meteorology Research Centre
CHAMP	Challenging Mini-satellite Payload for Geophysical Research and Application
CLIVAR	CLImate VARiability and Predictability Study
COADS	Comprehensive Ocean Atmosphere Data Sets
DEM	Digital Elevation Model
DIS	Data and Information System
DNMI	Det norske meteorologiske institutt
DORIS	Doppler Orbitography and Radiopositioning Integrated by Satellite
D-PAF	German Processing and Archiving Facility
DRS	(ESA) Data Relay Satellite
DSP	Digital Signal Processing
ECMWF	European Centre for Medium Range weather Forecasting
EM	Engineering Model
EMB	ElectroMagnetic Bias
FDGDR	Fast Delivery Geophysical Data Record
FDMAR	Fast Delivery Marine Abridged Record
FFT	Fast Fourier Transform
FM	Flight Model
FM	Frequency modulation
FNMOC	Fleet Numerical Meteorological and Oceanography Center
FOCC	Flight Operations Control Centre
FOS	Flight Operation Segment

GAIM	Global Analysis Interpretation and Modelling
GCOS	Global Climate Observing System
GCTE	Global Change and Terrestrial Ecosystems
GDR	Geophysical Data Record
GEWEX	Global Energy and Water-cycle EXperiment
GFO	GEOSAT Follow-On
GLAS	Geoscience Laser Altimeter System
GLONASS	(Russian) GLObal NAvigation Satellite System
G-M-S	GOMOS-MIPAS-SCIAMACHY
GOCE	Gravity Field and Steady State Ocean Circulation Explorer
GODAE	Global Ocean Data Assimilation Experiment
GOMOS	Global Ozone Monitoring by Occultation of the Stars
GOOS	Global Oceans Observing System
GPS	Global Positioning System
GRACE	Gravity Recovery and Climate Experiment
HDP	Human Dimensions of global change Programme
IB	Inverted Barometer correction
IF	Intermediate Frequency
IGAC	International Global Atmospheric Chemistry Programme
IGBP	International Geosphere-Biosphere Programme
IGDR	Interim Geophysical Data Record
IMAR	Interim Marine Abridged Record
IPCC	Intergovernmental Panel on Climate Change
IRI	International Rice Institute
JGOFS	Joint Global Ocean Flux Study
KNMI	Koninklijk Nederlands Meteorologisch Instituut
LFM	Linear Frequency Modulation
LOICZ	Land-Ocean Interactions in the Coastal Zone programme
LRAC	Low rate Reference Archive Centre
LRR	Laser Retro-Reflector
LT	Local Time
LUCC	Land Use/Cover Change Project
MAR	Marine Abridged Records
MAR	Mean Accumulation Rate
MERIS	Medium Resolution Imaging Spectrometer
MIPAS	Michelson Interferometer for Passive Sounding
MSS	Mean Sea Surface
MWR	Microwave Radiometer

NAO	North Atlantic Oscillation
NCEP	(US) ational Centre for Environmental Prediction
NOAA	(US) National Oceanic & Atmospheric Administration
NPOESS	(US) National Polar Orbiting Operational Environmental Satellite System
NRC	(US) National Research Council
NRT	Near Real Time
NSES	National earth Station providing ESA Services
OI	Optimal Interpolation
OOSDP	Ocean Observing System Development Panel
OPR	Ocean Product Records
PAC	Processing and Archive Centre
PAGES	PAst Global changES
PDAS	Payload Data Acquisition Station
PDCC	Payload Data Control Centre
PDHS	Payload Data Handling Station
PDS	(Envisat) Payload Data Segment
PEB	Payload Equipment Bay
PRARE	Precise Range And Range-rate Equipment
PRF	Pulse Repetition Frequency
RA-2	Radar Altimeter - 2
RMS	Root mean square
RSS	Root sum of squares
SAR	Synthetic Aperture Radar
SAW	Surface Acoustic Wave
SCIAMACHY	SCanning Imaging Absorption SpectroMeter for Atmospheric CartograpHY
SGDR	Sensor Geophysical Data Record
SHOM	Service Hydrographique et Océanographique de la Marine
SLR	Satellite Laser Ranging
SNR	Signal to Noise Ratio
SOAP	System for Ocean Analysis and Prediction
SPARC	Stratospheric Processes and their Role in Climate
SPOT	Satellite Pour l'Observation de la Terre
SSB	Sea State Bias
SSM/I	Special Sensor Microwave/Imager
SST	Sea Surface Temperature
START	Global Change System for Analysis, Research and Training
SWH	Significant Wave Height

TBC	To Be Confirmed/Chosen
TEC	Total Electron Content
TECU	Total Electron Content Units
TMR	TOPEX Microwave Radiometer
TOPEX/POSEIDON	US/French joint project, consisting of the US satellite Topex (Topography experiment for ocean circulation) carrying a French altimeter (Poséidon)
TRMM	Tropical Rainfall Measurement Mission
TT&C	Telecommand, Telemetry and Control
TWT	Travelling Wave Tube
UDS	User Data Segment
UKMO	United Kingdom Meteorological Office
UNEP	United Nations Environmental Program
USO	Ultra-Stable Oscillator
UTC	Universal Time Coordinated
WAM	Wave Model
WCRP	World Climate Research Programme
WMO	World Meteorological Organisation
WOCE	World Ocean Circulation Experiment
WWW	World Weather Watch
XBT	Expendable Bathy-Thermograph

1. Introduction

Following the success of ERS-1and ERS-2 in monitoring the Earth and its Environment (ESA SP-1176/1, ESA SP-414), as well as the endorsement of the Agency's Earth Observation Programme by the European Ministers at their meetings in 1991 and 1992, ESA is now moving towards the implementation of the Envisat payload and the preparation of the Envisat mission. The launch is scheduled for the second half of 2000.

The Agency's Earth Observation strategy, which has been developed in collaboration with the user community and representatives of the ESA member states, identifies five basic objectives, namely:

- Monitoring of the Earth's environment on various scales, from local or regional to global.
- Management and monitoring of the Earth's resources, both renewable and non-renewable.
- Continuation and improvement of the service provided to the world-wide operational meteorological community.
- Contributing to the understanding of the structure and dynamics of the Earth's crust and interior.
- Initiating and consolidating services for application communities.

The realisation of these objectives forms the basis of the ESA Earth Observation Programme, which includes the ERS-1 mission (about 5 years of operation from July 1991 until July 1996, and from then on kept in stand-by-mode for ERS-2), the presently operating ERS-2 mission (launched in April 1995), the approved Envisat mission and Metop series and the planned Earth Explorer and Earth Watch Missions.

Envisat is an advanced Earth observing satellite designed to provide measurements of the atmosphere, ocean, land and ice over a five year period. As the successor to the highly successful ERS-1 and ERS-2 satellites it will provide direct continuity of measurement with most ERS instruments, thereby extending to more than 10 years the long term data sets available for global environmental monitoring, and furthering many operational and commercial applications.

As a total package the capabilities of Envisat exceed those of any previous or planned Earth observation satellite. The payload includes three new atmospheric chemistry instruments. There is also an Advanced Synthetic Aperture Radar (ASAR) which can collect images over a wide swath, together with new low resolution and dual polarisation capabilities. A new imaging spectrometer (MERIS) is included for ocean colour and vegetation monitoring, and there are improved versions of the ERS radar altimeter, microwave radiometer, and visible/near infra-red radiometers, together with a new very precise orbit measurement system. An overview of the overall Envisat mission objectives is provided in ESA SP-1218.

In this report we provide a detailed assessment of the dual frequency radar altimeter (RA-2) to be implemented on Envisat. It addresses the integrated altimeter system including the microwave radiometer and positioning systems, the instrument observation and mission requirements, and the algorithm maturity and geophysical parameter retrieval. In addition it provides a brief outline of calibration and validation exercises, which are discussed in more detail in *Francis and Roca (1998)*.

2. The Altimetric System and Mission

2.1. The Mission

Envisat, which will be operated in a 35 day repeat cycle, is intended to make a significant contribution to environmental studies, notably in the areas of atmospheric chemistry, oceanography (including marine biology of the ocean surface), the cryosphere and the land surface. By so doing, in addition to providing data relevant to the monitoring of the state of the Earth's climate, it will help to increase understanding of the various processes involved, which is a pre-requisite for the development of better climate models. Moreover, Envisat will seek to enhance our capability to monitor and manage the Earth's resources and contribute to a better understanding of solid-Earth processes. Envisat is also intended to consolidate the ERS operational applications, in particular as related to the operational monitoring of near surface wind speed, sea state and sea ice.

The dual frequency RA-2 has an essential role to play in the Envisat mission (Table 2.1). Operating over oceans, its data can be used to monitor sea level, thereby supporting research into ocean circulation (and the associated transfers of energy) and sea level change as well as providing observations of the sea floor, surface and marine geoid characteristics. From the shape of the radar pulse, it is possible to determine near sea-surface wind speeds and significant wave heights. These data are important for weather and sea-state forecasting.

RA-2 will also be able to map and monitor sea ice and polar ice sheets and hence the energy/ mass balances of major ice sheets, including the

Discipline	Geophysical Quantity	Contribution from RA2/MWR
Atmosphere	Water vapour content	MWR
	Precipitation	RA-2/MWR (research)
	Ionosphere	RA-2
Land	Surface Elevation	RA-2
Ocean	Sea Level Topography	RA-2
	Mean Sea Level	RA-2
	Waves	RA-2
	Wind Speed	RA-2
Sea Ice/Ice Sheet	Topography/Elevation	RA-2
Gravity	Marine Gravity Anomalies	RA-2

Table 2.1: Contribution to the Envisat mission objectives from the RA-2/MWR-2. Note that the precipitation retrieval (or rainfall estimates) is currently a relatively new research topic (see Section 4)

Antarctic. In addition to operating over ocean and ice, however, RA-2 can also be used over land surfaces. This is a new feature as, from its observations of altitude and reflectivity, it is possible to determine land surface elevation, and surface characteristics.

RA-2 guarantees the continuity of the ERS altimeter data, thereby ensuring a long-term data set for use in climate studies such as sea level rise. It will also complement the data provided by the TOPEX/ POSEIDON mission (and later on Jason) and the Geosat Follow-On (GFO) mission, by filling in many gaps in surface coverage that limit the accuracy with which the sea level can be determined. This knowledge is of fundamental importance for mesoscale ocean circulation studies.

2.2. The Instruments

The integrated radar altimeter instrument system includes, in addition to the dual frequency altimeter (RA-2), a microwave radiometer (MWR), the Doppler Orbitography and Radio-positioning Integrated by Satellite (DORIS) system and the Laser Retro-Reflector (LRR). In order to improve performance the system includes several new, important modifications to the ERS altimeter system. Moreover, an on-board processor will enable RA-2 to automatically adapt its radar characteristics to surface characteristics. In particular, it should be noted that:

- ocean, ice sheet and land surface topography will be measured to higher accuracy than possible with ERS, and the new system will function over terrain which cannot be tracked by ERS.
- the synergetic use of RA-2/MWR, together with MERIS, AATSR and ASAR will provide unique and comprehensive observations of ocean processes at mesoscale, regional and global scale; at time scales up to the duration of the Envisat mission.
- RA-2/MWR guarantees the long term continuity of ERS radar altimeter data and, by overlapping of the two altimeter missions in time, accurate measurements of sea level changes at the millimetre per year scale can be achieved from the cross calibration exercises.

In the following sections the individual sensors of the integrated radar altimeter system are further described and complemented with a dedicated section on the satellite orbit.

Figure 2.1: RA-2 Operating Configuration

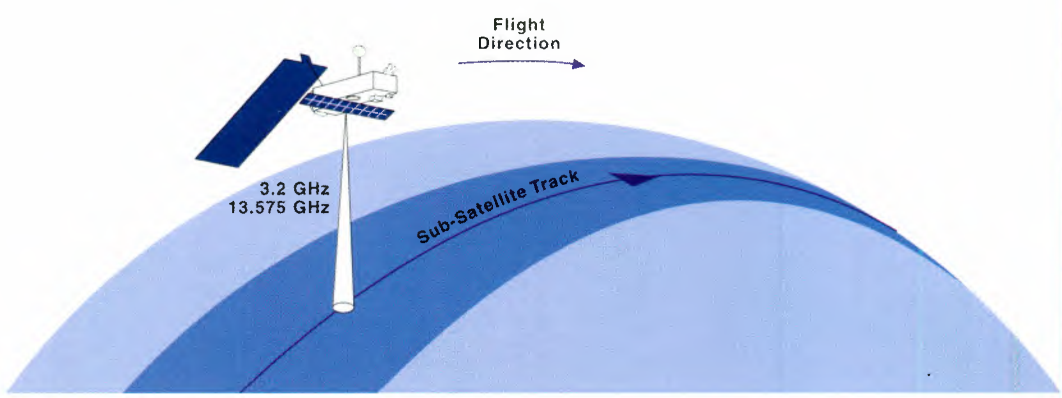

Table 2.2: RA-2 New Features and Developments with Respect to ERS-1/2

New Features	New Developments	Added Capabilities
Model-free tracker	Signal processor hardware and software	Improved height and reflectivity of non-ocean surfaces
	High speed 128-point FFT	Robust operation versus surface parameter changes
Adaptive height resolution	Chirp generator with 3 different bandwidths	Optimum resolution selection
	Onboard resolution switching	Improved tracking over rugged terrain
Second operating frequency	Dual frequency antenna (13.575/3.2 GHz)	Correction of range errors due to ionosphere
	S-band solid state amplifier	Improved characterisation of the surface scatterers

2.2.1. The Radar Altimeter (RA-2)

The RA-2 is a two-frequency, nadir-pointing, pulse-limited radar operating, via a single antenna dish at 13.575 GHz (Ku-band) and at 3.2 GHz (S-band) (see Figure 2.1), enabling correction of errors introduced by ionospheric fluctuations. In comparison to the ERS-1 radar altimeter, its design has several new features intended to measure echoes from ocean, ice and land surfaces with improved accuracy and without interruption. These new features and developments with respect to ERS are listed in Table 2.2.

The main operating frequency of RA-2 (see Table 2.3) has been shifted to 13.575 GHz (to avoid electromagnetic interference from "Fixed Satellite Earth to Space Services" which have recently been allocated new operating frequency bands). In order to operate the secondary frequency channel at 3.2 GHz, the antenna feed has been redesigned. A solid-state power amplifier, a transmit/receive switch

Table 2.3: Summary of RA-2 Design Parameters (* Note that individual echoes are also available)

Design Parameter	Main Channel	Common	Secondary Channel
Range (km)		769 to 825	
Operating frequency (GHz)	13.575		3.2
Pulse length (μs)		20	
Bandwidth (MHz)	320, 80, 20		160
Transmitted peak power (W)	60 (TWT)		60 (solid state)
Pulse repetition frequency (Hz)	1795.33		448.83
Number of samples per echo	128		64
Echoes averaged on board *	100		25
Antenna diameter (m)		1.2	
Power consumption (W)		161	
Mass (kg)		110	
Data rate (nom./max.) (kbit/s)		100	

and a low noise amplifier have been added. The subsystem that produces the necessary reference signals and the receiver have also been modified to support operation at this new frequency.

It should also be noted that there is no on-board autonomous tracking of the S-band echo. Instead, based on the information derived on-board from the Ku-band tracker (notably signal position and strength), a 20 ms time window dedicated to the collection of the S-band echo samples is implemented. The S-band time window is shifted by a fixed amount with respect to the Ku-band time window (equal to the time difference between transmission of the Ku-band pulse and the transmission of the S-band pulse). The receiver gain during reception of the S-band echo is adjusted by adding a fixed amount with respect to the Ku-band echo reception. The S-band waveforms are always collected with the same resolution (160 MHz chirp signals corresponding to about 95 cm vertical resolution).

Both the hardware and the software of the on-board processor are completely new. A dedicated Digital Signal Processor (DSP) performs a Fast Fourier Transform (FFT) on twice as many (128) digital samples as the ERS-1 instrument (and in less than half the time). The new algorithms that produce the error control signals are highly linear and independent of echo shape. These characteristics, along with the doubling of the number of samples, make the RA-2 operation more tolerant to changes in surface topography.

The width of the tracking window is autonomously selected on-board from three values. This is achieved by changing the radar altitude resolution while maintaining the same number of samples. When the radar echo is about to move out of the tracking window, due for example to a sudden change in surface elevation, the window is broadened to recapture it. This will allow uninterrupted radar operation over all kinds of surfaces, including their boundaries, and will avoid the need for dedicated operating modes commanded from the ground.

The radar pulse generator, based on Surface Acoustic Wave (SAW) devices, has been modified to generate Linear Frequency Modulated (LFM) pulses (known as 'chirps') in three different bandwidths, selectable by the on-board signal processor.

The Pulse Repetition Frequency (PRF) of the main channel has been increased to about 1800 Hz, to allow the on-board averaging of more independent measurements per second. A fast DSP has been selected in order to allow each echo to be processed before the next one is received.

The RA-2 measures the transit time and radar backscatter power of individual transmitted pulses. The transit time is proportional to the satellite's altitude above the ocean, land, or ice surface. Over ocean surfaces the measured range is accurate to better than 2.5 cm (see Table 2.4). Over the ocean the magnitude and shape of the returned echoes also contain information about the characteristics of the reflecting surface, from which it is possible to retrieve geophysical parameters such as significant wave height, wind speed, and sea ice edge location.

Some further changes have been necessary, both to meet the new environmental requirements set by the Envisat platform and in order to cope with a mission lifetime of 4 to 5 years. All of the electronic boxes are fully redundant, and cross-strapping between five major assemblies means that 32 different hardware configurations will be possible, assuring the necessary reliability. All of the units are housed in the Payload

Parameter	Range	Accuracy
Satellite height	769 to 825 km	< 4.5 cm (highest resolution)
Backscatter coefficient (wind speed)	-10 dB to +50 dB	< 0.4 dB (bias) < 0.2 dB (residual)
Waveheight	0.5 m to 20 m	< 5 % or 0.25 m
Measurement datation	± 100 µs w.r.t. UTC	

Table 2.4: RA-2 Instrument Performance Specifications

Equipment Bay (PEB) of the platform, which also provides both mechanical support and thermal control for the complete instrument.

2.2.2. The Microwave Radiometer (MWR)

The MWR is a nadir-viewing, two-channel, passive microwave radiometer operating at 23.8 and 36.5 GHz. At these two frequencies, it receives and measures microwave radiation generated and reflected by the Earth, as schematically illustrated in Figure 2.2. The signals received can be related to surface temperature but, most importantly, they provide an estimate of the total water content in the atmosphere. MWR has a 20 km diameter field of view.

The main objective of the atmospheric humidity measurements is to provide the data required for tropospheric path correction of the radar altimeter, which is influenced both by the integrated atmospheric water vapour content and by liquid water. Without the MWR data, the altimeter measurement accuracy would be degraded. In addition, the MWR measurements are useful for the determination of surface emissivity and soil moisture over land, for surface energy budget investigations in support of atmospheric studies and for ice characterisation.

The MWR instrument, which is of the same design as that on the ERS-1/2 satellites, compares received signals with signals from a reference load at a known temperature. On-board calibration will be performed using a sky horn pointing to deep space (i.e. cold calibration at 4K), with an internal load supplying the hot reference.

Figure 2.2: MWR Operating Configuration

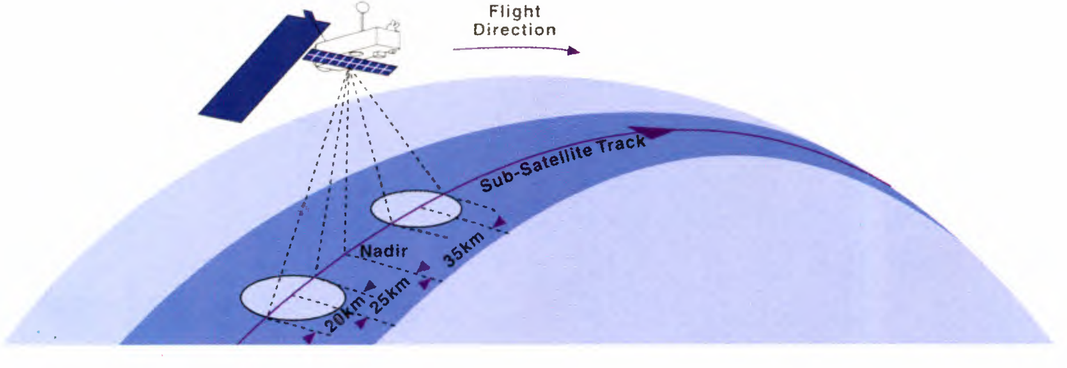

Table 2.5: MWR Performance Parameter and Budget Data

Operating frequencies	23.8 GHz (K-band), 36.5 GHz (Ka-band)
Dynamic range	3K to 300K
Absolute radiometric accuracy	Better than 3K
Radiometer type	Dicke
Operation	Continuous full orbit
Data rate	16.7 kbit/s
Mass	25 kg
Power	23 W

The MWR performance characteristics and budget data are listed in Table 2.5.

2.2.3. Doppler Orbitography and Radio Positioning Integrated by Satellite

DORIS is a radio-electrical Doppler measurement system which can be used to determine the satellite's exact position in space. Versions of this instrument are currently flying on the Spot-2, Spot-4 and TOPEX/POSEIDON missions. It is also planned to fly on Spot-5 and Jason.

DORIS measures the Doppler frequency shifts of both VHF and S-band signals transmitted by ground beacons (Figure 2.3). Instrument noise is equivalent to an error of about 0.5 mm/s in radial velocity, corresponding to absolute determinations of position to better than 10 cm. The precise measurement is made at S-band, with the VHF signal being used to correct for ionospheric effects. The DORIS performance characteristics are given in Table 2.6.

Precise positioning is of fundamental importance to several aspects of the Envisat mission. In particular, RA-2 only measures instantaneous altitude, whereas use of this data on a global scale requires a precise knowledge of the orbit. When relying only on tracking by Satellite Laser Ranging (SLR), the accuracy of radial positioning will be limited to about 25 cm. This would undermine many of the mission objectives of RA-2, including large-scale oceanography, global and basin scale circulation studies, as well as the global monitoring of changes in sea level. It would also be impossible to monitor the mass balance of the ice-sheets. All these objectives as well as the gravity field mission objectives are therefore particularly dependent on the information provided by the DORIS system.

Figure 2.3: DORIS Operating Configuration.

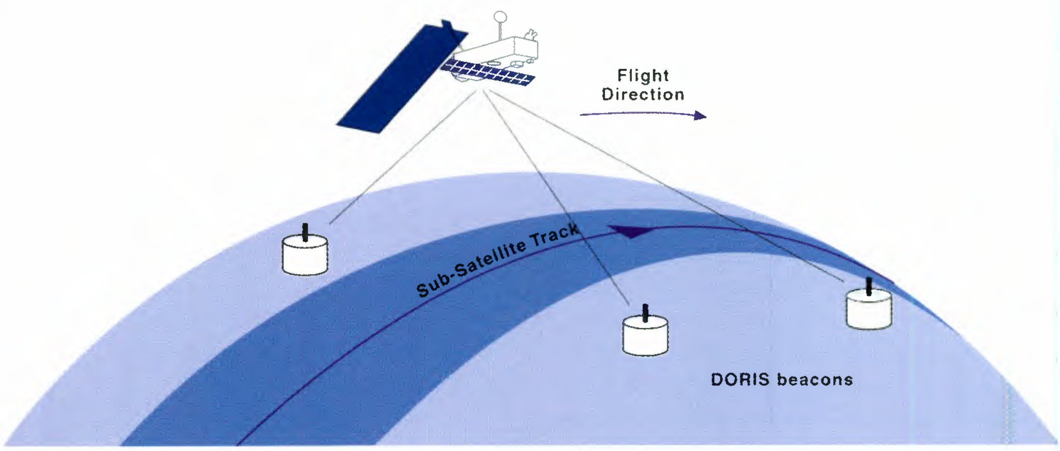

Measurement frequency	2.03625 GHz
Doppler measurement for ionospheric correction	401.25 MHz
Position accuracy - real time	1 m for the radial component
Position accuracy – restituted	0.05 m radial
Velocity accuracy - real time	1 mm/s
Velocity accuracy – restituted	0.4 mm/s
Operation	Continuously over full orbit
Data rate	16.7 kbit/s
Mass	91 kg (inclusive ICU)
Power	42 W

Table 2.6: DORIS Performance Parameters and Budget Data

There is currently a ground network of about fifty stations distributed around the globe and this network is growing steadily. In its existing form, the network would provide about 75% global coverage for Envisat. Given the geographical distribution of the ground beacons, DORIS offers a homogeneous and quasi-global coverage, with small gaps that may occur between consecutive "visibility" circles. Precise orbits computed for the SPOT satellites demonstrate that the present distribution of stations ensures orbit computation with a high degree of accuracy. In addition, since the DORIS system has a multi-mission purpose, the enhancement of the DORIS network will of course also benefit Envisat orbit determination.

2.2.4. The Laser Retro-Reflector (LRR)

The LRR is a set of passive reflectors designed to allow ground-based laser stations to measure precisely the distance to the spacecraft. It will be used to complement the DORIS instrument for the restitution of the precise Envisat orbit. The LRR thus functions both as a backup and calibration device for the DORIS instrument.

2.3. Orbit Characteristic

The reference orbit characteristics for Envisat are listed in Table 2.7, and indicate that the orbit will be a high inclination, sun-synchronous, near circular polar orbit with an altitude of 799.8 km. The local solar time at the descending node will be 10:00 a.m. The repeat cycle is 35 days with

Orbits per day	14 11/35
Repeat cycle	35 days (501 orbits)
Orbit period	100.59 minutes
Ground track separation at equator	80 km
Mean local solar time of descending node	10:00 LT
Inclination	98.55°
Orbit radius	7159.5 km
Orbit velocity	7.45 km/s
Mean altitude	799.8 km

Table 2.7: Reference Orbit Characteristics for the Envisat Mission

Figure 2.4: Visualisation of the 35 day repeat cycle for a selected region in the western Mediterranean. Numbers indicate the orbit number between 1 and 501. Sub-cycles of 3 days and 17 days are indicated

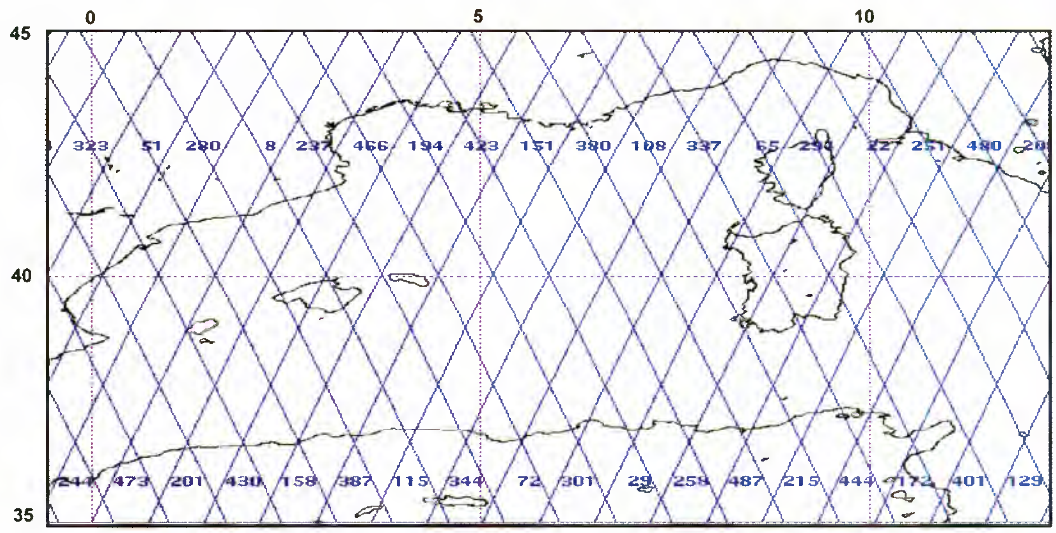

sub-cycles of 3 days and 17 days as indicated in Figure 2.4. The ground track separation at the equator is 80 km and decreases with latitude. Because of their measurement principles and their narrow fields of view, the MWR and RA-2 instruments do not provide global coverage, but provide a tight net of measurements over the globe. Changes of the orbital period, associated with altitudes between 770 km and 825 km, are possible during the mission.

The Envisat orbit maintenance strategy ensures that the deviation of the actual ground track from nominal is kept below 1 km and that the mean local nodal crossing time matches the nominal to better than 5 minutes. Drag forces act to gradually lower the satellite orbit, which also makes the orbit period shorter. In turn, the satellite ground track drifts eastward (with respect to the Earth). A drift away from the reference ground track will lead to insufficient knowledge of the cross-track geoid and ice sheet slopes, making it difficult, if not impossible, to refer these measurements back to the reference ground track and merge them in the local time series. Hence, the orbit will have to be maintained within ± 1 km of the reference track (i.e. the deadband width), requiring periodic manoeuvering of the satellite into a higher orbit.

The orbit maintenance strategy aims to minimise disturbances to the payload operation. In-plane manoeuvering, nominally twice (possibly more frequently) a month, will not interrupt the operation of most sensors. Out of plane corrections, required every few months, will be performed in eclipse to avoid the potential risk of sensors viewing the sun. Since extensive manoeuvering of the satellite is undesirable, both from the point of view of fuel consumption and precise orbit computation, the relaxation of the deadband width should take into account all instruments and the estimated impact on the final error budget for each aspect of the thematic Envisat mission.

2.4. Ground Segment Overview

The Envisat-1 Ground Segment will provide the means and resources to manage and control the mission, to receive and process the data produced by the instruments and to disseminate and archive the generated products. Furthermore, it will provide a single interface to the users to allow optimum utilisation of the system resources in line with the user needs. The architectural structure and elements of the Ground

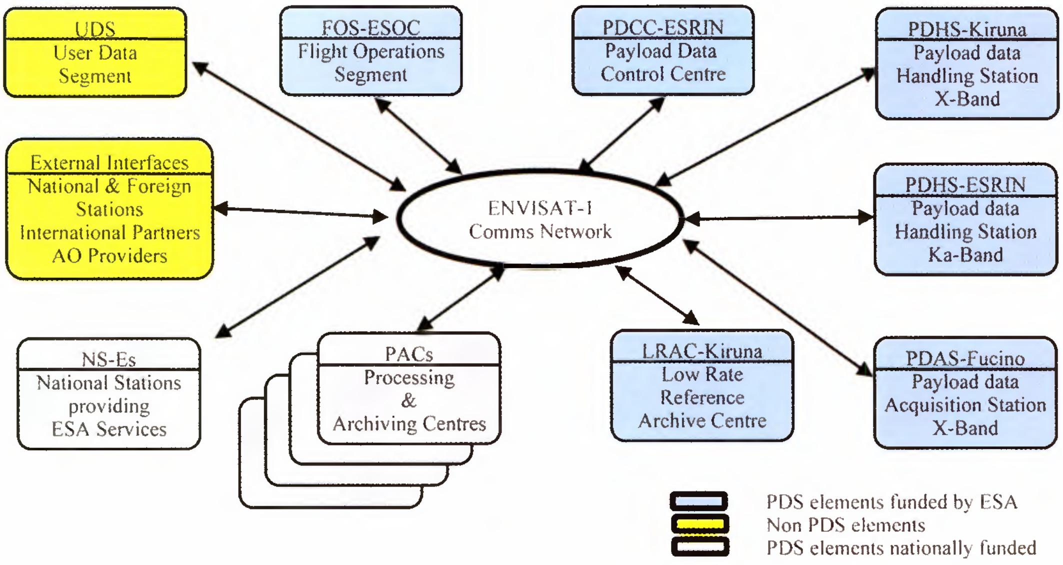

Figure 2.5: Ground Segment Architectural Structure and Elements

Segment are illustrated in Figure 2.5.

The Ground Segment can be split into two major elements:

- the Flight Operation Segment (FOS) which is responsible for the command and control of the satellite;

- the Payload Data Segment (PDS) which is responsible for the exploitation of the instrument data.

The satellite to ground communication links will rely on various ground stations including Kiruna, Fucino, Svalbard and Villafranca (the latter as Tracking, Telemetry and Command back-up) and the ESA Data Relay Satellite (DRS) system Artemis which will provide real-time communication between Envisat-1 and ground, even when the satellite is out of visibility of the ground stations. This will enable the use of the high rate sensors whose data cannot be stored on board, optimise the management of tape dumps and enhance the visibility for command and control. Additional national and ESA Ground Stations will be involved.

2.4.1. The Flight Operation Segment (FOS)

The FOS is composed of the Flight Operations Control Centre (FOCC) located at ESOC Darmstadt and the associated command and control stations. It provides control of the Envisat satellite through all mission phases.

The Flight Operations Control Centre will control all FOS operations:

- satellite operation planning based upon the observation plans prepared at the Payload Data Segment (PDS);

- mission planning interface with Artemis;

- command and control of the Envisat-1 satellite;

- up-loading of operation schedules on a daily basis via the Telemetry, Tracking and Command (TT&C) station at Kiruna-Salmijärvi.

Furthermore the FOCC will support:

- the satellite configuration and performance monitoring;
- software maintenance for the spacecraft and the payload elements;
- the orbit prediction, restitution and maintenance.

The FOCC also provides all the communication interfaces, internal to the FOS as well as external interfaces to the PDS and the specific entities supporting the Mission Operation.

2.4.2. The Payload Data Segment (PDS)
The PDS will provide all services related to the exploitation of the data produced by the instruments carried on-board the Envisat-1 satellite:

- all payload data acquisition for the global mission;
- all regional data acquisition performed by ESA stations;
- processing and delivery of ESA Near Real Time Products;
- archiving, processing and delivery of ESA off-line products with the support of Processing and Archiving Centres (PACs);
- interfaces with national and foreign stations acquiring regional data;
- interfaces to the User Community, from order handling to product delivery.

The PDS comprises all ground segment elements related to payload data acquisition, processing and archiving. It also includes the user interface facilities which enable Envisat services to the User Community. The ESA provided Centres and Stations include:

- the Payload Data Control Centre (PDCC) at ESRIN;
- the Payload Data Handling Station (PDHS) at ESRIN and Kiruna;
- the Payload Data Acquisition Station (PDAS) at Fucino;
- the Low Rate Reference Archive Centre (LRAC) at Kiruna.

In addition the Centres and Stations procured nationally include:

- the Processing and Archiving Centre (PAC's) located in ESA member states;
- the National Stations providing ESA Services (NSES) and located in Programme Participating States.

The PDS will also interface with National and Foreign Stations duly authorised to receive Envisat-1 Regional data. All PDS centres and stations will be coordinated by the Payload Data Control Centre (PDCC), which is in charge of instrument and ground segment planning and of the overall PDS monitoring and control. The PDCC will interface with the Flight Operation Control Centre (FOCC) for all mission planning activities.

From the user's viewpoint, there is one unique interface to the Envisat Ground Segment called the User Service Facility (included in the User Data Segment (UDS) shown in Figure 2.5) through which all users will submit order requests and be provided with data products.

2.5. Product Overview

This section describes the data products and algorithms in the context of the observational and mission requirements which are provided to the users by the User Service Facility.

On the ground, the samples of the return echoes will be processed according to well-established models and corrections and calibrations will be applied to estimate time delay, radar cross-section and standard deviation of the height distribution of the elementary surface reflectors. In this way, it will be possible to retrieve the range from satellite to target, the magnitude of the wind speed and significant wave height, respectively. This will be achieved on a continuous basis using four different waveform retrackers working in parallel.

The four retrackers are the ocean retracker, the sea-ice retracker, the ice-1 retracker, and the ice-2 retracker. The ocean, the ice-1 and the ice-2 retrackers work on both the Ku-band and the S-band waveforms while the sea ice retracker only works on the Ku-band waveforms. The four retrackers will produce four different estimates of the range measurements, which will be put into the geophysical (Level 2) products. These estimated range measurements, from the different retrackers, will not be corrected for the various geophysical effects. The corrections will, however, be supplied in the product. The wet tropospheric correction estimated by the microwave radiometer is also included in the Level 2 products.

Two strong specific requirements have been stressed by the user community:

- The products have to be global (i.e., not segmented by surface type);
- The products need to be segmented in pole to pole ascending and descending pass files.

This has been taken into account for all the geophysical products except for the near real-time (NRT) products which are constrained by downlinking of the data; their segmentation will be driven by the constraints of the dump over the ground station.

The RA-2/MWR products are formatted according to the ENVISAT Payload Data Segment structure (see ESA SP-1221).

2.5.1. RA-2 products

The RA-2 Product Tree is shown in Figure 2.6. This shows the input/output relationships between the different RA-2 products and that between the RA-2 processing chain and the MWR and the DORIS processing chains.

Level 0 is the raw data generated from the data stream of Instrument Source Packets (already demultiplexed per instrument).

The Level 1B product is a conversion of the Level 0 product to a product presented in calibrated engineering units, in which all the steps demanding a detailed knowledge of the instrument itself have been carried out. These steps include decoding the source packet, applying characterisation and calibration data, computing the time-tag in UTC and presenting the instrument measurements (waveforms) in engineering units. This product reflects the structure and contents of the RA-2 source packet.

Level 2 is the science product that will be distributed to users. It basically consists of three main products: GDR (Geophysical Data Record), SGDR (Sensor GDR) and MAR (Marine Abridged Records).

- The GDR is the "traditional" altimeter product, consisting of once per second measurements processed to Level 2. The range measurement between the surface and the satellite appears as a key parameter and exists in three forms: FDGDR (Fast-Delivery Geophysical Data Record), IGDR (Interim Geophysical Data Record) and GDR. They essentially represent the same product, differing in their temporal

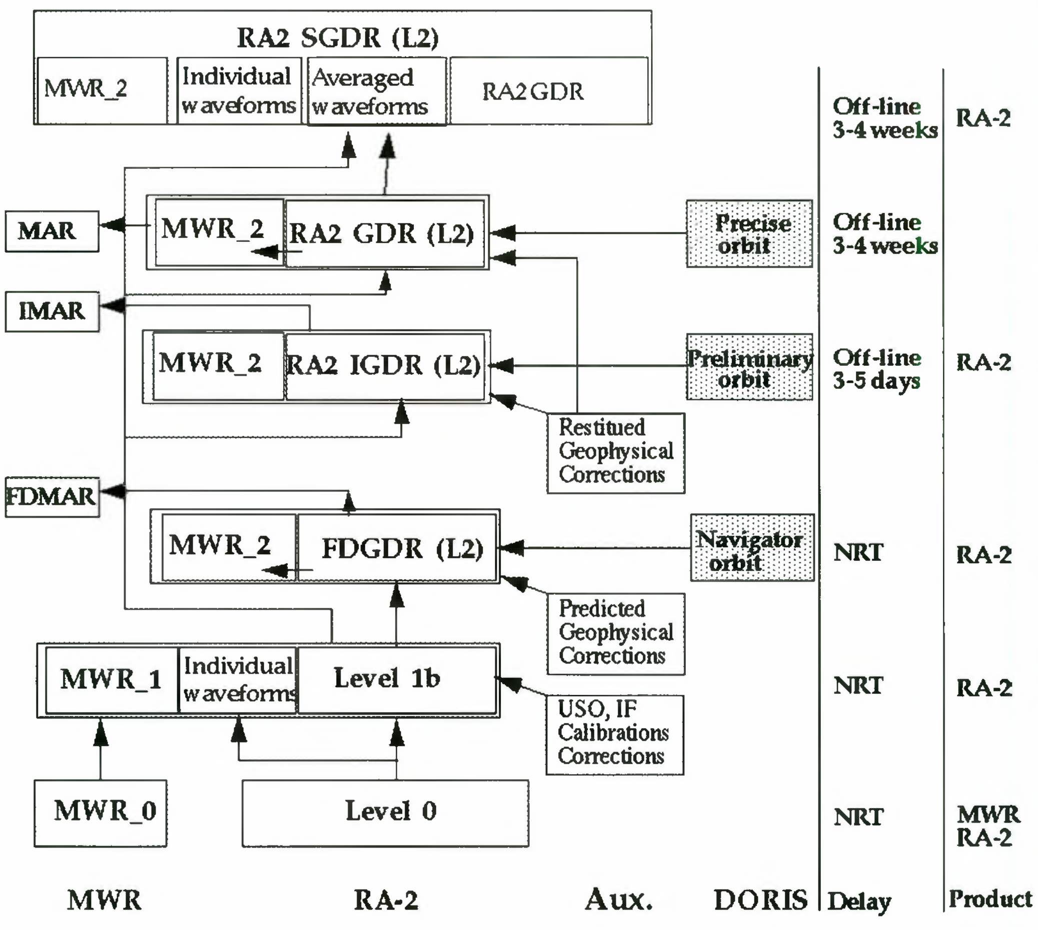

Figure 2.6: Structure of the RA-2 Product Tree

availability and therefore in the quality of the corrections (geophysical or engineering calibration). Both FDGDR and IGDR are intermediate products. The FDGDR is produced in less than 3 hours and then replaced by the IGDR (after 3-5 days, depending on the availability of the preliminary DORIS orbit). This, in turn, is substituted by the GDR (after 3-4 weeks, depending on the availability of the precise DORIS orbit). The GDR is generated by applying the same processing as for FDGDR (the four retrackers are re-run) on the Level 1B waveforms corrected for long term instrument errors, i.e. IF calibration, USO drift.

- A MAR product containing an ocean oriented (only ocean retracker) subset of the FD/I/GDR is made available for meteorological and oceanographic applications. The subsets are called, respectively, FDMAR, IMAR and GMAR.

- The SGDR is essentially the same product as the GDR, with waveforms added to the product. The SGDR is generated from the consolidated Level 1B (waveforms corrected for long term instrument variations) and from the GDR (same geophysical corrections).

Table 2.8: RA-2 Level 2 product overview

RA-2 Level 2 Product		
Type	**Time Requirements**	**Comments**
Fast Delivery Geophysical Data Record (FDGDR)	< 3 hours	4 retracking algorithms specific to surface type (ocean, ice*2, sea ice). DORIS navigator orbit. MWR corrections. Geophysical corrections and ECMWF forecast meteorological corrections. Includes MWR Level 2 independent data set.
Interim Geophysical Data Record(IGDR)	off-line 3-5 days	Same product structure as FDGR. Time ordered. 4 retracking algorithms specific to surface type (ocean, ice*2, sea ice). DORIS preliminary orbit. Predicted USO drift and IF corrections. MWR corrections. Analysed geophysical corrections and ECMWF analysed meteorological corrections. Includes MWR Level 2 independent data set
Geophysical Data Record (GDR)	off-line 3-4 weeks	Same product structure as IGDR. 4 retracking algorithms specific to surface type (ocean, ice*2, sea ice). DORIS precise orbit. Restituted USO drift and IF corrections. MWR corrections. Analysed geophysical corrections and ECMWF analysed meteorological corrections. Includes MWR Level 2 independent data set
Marine Abridged Records (MAR) - FDMAR - IMAR - GMAR	< 3 hours offline 3 – 5 days offline 3 – 4 weeks	Extracted from FD/I/GDR with ocean retracker only
Sensor GDR -(SGDR)	off-line 3 - 4 weeks	Waveforms appended to GDR in an independent data set. Includes MWR Level 2 as an independent data set. Individual waveforms appended in an independent data set.

Table 2.8 summarises the RA-2 Level 2 data products to be generated and disseminated under ESA responsibility.

2.5.2. MWR Products
Each channel of the microwave radiometer operates in Dicke mode, comparing the antenna temperature to an internal reference temperature at a switching frequency of 1 kHz. The output signal from the synchronous detector is integrated and sampled every 150 ms and transmitted to the ground as a numerical count, together with the reference load temperature and various internal temperatures (further investigation is possible to improve the radiometric resolution).

The MWR data at Level 0 are the raw data generated from the data stream of Instrument Source Packets (already de-multiplexed per instrument).

The Level 1B data are converted from Level 0 following the same procedure as for the RA-2 Level 1B product. The Level 1B data are packaged into an independent Measurement Data Set and then merged into the Level 1B RA-2 product.

The Level 2 data are stored as an independent Measurement Data Set of Level 2 RA-2 products. The specific characteristics of the MWR Level 2 Measurement Data Set are:

- one record every 1.2 seconds (source packet "blocking" retained)
- time-tag
- geolocation
- calibrated brightness temperatures from both channels and their standard deviations
- annotation data
- water vapour, liquid water and wet tropospheric correction
- RA-2 Ku- and S-Band sigma-0
- RA-2 significant wave height.

2.6 Calibration and Validation

At the end of the Envisat programme, ESA will have acquired more than a decade of altimetric measurements. As well as the science and application objectives defined in this document, combining ERS-1, ERS-2 and Envisat data should make possible long term studies and monitoring of the glaciological and oceanographic parameters which play a key role in climate changes. However, in order to provide a satisfactory basis for ensuring the stable retrieval of geophysical parameters, the values derived from satellite measurements need to be calibrated and validated by comparison with in-situ measurements and other satellite measurements. Details of the ESA Calibration and Validation Plan are reported in "RA-2/MWR Detailed Calibration and Validation Plan" *(Benveniste et al., 1998)* and "RA-2 In-Orbit Absolute Range Calibration Plan *(Francis and Roca, 1998)*, of which a summary is given below.

It is necessary to be able to relate the RA-2 and MWR measurements to a general reference system and to know their stability. In other words it is necessary to calibrate the data and determine their drift with time. Both the engineering quantities in the Level 1B product (this is the normal situation) and the geophysical quantities in the Level 2 product can be calibrated.

Calibration can be performed in an absolute sense, by reference to independent measurements, or it can be performed relative to similar measurements from other satellites when one is interested primarily in the continuity of a data-set rather than its absolute value.

Once the measurement system has been calibrated, it is possible to determine the quality of the parameters in the data products by comparison with expected values, such as from models or from dedicated in-situ measurements. This activity is called validation.

Some (generally geophysical) parameters are extremely difficult to calibrate in a formal way as the independent knowledge of the parameter may have some uncertainty, typically due to limitations of existing measurement systems (e.g. significant waveheight). In such cases "calibration" may be based on pre-launch measurements only. Validation may then be performed, which in turn may lead to a re-evaluation of the calibration.

The RA-2 measurements of range will extend a continuous time-series started by ERS-1 in 1991. The continuity of this time series needs to be established by a relative calibration (as performed between ERS-1 and ERS-2) but there is also the need to secure the absolute calibration of range after such a long interval.

The specific objectives of the Envisat RA-2 and MWR calibration/validation activities are the following:

- for the Envisat RA-2:

- absolute calibration of the three main measured geophysical parameters: height (via range), significant wave height and wind speed (via sigma-0),
- and relative calibration against ERS and other altimetric missions of these three parameters,

- for the Envisat MWR:

- absolute calibration

and

- relative calibration against ERS of MWR brightness temperatures and water vapour,

- long-term drift detection for all parameters.

The accuracies to which the parameters need to be calibrated (for both RA-2 and MWR) are given in Table 2.9 a.

Range/Sea-Surface Height
The absolute range calibration requirements are very stringent, being 5 times more demanding than the absolute bias calibration of ERS-1.

Table 2.9 a: Calibration objectives for RA-2 and MWR measurements. The Relative Bias is that with respect to other altimeters. The slope in windspeed and waveheight refers to the slope of a regression line when comparing RA-2 data to other sources

Parameter	Bias	Rel. Bias	Drift	Dynamic Range
range (engineering parameter)	10 mm	1 mm	1 mm/year	N/A
sea-surface height	10 mm	1 mm	1 mm/year	N/A
sigma-0 (dual frequency)	±0.5 dB			5 - 20 dB
windspeed	10 cm/s	2 cm/s	2 cm/s/year	3 - 20 m/s
windspeed slope	3 %	1 %		
significant waveheight	3 cm	1cm	1 cm/s/year	1 - 10 m
significant waveheight slope	4 %	1 %		
brightness temp (dual freq)	3K	0.1K	0.5K/year	100 - 350K
wet tropospheric correction	2.5 mm	1.0 mm	1 mm/year	0 - 50 cm

The drift requirements are also challenging and exceed the performance of the 5-year TOPEX time series collected at the Harvest site. However, it must be noted that:

- a large number of measurements will reduce random errors;
- multiple measurement sites will reduce the susceptibility to systematic errors;
- drift is insensitive to systematic errors and may be determined at a high-quality single site.

These points, combined with the mission constraints, particularly the 35-day orbit, which provides a dense coverage with infrequent revisits, have led to the concept of a combination of relative calibration and absolute calibration in a region. The relative calibration will be based on the experiences gained during the cross-calibration of ERS-1 and ERS-2, and is described in "RA-2/MWR Detailed Calibration and Validation Plan" *(Benveniste et al., 1998)*.

The absolute calibration concept has been elaborated in the "RA-2 In-Orbit Absolute Range Calibration Plan" *(Francis and Roca, 1998)* and reviewed by the scientific community at the "RA-2 Absolute Range Calibration Workshop", El Muntanyà, 1998. A summary of the concept is provided here - many more details, including justification for the selection, are provided in the referenced document.

The range calibration will be primarily focused in the north-western Mediterranean and will be based on the determination of sea-level. There are three key measurements:

- The altimeter range, corrected for propagation effects and sea-state bias. Propagation corrections will be derived from in-situ measurements in the calibration region, supported by modelling. Dedicated instrumentation will include dual-frequency GPS receivers (some mounted in buoys) and upward-looking microwave radiometers.
- The orbital height above the ellipsoid. This will be derived by dedicated trajectory fitting over the calibration region, exploiting simultaneous laser tracking.
- The sea-surface height above the ellipsoid. This will be derived from a number of high-quality, open-sea sites (platforms, small islands or GPS buoys) complemented by available shore-based sea-level measurements which will have to be extrapolated to the altimeter tracks. In this activity the mean sea surface, derived from the ERS measurements along the same tracks, will be used.

The range measured at S-band will follow the same approach as that used at Ku-band but it must be calibrated independently so that it may be used for the ionospheric correction. This means that the ionospheric delay needs to be determined by independent means. This will be done by assimilation of high-density dual-frequency GPS data (plus other available data types such as those from DORIS) in the calibration region, into ionospheric models which are now in development.

Within this very briefc overview there are some important points to note:

- *Exploitation of other altimeter satellites:* it has been recognised that by placing the highest quality measurement systems at cross-overs between Envisat and Jason (for example) and performing relative calibration globally between these two altimeters, the effective number of measurements of Envisat is increased. This important characteristic unites absolute and relative calibration activities.

- *Determination of drift:* this will be based on a dedicated site on the ground-track fully equipped with instrumentation, possibly including a transponder. Drift in the Level 2 parameters may also be measured by the use of regional/global tide gauge networks.

The relative range calibration will provide a unification of the Envisat data stream with those of ERS and other altimeters (TOPEX/Poseidon, GFO, Jason). The requirements, which are very stringent compared to those on the absolute bias, have been achieved, for the cross-calibration of ERS-2 and ERS-1, by using the millions of globally distributed data included in three 35 day cycles. Similar methodology, but improved, using previous experience, can also be applied to Envisat. The methods are listed in Table 2.9 b.

Relative range calibration will exploit three techniques:

- comparison of collinear tracks between ERS and Envisat. Although based heavily on experience with ERS-1 and ERS-2 there are a number of differences:

  • the time separation on the ground-track is 30 minutes (instead of 1 day);

  • Envisat has a dual-frequency ionosphere correction unlike ERS - the 30 minute difference in mean local solar time may be compensated more easily than by modelling for ERS;

  • precision tracking systems and mass/geometry are different for the two satellites so there may be slight differences in orbit restitution;

  • the retracking applied to the waveforms in the Level 2 processing is different.

- comparison of global cross-over data with other contemporary altimeter satellites (e.g. ERS, Jason etc.): this approach permits the use of data from satellites in different orbits;

- comparison of Mean Sea Surface (MSS) derived from other contemporary altimeter satellites.

SIGMA-0

Historically sigma-0 has only been calibrated relatively, between satellites. Where an overlap between missions did not occur this has been carried out with the aid of a model linking wind speed to sigma-0. This has lead to a number of empirical corrections, of up to several dB's, to the altimeter measurements, based on pre-launch measurements. This approach proved satisfactory where the objective was ultimately to derive the wind speed measurement itself and when it could be assumed that this was solely a function of sigma-0.

However this is no longer the situation and an absolute calibration of sigma-0 is needed for more theoretically-based studies of ocean surface properties. Applications of sigma-0 over land have been identified, in forestry for example. There are potentially three ways to achieve this, described below and listed in Table 2.9 b:

- Using a dedicated transponder. This can be based on an existing ERS transponder (with refurbishment), a new design derived from the ERS scatterometer transponder, or a specialised transponder derived from adapted RA-2 test equipment. Preliminary investigation of the performance of these systems indicates that

Table 2.9 b: Summary of calibration and validation methods for the primary measurements from RA-2/MWR and corrections to be applied to the RA-2

Parameter	Method	Comments	Expected Performance
Range	*Absolute:* • regional calibration • transponder *Relative:* • comparison of MSS model (ERS, T/P, Jason) • comparison of collinear tracks (ERS) • comparison of global cross-overs (ERS, T/P, Jason)	 • to monitor drift • 30 minute separation	1 cm 1 mm/yr 5 mm 1 mm 3 mm
Sigma-0	*Absolute:* • transponder • reference to natural target • radiometer-like power measurement *Relative:* • comparison of collinear tracks (ERS) • histogram comparison (ERS, T/P, Jason)	• new development • refurbished ERS • rebuilt RA-2 test equipment (RSS) • local scatterometer • space/time sampling to be checked • feasibility under investigation • 30 minute separation • bad ERS histograms	0.2 dB 0.4 dB TBC unknown better than ERS-1/ERS-2 0.1 dB
Windspeed	*Absolute:* • comparison with ECMWF fields • comparison to buoys	• large dynamic range • few measurements • low probability of extreme winds	8 cm/s 3 cm/s
Significant Waveheight	*Absolute:* • comparison with ECMWF fields • comparison to buoys *Relative:* • comparison of collinear tracks (ERS)	• assimilates RA data • large dynamic range • few measurements • low probability of extreme waves • 30 minute separation	10 cm 15 - 20 cm
Total Electron Content	*Validation:* • assimilation of GPS/DORIS data into ionospheric model model for global comparison • additional assimilation of PRARE and ionosonde TBC • tomography from GPS measurements	*Calibration* is performed as part of absolute range calibration • new approaches to assimilation in development • new development: probably needs space-based GPS receivers	0.5 TECU [1 mm at Ku- band]
Brightness Temperature	• synthesise brightness temperature using radiative transfer model - input data from ECMWF/radiosondes	• well-established technique	3 K
Water Vapour Column	• comparison with dual-frequency GPS • Comparison with upward-looking microwave radiometer • comparison to radiosonde data	• new technique offering good performance • best results from GPS receivers at sea • best results from radiometers at sea	5-7 mm

the required performance can be achieved.

- Measuring the sigma-0 at sea using a dedicated nadir-viewing measurement system, simultaneously with terrestrial measurements.

- An innovative technique is under investigation in which the receiver chain of the RA-2 might be able to operate as a coarse microwave radiometer. By assuming that the transmitter power is well known and that the upwelling microwave radiation can be well modelled, this could allow the absolute gain of the receiver to be determined and ultimately the calibration of sigma-0.

Absolute calibration of sigma-0 will be performed in both Ku- and S-band. It is worth noting that the relative sigma-0 between Ku- and S-band is not very well known.

Cross-calibration of sigma-0 with results from other satellites can exploit the methods already used during the ERS-2 cross-calibration with ERS-1 (see Table 2.9 b). The 30 minute time separation between Envisat and ERS, compared to 1 day for ERS-1/ERS-2, will provide much better correlation in the collinear tracks method.

As there are no other S-band radar altimeters available, cross-calibration cannot be used for the S-band channel - only the absolute calibration methods can be used.

Windspeed
Topics which need to be addressed in establishing the calibration and validation of wind speed are the following:

- measurement capabilities, including performance and spatial/temporal sampling, of independent systems (buoys, airborne and spaceborne scatterometers);

- characteristics (accuracy, spatial/temporal sampling) of available meteorological models;

- stability assumptions in comparing wind measurements to surface friction speed;

- results and experience from previous cal/val activities (e.g. ERS)

- improvement of the wind retrieval model.

Cross-calibration of windspeed with results from other satellites can exploit the methods identified in Table 2.9 b.

Significant Waveheight
Topics which need to be addressed in establishing the calibration and validation of significant waveheight are the following:

- measurement capabilities, including performance and spatial/temporal sampling, of independent systems (buoys etc.);

- characteristics (accuracy, spatial/temporal sampling) of the WAM model;

- results and experience of cal/val activities using these data sources (e.g. ERS).

Cross-calibration of significant waveheight with results from other satellites can exploit the methods identified in Table 2.9 b.

Total Electron Content (TEC)
The ionospheric correction will be generated through the dual frequency (S-band) measurements. As mentioned earlier, the S-band has to be independently calibrated and so dedicated measurements have to be made of TEC in the calibration region.

This is described in detail in "RA-2 In-Orbit Absolute Range Calibration Plan" *(Francis and Roca, 1998)*. Validation of the global TEC measurements can be carried out using similar techniques. The major approaches are based on the use of dual-frequency GPS and dual-frequency DORIS data, coupled with the use of assimilation tools in order to properly take into account the part of the ionosphere lying below the satellite altitude.

Brightness Temperatures and Water Vapour

The requirements can be achieved with the methods used for previous microwave radiometers (see Table 2.9 b). Further refinements to the water vapour retrieval are envisaged by using altimeter sigma-0 as a proxy for a third radiometer channel.

3. Measurement Accuracy

3.1 RA-2 Instrument Error Overview

The aim of this section is to provide an overview of the error sources which affect the performance of the Radar Altimeter.

An accurate analysis was performed by Alenia Aerospazio in order to investigate the errors in the engineering parameters, time delay, Sigma-0 and Sigma-S (rms height of the specular points relative to the mean sea level, numerically one quarter of the significant wave height (SWH)). An error budget was then derived from theoretical or mathematical analyses and simulations, always considering the worst case, to be used as a tool to identify problems during the development of the instrument. This analysis assumes that errors combine together in a maximum sense, e.g. all sidelobe energy concentrates at one frequency; the worst case.

Once the instrument has been built, ground testing is carried out to demonstrate that the specifications are met under the worst case scenario. The results presented below are based on tests carried out on the Flight Model (FM), as test results are more representative than theoretical analysis. The FM has been through acceptance testing. Results from this test are supposed to demonstrate extreme conditions, rather than typical behaviour of the instrument under normal conditions. For this reason in-flight performance can already be expected to be better than the results described below.

Nevertheless, some results from the FM-tests of the instrument (in its nominal or more typical conditions) have been used to demonstrate the real behaviour of the instrument as closely as possible.

3.1.1 Types of Error

The existing errors are classified according to their time dependence as bias, drifts, harmonics and random errors. Different methods can be used to define the way in which they are compiled. The one described below (where the index i refers to the individual contribution for each type of error) is that defined in the RA-2 requirement specification which has to be followed when comparing test results against the specifications. Many other methods could be defined and give valid results, but the traceability against the specifications would be lost.

Bias Error: A bias error is defined as an error which is stable during the whole mission. The bias is constant through the mission but it can be a function of any other parameter. Unless decorrelation of the bias error can be demonstrated, the total bias error should be derived as follows:

$$b_T = \sum_i |b_i| \qquad (3.1)$$

Quasistatic Errors (Long Term Drifts): A quasistatic error is defined as an error which slowly varies with time without any periodic character. Different rates of change during the mission, as well as step changes, are allowed. Unless decorrelation of the quasistatic errors is demonstrated, they are summed as follows:

$$q_T = \sum_i |q_i| \qquad (3.2)$$

Harmonic Errors: A harmonic error is defined as an error oscillating with a defined period and with a mean value equal to zero. The typical periods are one full orbit or half an orbit. The amplitude and the phase of the oscillation may vary with time (i.e. drifting). They are added quadratically:

$$h_T = \left[\sum_i h_i^2\right]^{1/2} \qquad (3.3$$

Random Errors: The random error is defined as one that varies in a stochastic way (random process). They also must be added up quadratically:

$$e_{rss} = [b_T^2 + q_T^2 + h_T^2 + \sigma_T^2]^{1/2} \qquad (3.5)$$

where σ_T is the standard deviation of the corresponding random error (assuming a Gaussian distribution).

Total error: The total error is derived as follows:

$$e_{rss} = [b_T^2 + q_T^2 + h_T^2 + \sigma_T^2]^{1/2} \qquad (3.5)$$

Table 3.1: Summary of the range errors and their associated sources. Note that for the ionospheric induced errors (*) after correction does not account for the sea state bias error

Error Sources	Non-corrected Effect (cm)	Residual Error After Correction (cm)	Type of Error	Comments
Instrument Corrected Range	-	2.38	random	SWH = 4 m (from FM testing)
Ionosphere	0-50	0.3	random	Real time use of the 2nd RA-2 frequency (S-Band)*
IF Amplitude Distortions	0.3	neg.	drift	Error budget (influence waveform shape)
USO Long Term Drift	5	neg.	drift	Error budget (drift of primary timing standard)
USO Temperature Variations	0.53	0.53	harmonic	Error budget
Residual after internal calibration		0.3	harmonic	Error budget
Residual bias after external calibration		1	bias	Objective (Abs. Range Cal/Plan under dev.). It absorbs all bias error
Total Error		2.67		Following the above definition of compilation

Table 3.2: Sigma-0 and Sigma-S performance summary

Parameters	Residual After Calibration	Type of Error	Comments
Sigma-S	4.1 cm	random	Sigma-S = 1m (SWH = 4 m) Sigma-0 = 0 dB 1 sec. average
Sigma-0	0.52 dB	rms	Sigma-0 = 10 dB (SWH = 4 m) (driven by the antenna gain uncertainty)

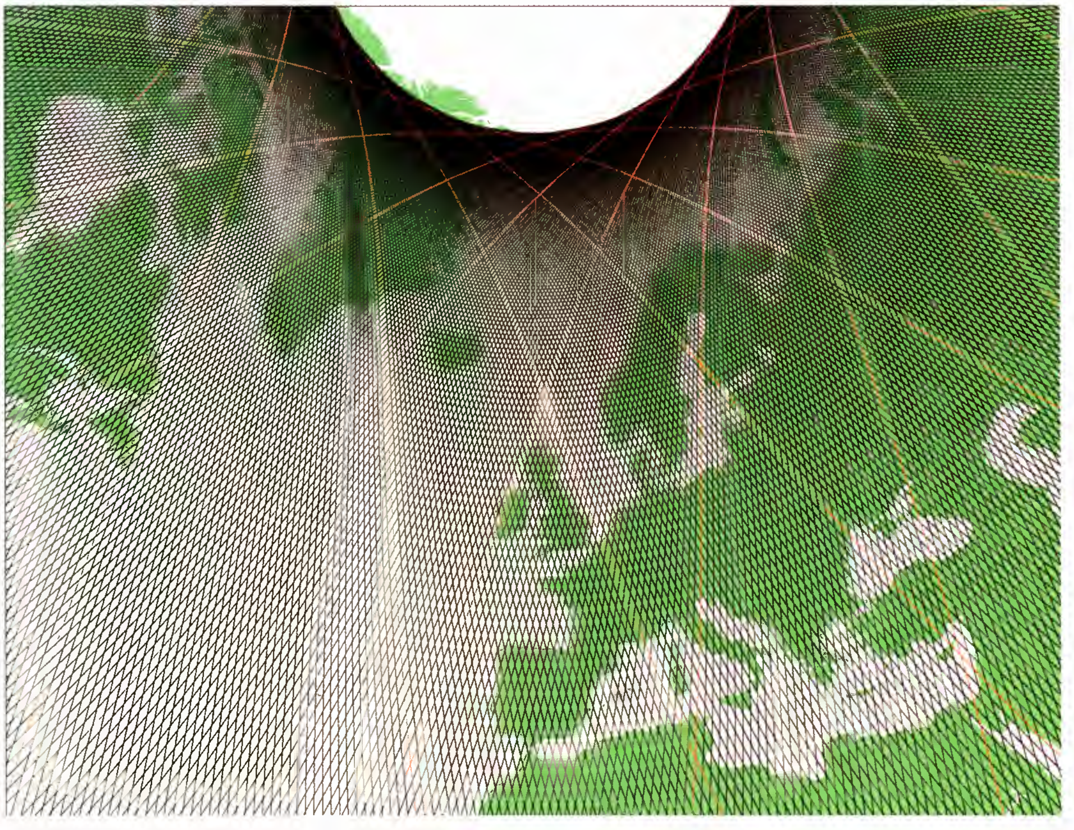

Figure 3.1: Ground track pattern (coverage) obtained after 35 days

Table 3.1 summarises the ranges of these various instrument errors. All lie within the specification.

Results derived from the EM testing of Sigma-S and Sigma-0 performance for typical situations, are provided in Table 3.2. Bias errors also exist but are not shown as they reflect hardware problems already solved in the Flight Model.

3.2. Orbit

In its near-polar orbit the altimeter will sample the ocean, land, lakes and ice up to 82° N/S, covering the majority of global land ice. The 35-day repeat period is a near optimum for the spatio-temporal sampling of mesoscale ocean phenomena. The ground track pattern (Figure 3.1) created by the 501 orbital revolutions of the satellite during one repeat period is sufficiently dense to observe Kelvin and Rossby waves in equatorial regions, mid-latitude eddies, and it can even pick up the smaller scale variability at high latitudes. At the same time the repeat period of 35 days is sufficiently short to follow the evolution of these features in time. Towards the poles, where the cross-track spacing rapidly decreases, ice caps can be mapped to high resolution and their seasonal and long-term variations can be monitored. Because Envisat will follow the same ground track as ERS-2 and ERS-1, an intermittent, but almost continuous time series of local sea height variations along the ground tracks can be constructed which will span over 15 years by the end of the Envisat mission. Continuity of the time series will enable the full separation and characterisation of oceanic tides and variability on various temporal scales, ranging from a few hours to a decade.

Satellite tracking is the only means available to tie altimeter height measurements into a global reference frame. Precise orbit computation, based on these tracking data and various dynamical models, ensures the continuity of this link over regions where there is no immediate tracking. The accuracy with which the absolute sea level, land or ice elevation is inferred, by differencing the orbital altitude and the altimeter height measurement, is always limited by the precision of the orbit computation. The radial orbit error remainsl one of the largest errors in recovering sea surface heights from altimetry. SAR interferometry also demands ever increasing precision of the orbit computation in the cross-track direction to determine the baseline between two SAR images accurately.

Major advances have been made during the ERS mission in the accurate restitution of the orbit. Starting with radial orbit errors of around 150 cm in 1991, the best available orbits are now accurate to better than 5 cm. This was achieved by adopting improved models for the satellite surface forces and the gravity field, and by adding altimeter crossover data in the orbit determination (as long as tracking by the Precise Range and Range Rate Equipment (PRARE) was not widely available). As altimeter corrections become more accurate, the requirements for orbit precision will also increase. While a variance of the radial orbit error of 5 cm with a long term stability of 2 cm is currently being achieved *(Scharroo and Visser, 1998)*, these values need to be reduced to 3 cm and 1 cm, respectively, in the time frame of the Envisat RA-2 operation. This would allow full recovery of small, large scale and long period changes in sea level and ice sheet elevation. Experience has shown that such demands on the orbit precision can only be met when the satellite enjoys a good global tracking coverage and the orbit determination procedure is flexible enough to adapt to new insights and computational models.

Satellite Laser Ranging (SLR) appears to be too sparse to compute ERS-1 orbits to better than 15 cm radially. Its sparsity is caused by the poor geographical distribution of laser systems (mainly located in Europe and the United States), the need for costly human operation and its weather dependence. The DORIS system will circumvent all of these drawbacks as it is virtually stand-alone, has all-weather capability and provides almost (approximately 75%) global coverage. Current experience with DORIS tracking on SPOT-2 (which has a similar orbit to Envisat) suggests that orbital precisions of better than 10 cm are readily achievable; more thorough evaluations show that radial orbit accuracies of 5 cm could be reached. It should be noticed that, apart from differences in the shape and size of the satellite and the DORIS instrument itself, the frequency of manoeuvres and solar activity may be seen as major differences between SPOT-2 and Envisat. It is therefore expected that some experience of Envisat orbit determination will have to be gained before knowledge of its orbits will acquire its final precision. When enhanced by exploiting SLR tracking, even higher accuracies may be achieved.

The choice of the gravity field model has an unquestionable impact on the computed orbit. A gravity field model that is well suited for low-inclination satellites may have serious defects when used to compute the high-inclination orbits of ERS or Envisat. The GRIM4 derived models that have been used so far for the ERS orbit computation at D-PAF have been shown to induce large geographically correlated orbit errors. Although these would not effect the relative sea surface height time series, they limit the applicability of the altimetric measurements for resolving ocean dynamic topography or for the accurate reconstruction of mean sea level and ocean tides at medium wavelengths. In particular they hamper the merging of altimetric measurements and derived products from satellites in different orbits, e.g. TOPEX/POSEIDON and Geosat Follow-On (GFO), each of which has a unique pattern of geographically correlated orbit error.

It is widely argued that, when orbit computations use the same gravity field for all altimeter satellites, there is no mismatch between the gravity-induced orbit errors so they cancel when differencing the different data sets. This is, however, not true. Because of their distinct inclination, repeat cycle, altitude and choice of orbital arc length, gravity model errors impact differently on the computed orbital altitude. Currently, the best choice of gravity model is considered to be one that introduces the smallest errors for each particular mission. Tailored models, tuned to a particular satellite mission are therefore the best candidates for the orbit computation, as long as these act within the error margins of a general-purpose model. With the long-term operation of ERS-1 and ERS-2, sufficient data will be available for the construction of such a gravity field tuned to these satellites, which is then equally suitable for Envisat. At the accuracy many oceanographers seek at longer time scales, it will be crucial to merge the altimeter measurement series from different altimeter missions. Also to be considered are the possible availability of generic gravity models derived from the CHAMP, GRACE and GOCE type missions, which could be of great benefit for Envisat as well as other altimetry missions (see section 4.10).

The operation of the satellite and the production of fast-delivery and precise altimeter products will require the generation of predicted, fast-delivery, and precise orbits. Scientific research will most likely focus on the precise orbits, which therefore require the greatest attention and continuity. To make aa multi-satellite altimeter time series from ERS-1, ERS-2 and Envisat, the orbits of each of the satellites must be in the same reference frame and be based on the same gravity field model. It is likely that the adoption of the most suitable gravity models for Envisat requires a regeneration of all ERS-1 and ERS-2 orbits to ensure this continuity.

The precision of the orbital altitude is also related to the measurement timing accuracy. Due to the vertical velocity of the satellite (which can vary from 0 to about 25 m/s), each millisecond error in the time tag associated with the altimeter measurements can introduce an error of up to 2.5 cm in the inferred sea level. When the timing error is stable it causes a 1- and 2-cycle per revolution height error around the orbit; when it is variable it induces additional correlated noise or drifts. Timing must be accurate to about 0.2 ms, with a long-term stability 0.05 ms, in order to reduce the signal below 5 mm amplitude and to avoid drifts of more than 1 mm/year.

As for previous missions, preliminary orbits (2-3 days availability) with a radial accuracy better than 10 cm will be provided. In comparison, precise orbits will have an expected radial accuracy better than 5 cm. In addition, for the first time, a real time DORIS orbit using onboard navigation capability will be made available to near real-time users. This orbit is expected to have better than 100 cm accuracy, with an accuracy goal of about 35 cm. Tests of this new DORIS capability are being conducted on the SPOT-4 satellite.

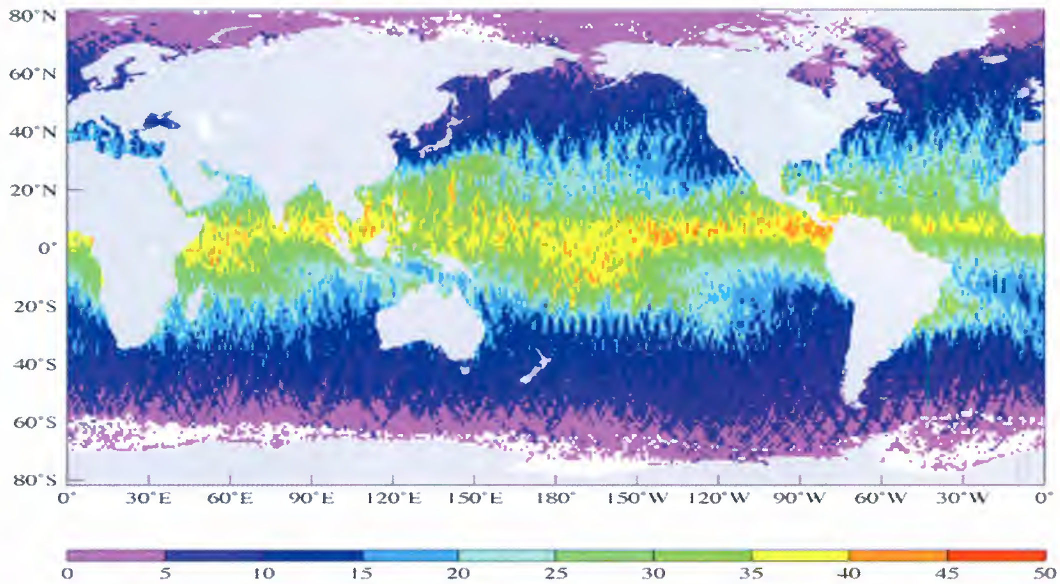

Figure 3.2: Dry tropospheric corrections in cm, based on the ECMWF model atmospheric pressure grids. Largest corrections are seen in the sub-polar regions, due to strong atmospheric low pressure systems

3.3. Errors and Corrections Due to the Environment

Corrections to the range measurement due to the environment, arise from two sources: delays in propagation of the radar pulse through the atmosphere, and sea surface height variations which are not related to ocean circulation. The latter includes effects due to surface waves (the sea state bias), atmospheric pressure variations (the inverted barometer effect) and tides. Uncertainty in the underlying geoid is also considered in the context of these geophysical corrections.

3.3.1. Atmospheric path delays

There are three path delay corrections caused by the atmosphere:

- delays caused by air molecules in the troposphere, i.e. the "dry troposphere" correction, which is proportional to atmospheric pressure at the sea surface;
- delays caused by water molecules in the troposphere, i.e. the "wet troposphere" correction, which is proportional to the total precipitable water content in the atmosphere;
- delays caused by electrons in the ionosphere, i.e. the "ionospheric" correction, which is proportional to the vertically integrated electron content between the satellite and the sea surface.

Dry Troposphere

The dry troposphere correction (DTC) is not based on direct satellite measurements, but rather on numerical weather model analyses. Model grids of sea-level atmospheric pressure, typically generated every 6 or 12 hours, are interpolated to the satellite ground track position and time. The correction is computed from the interpolated sea level pressure (P) and geodetic latitude (ϕ), according to Saastamoinen (1972):

$$\mathrm{DTC\ (mm)} = 2.227 \times (1.0 + 0.0026 \cos 2\phi) \times P\ \mathrm{(mbar)} \qquad (3.6)$$

Figure 3.2 shows a typical distribution of the dry tropospheric correction from cycle 26 of ERS-2. The average value of this correction is about 2.3 metres, with spatial and temporal variations of 10-15 cm.

Wet Troposphere

The wet troposphere correction (WTC) can be calculated from weather model grids of total precipitable water. However, every altimetric mission since GEOSAT has included a microwave radiometer, allowing the wet troposphere correction to be directly estimated along with the range. The radiometer measures two or three "brightness temperatures" at different microwave frequencies, and the water vapour content is computed from these brightness temperatures. The wet tropospheric correction is calculated from the total precipitable water (W) according to *Tapley, et al. (1982)*:

$$\text{WTC (mm)} = 63.6\,W \quad (\text{g cm}^{-2}) \qquad (3.7)$$

The measured wet tropospheric correction in mm is better than that based on weather model grids, but rain cells and contamination by land or sea ice can invalidate the measurements. In such instances the model-based wet tropospheric correction serves as a backup. Figures 3.3 a and b show the distribution of wet corrections from ERS-2 cycle 26, using the measured (MWR radiometer) and model (ECMWF analysis) values, respectively. The average value of this

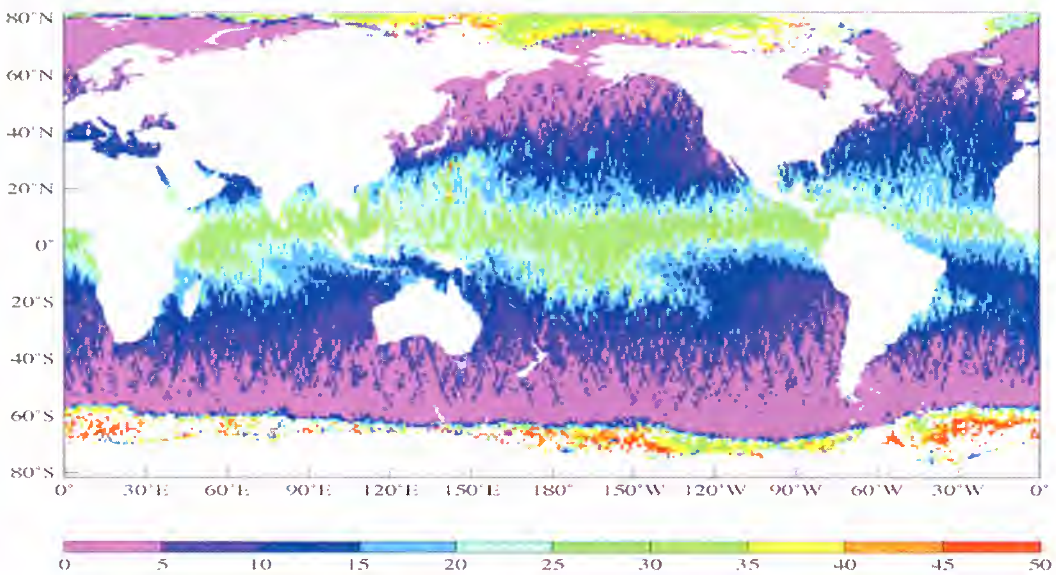

Figure 3.3a: Wet tropospheric corrections in cm, from the on-board radiometer measurements of water vapour content. Largest corrections are seen in the high-humidity tropical regions. Artifacts from sea-ice contamination are seen in the polar regions.

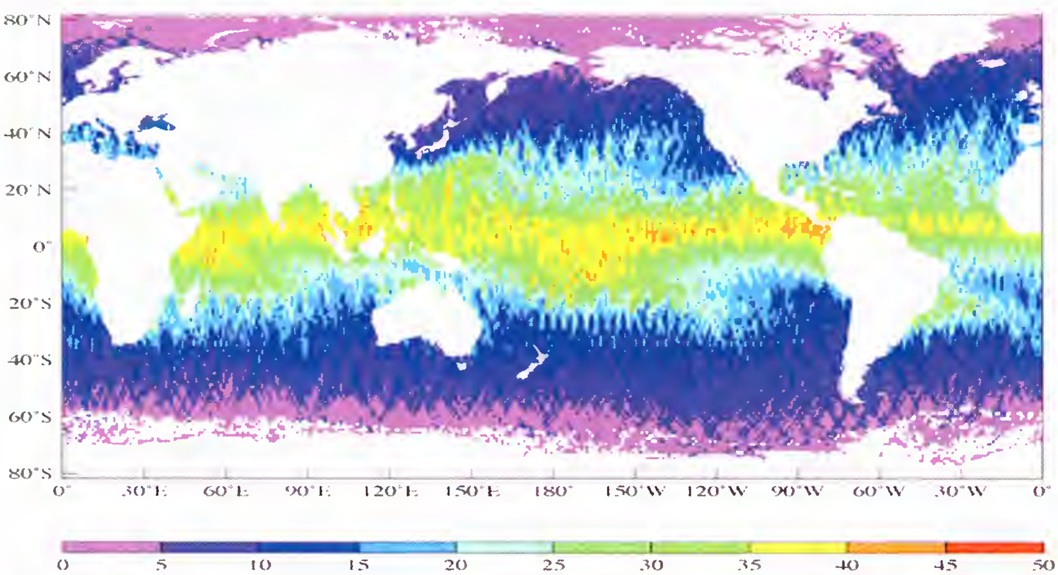

Figure 3.3b: Wet tropospheric corrections in cm, based on the ECMWF model water vapour grids.

correction is about 25 cm, with variations of 20-25 cm. The largest wet corrections are seen in the high humidity tropical regions.

Attenuation of the radar signal by rain and liquid water in the atmosphere is related to the wet troposphere correction, but is much less straightforward to estimate. This effect is manifested as a reduction of returned power from the radar signal, rather than as a path delay in the round trip travel time. Usually, edit criteria based on the backscatter power, automatic gain control (AGC), or scatter of the high-rate range measurements are used to remove data contaminated by rain. *(Quartly, 1997).*

Ionosphere

Prior to TOPEX/Poseidon, the ionospheric correction had to be estimated using ionospheric models such as the *Bent (1973)* or IRI95 *(Bilitza, 1997)* model. Estimates of total electron content (E) were used to calculate the ionosphere correction:

$$\mathrm{IC\,(mm)} = 40250 \times E\ (\text{electrons m}^{-2}) \,/\, [f(\text{Hz})]^2 \qquad (3.8)$$

where f is the altimeter frequency (in Hz). Typical electron content values are on the order of 10^{17}-10^{18} electrons per square metre. The Ku-band altimeter frequency is about 13.8 GHz, so the ionospheric correction is in the order of 2-20 cm.

The quadratic frequency dependence in Equation 3.8 is utilised to make direct estimates of this correction from dual-frequency altimeters such as on TOPEX and Envisat's RA-2. The difference in path delay seen by range measurements at the two altimeter frequencies is used to estimate the ionospheric correction. As with the wet tropospheric correction, the measured ionospheric correction is preferred, with the model-based ionospheric correction serving as a backup. It should be noted that Envisat may make use of its dual-frequency DORIS measurements to serve as another source of ionospheric correction, as is currently done for TOPEX/POSEIDON *(Imel, 1994).* The fact that the spectral content of the DORIS correction and the bi-frequency altimeter correction may be different will bring useful information to ionospheric science. The comparison of DORIS and altimeter ionospheric corrections during a period of high solar activity may bring fruitful information as well, as this case was not encountered by TOPEX/POSEIDON.

All three atmospheric corrections have a zonal structure, with larger N-S gradients than E-W gradients. The wet and dry troposphere corrections vary seasonally as well as on synoptic (meteorological) time scales due to local weather systems. The ionospheric correction, however, is a strong function of local time, being weak at night and maximum at local afternoon. The ERS and Envisat orbits are sun-synchronous, with descending tracks crossing the equator at local morning, and ascending tracks at local evening. This diurnal effect is illustrated in Figures 3.4 a & b using ascending and descending tracks, respectively, from cycle 26 of ERS-2. The magnitude of the ionospheric correction is about 50% greater for the descending orbits (10:30 local equator crossing time) compared to the ascending orbits (22:30 local equator crossing time). During peaks in solar activity, as will occur during the early years of the Envisat mission, the ionospheric correction can reach values as high as 20-25 cm.

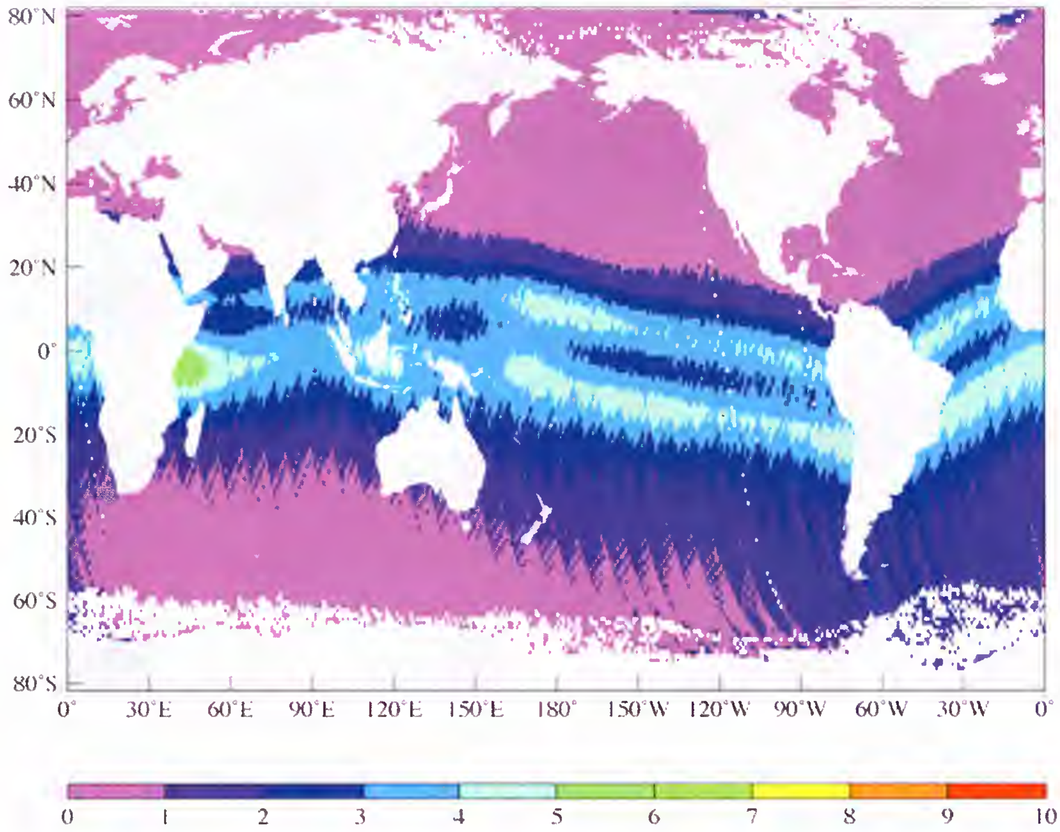

Figure 3.4 a: Ionospheric corrections in cm, from ascending passes of ERS-2's cycle 26. Largest corrections are seen in the equatorial "electro-jet". The local time of each ascending equator crossing is ~22:30

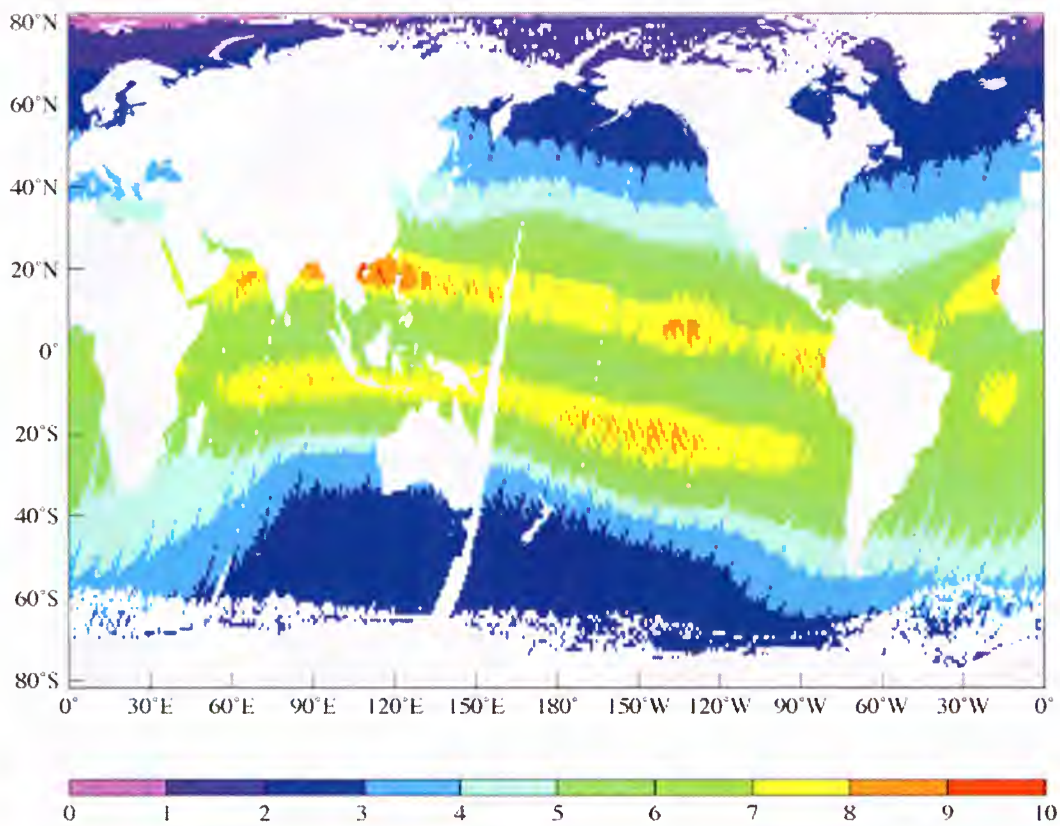

Figure 3.4 b: Ionospheric corrections in cm, from descending passes of ERS-2's cycle 26. The local time of each descending equator crossing is ~10:30, and therefore the corrections are much greater than for the ascending night-time passes

3.3.2 Sea State Bias

The interaction of the altimeter's radar pulse with the sea surface results in a combination of effects known collectively as the sea state bias (SSB). The SSB includes the electromagnetic bias (EMB), the skewness bias and the tracker bias.

The EMB arises because the radar pulse is preferentially reflected by wave troughs rather than wave crests. This results in a bias towards the troughs, making the range measurement too long. The EMB varies with the radar frequency. Skewness is a property of ocean waves which affects the shape of the altimeter pulse's return waveform. The difference between the model waveform shape (which assumes a Gaussian sea surface) and the measured (skewed) waveform leads to a bias. The skewness error is proportional to significant wave height (SWH) and can be approximated by λ*SWH/24, where λ is the skewness of the sea surface elevation *(Srokosz, 1986)*. Typical values of λ are between 0.1 and 0.3. The tracker bias is related to the implementation of the tracking algorithm, and is roughly proportional to SWH. The tracker bias is thus unique to each altimetric system.

In practice, simple parametric models of the SSB are used. These generally express the SSB as a function of the wind speed, U, and the significant wave height, SWH. The model's coefficients are empirically determined to minimise the measured sea level variations either at crossover points or along repeat tracks. The general functional form of most SSB algorithms is:

$$\begin{aligned} SSB = SWH\,(a_1 + a_2 \times SWH + a_3 \times U \\ + a_4 \times SWH^2 + a_5 \times U^2 \\ + a_6 \times SWH \times U) \end{aligned} \tag{3.9}$$

Once the optimal functional form is determined (specifying which of the above terms are significant), the coefficients are estimated, to yield the final algorithm (e.g. *Gaspar et al., 1994)*.

For an early version of the ERS-1 Ocean Products (OPR), *Gaspar and Ogor (1994)* determined that a simple linear dependence on SWH was optimal, with a_1 =- 0.055 and all other coefficients set to zero: SSB = -5.5% SWH (mm). The corrections based on this formulation of SSB are illustrated in Figure 3.5. In regions of high wave activity (SWH around 10 m) the SSB can be as large as 55 cm.

As orbit errors are expected to be on the order of 3-5 cm for Envisat, the error due to the lack of knowledge of the SSB has become a major error source. It is now estimated that the SSB error for TOPEX is at the 2.5 cm rms level, and can rise to 5 cm or more in the southern oceans. Several types of activity can be envisioned to address this problem: the development of more realistic theoretical models for SSB, experiments to obtain *in-situ* measurements of the SSB for a wide range of sea state conditions and the development of improved statistical approaches to extract the SSB signal from the altimeter data (e.g. *Gaspar and Florens, 1998*).

Height performance summary

The range performance results listed in Table 3.3 take account of the typical accuracies currently achieved with altimetry. Any improvement in the modelling of the predictions will also be reflected in these results.

3.3.3 Inverted barometer

Changes in atmospheric pressure at the sea surface cause local isostatic changes in sea level through the so-called "inverted barometer" effect. On average, a one millibar increase in surface pressure causes a depression in sea level of about one cm. This correction is directly proportional to

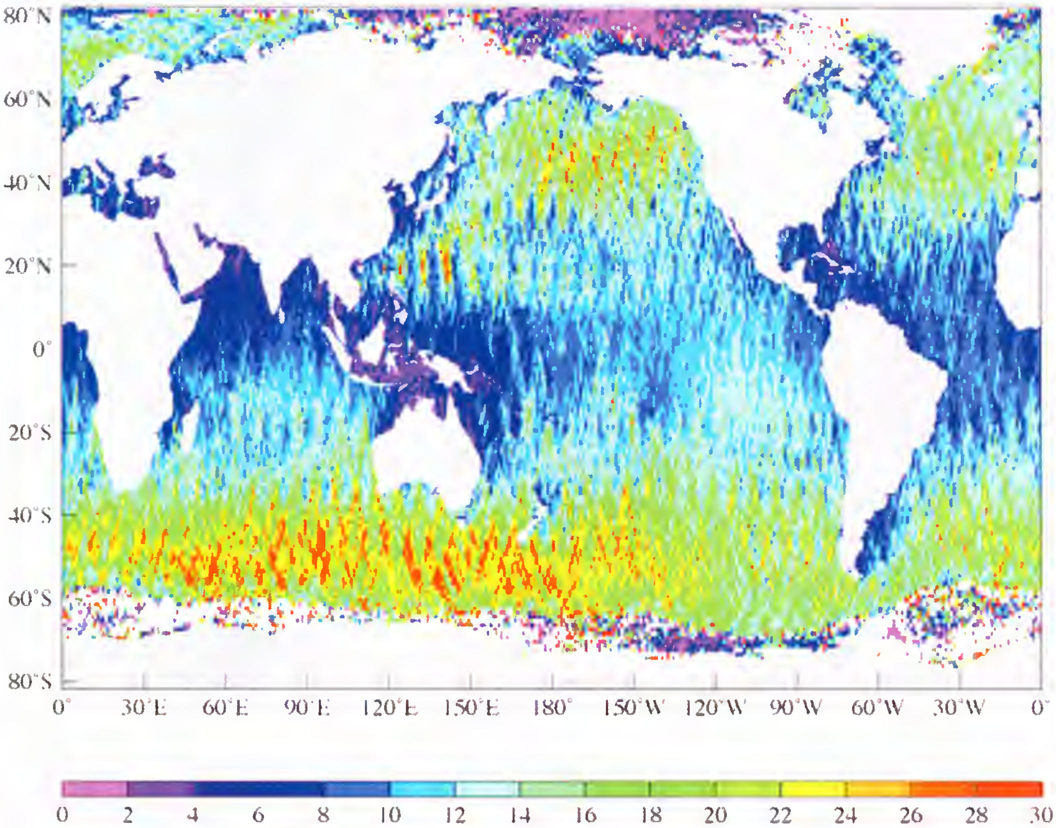

Figure 3.5: Sea state bias correction in cm, computed as 5.5% of SWH In regions of high sea state, such as the "roaring forties" in the southern hemisphere, values as high as 30 - 40 cm are reached.

Table 3.3: Summary of environmental correction errors.

Contributor	Non-corrected Effect (cm)	Residual Error After Correction (cm)	Comments
Instrument Error	-	2.67	Computed from above Table 3.1
Orbit		~ 5	Based on DORIS tracking of SPOT-2 which has a similar orbit to Envisat. No consideration of frequencies of orbit manoeuvres.
Ionosphere	2 -20 (25)	0.3	Real time use of 2nd RA-2 frequency (S-band)
Sea-State Bias	0-20	~2	Effect at RA-2 frequencies under study
Dry Troposphere	~230	0.2-2	Real time use of ECMWF prediction
Wet Troposphere	0-30	1-2	Real time use of MWR data

surface pressure, like the dry tropospheric correction, but is more than four times as large. Typically, the inverted barometer correction (IB) is computed from sea level pressure (P):

$$IB\ (mm) = -9.948 \times (P\ (mb) - 1013.3) \qquad (3.10)$$

This simple, local, formulation may not hold in certain areas such as the tropics and one must also account for the globally averaged (over ocean) sea level pressure at any given time (*Ponte, et al., 1991*).

Fluctuations in atmospheric pressure determine the variability in sea surface height. The full sea level response to atmospheric loading may include dynamical signals in addition to the isostatic effects (simple inverted barometer). *Van Dam and Wahr (1993)* and *Fu and Pihos (1994)* used altimeter data from GEOSAT and TOPEX/POSEIDON to look at the relationships between time series of sea level and barometric pressure. Linear regression analyses led them to conclude that significant deviations exist from the perfect inverted barometer response. A recent analysis by *Gaspar and Ponde (1997)* showed that observed departures of sea level response from the inverted barometer may not be due to artifacts or errors in analysed data. They strongly suggest the presence of adjusted sea level signals which are correlated with barometric pressure. Their analysis of barotropic model outputs, forced by winds and pressure, concluded that a definite correlation exists between both wind- and pressure-driven sea level signals and barometric pressure. This provides a possible dynamical basis for the observed behaviour of the regression coefficients.

When considering climatic mean sea level rise, the impact of these correlations of the inverted barometer correction has been studied by several groups. Indeed, even on such long time scales, the problem of choosing the right reference pressure in the inverted barometer regression (Equation 3.10) is not trivial, due to the way the satellite samples the ocean. If the reference pressure is chosen as (typically) 1013.3 mb, the mean sea level corrected for the inverted barometer exhibits a large artificial annual fluctuation. This results from the fact that the globally averaged surface pressure does not vanish at the annual frequency (*Minster et al, 1995*). A modified inverted barometric correction, obtained by averaging pressure data along the altimeter satellite tracks, also proves inadequate. The best approach is probably to use averaged surface pressure fields (over the ocean domain). While this has the benefit of having little impact on the interannual component and trends in mean sea level, it is still an imperfect solution for the seasonal sea level signal.

3.3.4 Tides

Ocean tides: Ocean tides have a dual role *vis à vis* altimeter measurements. On the one hand most oceanographers consider them as unwanted signals to be first removed from altimeter data, in order to recover ocean circulation signals. On the other hand, for tidal analysis, the use of altimetry in addition to other types of data and models advances our knowledge of tides. Accuracy requirements reconcile both categories of users, as they all want to derive them either globally or regionally to the best achievable accuracy. The Envisat situation with respect to tidal aliasing is exactly the same as for ERS-1/2; the principal semi-diurnal solar component (S2) aliases the altimetric height signals to very low frequencies. Nevertheless, progress in tide recovery procedures makes the situation much better than at the time of ERS-1.

Shum et al, (1996) provided a comprehensive review of a large series of ocean tide models developed in the framework of the TOPEX/POSEIDON mission. From the accuracy assessment they made, it appears that significant progress has been made in the recovery of ocean tides thanks to altimetry from Geosat, ERS and TOPEX/POSEIDON. At the present time, it is quite obvious that data assimilation techniques are among the most useful tools, together with purely empirical models. A large series of tests which compared model outputs to in-situ data (tide gauges, gravimeter data), and analysedaltimeter residuals resulted in the selection of two models (FES95.2 by *C. Le Provost,1992*; and CSR3.0 by *Eanes et al, 1989*) that are now widely known and used to correct altimeter measurements. It is now generally agreed that the major diurnal and semi-diurnal components of the tides are very well known at large scales, whilst shallow water tides are still a problem.

Progress is underway to determine the long period tides that may incorporate a response to luni-solar gravitational potential and a partial response to meteorological forcing. These two fields may benefit from the Envisat altimeter, as well as from other altimeter missions. Other fields of tide related science may deal with the effects of internal tides, meteorological influences (e.g. atmospheric forcing at the diurnal solar S1 frequency) and even, free-core nutation resonance on the estimates of diurnal tidal admittance (affecting the diurnal solar-lunar declinational K1 amplitude). This would also lead to improvement in the overall global modelling of tides. Besides these research activities, it should be noted that although many applications may be satisfied using the CSR3.0 or FES95.2 models the ultimate accuracy is still to be determined.

<u>Solid Earth tide and loading tide effects</u>: The Earth's crust is known to have elasticity and viscosity. Therefore, the tide-generating forces that dynamically act on the ocean masses also result in the appearance of tidal deformations in the solid body of the Earth. Earth tides may be regarded as being in equilibrium. The radial displacements of the Earth's surface may be represented as a linear function of the tide potential and the additional potential created by them. It is standard practice to use the so-called *Love* numbers to characterise the ratio of the solid earth tide to the equilibrium tide in the ocean and the ratio of the additional gravitational potential to the tidal potential.

As an example, the gravitational effect of ocean tides can be considered. Water masses have their own gravitational potential. Their redistribution under the action of tide-generating forces causes perturbations of the Earth's gravitational potential. Added to these are perturbations generated by deformations of the bottom of the ocean. The latter result from two causes: the attraction of the Earth by water masses (the self attraction effect) and its flexure under the action of additional load (the crustal loading effect). If the tidal elevations of the free surface and the bottom of the ocean are respectively designated by H_s and H_b, then the relative displacements of the ocean surface is $H = H_s - H_b$, where H_b is the sum of the direct action of tide generating forces and the combined effect of the crustal loading and self attraction of ocean tides.

The total gravitational potential of mass forces is a combination of the astronomical tidal potential and the additional potentials caused by the ocean and solid earth tides.

It is now well established that all the effects described previously are significant in terms of amplitude (several centimetres) and that they of course have to be taken into account in the interpretation of altimeter data sets for ocean circulation.

Polar tide: The polar tide has been described by many authors. *Lambeck (1988)* provides an extensive discussion of rotational tides in terms of definition and characteristics. In the oceans, the main tide induced by variations in the centrifugal force is the Chandler polar tide. This has a 14-month period and is driven by the *Chandler wobble*. In addition, an annual polar tide also exists which is driven by the seasonal term in the polar motion. Both of these tides originate from the variations in the orientation of the rotation axis relative to the crust. The polar tide has an amplitude of the order of a few millimetres. This makes it a significant correction for the altimeter measurements when used for oceanographic or geophysical studies of long periodic signals. A still open question is how close the polar tide is to equilibrium. Up to now, an approximation assuming equilibrium theory has always been used and considered as sufficient in altimeter data processing. This approximation is easy and acceptable provided the location of the pole is well known.

3.3.5 Geoid uncertainty

The geoid is the surface of equal gravitational potential which, on average, corresponds to the hypothetical ocean surface at rest. On the other hand, the mean sea surface, as calculated from several years of altimeter measurements, serves as a reference for other purposes when time variations are studied (see e.g. *Yi, 1995*). This section considers the errors in currently applicable geoid information, derived from spherical harmonic expansions, or from a combination of such an expansion with local ship or airborne gravity data.

High resolution spherical harmonic models are now available which extend to degree and order 360 (corresponding to a resolution of 0.5 degrees), *Lemoine et. al, 1996* (EGM96). However, such models utilise gravity derived from altimetric measurements and must be used with great care when interpreting altimetric data. Fortunately there are also so-called satellite-only models, EGM96 (*Lemoine et al, 1996*), GRIM4-S4 (*Schwintzer et al, 1997*). Models are also available which combine satellite data with surface gravity data, such as the degree 70 TEG-3 model (*Tapley, et al. 1996*).

Errors in these models can be described as the sum of a so called *commission error* (the error in each degree) and a *truncation error* (the error committed by stopping at a certain degree). According to *Pavlis (1997)* the geoid error is as shown in Table 3.11.

The truncation error, based on the Tscherning/Rapp degree-variance model is 16.7 cm, so the total error for EGM96 is around 0.5 m, globally. In areas with a smooth gravity field (like the North Sea) the error in geoid undulation differences will be smaller, down to 0.2 to 0.3 m for basin-wide distances. For such areas local detailed geoids might exist, which are computed from modern ship gravity measurements (see *Bruinje et al, 1997*, *Denker et al, 1997*). Geoid undulation differences in these regions have errors of 0.1 - 0.15 m for distances of 200 - 500 km (see *Tscherning, 1998*).

For the study of basin-wide oceanographic phenomena, with wavelengths longer than 1000 km, the numbers given in the table provide a rough indication of the corresponding errors for existing geoids. (The "degree" can be converted

Degree	By Degree	Cumulatively	CHAMP	GRACE	GOCE
2	0.1	0.1			
6	0.4	0.6			
10	0.9	1.8			
20	1.7	4.9	$\sim 10^{-1}$	$\sim 10^{-3}$	$\sim 10^{-2}$
30	2.3	7.9			
50	2.9	14.6	~1	$\sim 10^{-2}$	~0.1
75	3.4	20.6			
100	3.0	26.0	~30	~1	~0.1
180	2.2	34.7			
250			Kaula	Kaula	< 5
360	1.3	42.1			

Table 3.11: Geoid undulation commission error for the EGM96 model in cm. (Table 3 from *Pavlis, 1997*). For comparison the cumulative errors are indicated for CHAMP, GRACE and GOCE at selected degrees (*Balmino et al, 1998*). Kaula represents the average *a priori* known value.

to distance using 180/"degree" multiplied by 110 km.) Thus "degree" 30 corresponds to 660 km and the accumulated geoid commission error is 7.9 cm.

It is expected that the long-wavelength geoid uncertainty will decrease during the lifetime of Envisat, due to new spaceborne gravity data being made available from the CHAMP and GRACE missions.

3.3.6 Ice sheet and glaciers

Satellite radar altimetry is currently the most effective method of obtaining accurate elevation models of the Earth's large ice sheets and ice shelves. Models of a substantial part of Greenland have been available for some time. With the advent of ERS-1, coverage of Greenland is now complete, while coverage of Antarctica is complete up to 82° S, including very high spatial density measurements obtained from the 168 day repeat period of the ERS-1 geodetic mission. The absolute accuracy of the elevations obtained by altimetry is of order 1 metre for near horizontal surfaces. The accuracy of the elevations is degraded in regions of appreciable surface topography, to the extent that data is lost altogether. The regions of high gradient that occur at the edges of the ice sheets of Antarctica and Greenland are not well-covered by radar altimetry measurements. With the PRARE tracking system on ERS-2 the improved orbit determination can yield better accuracy in the elevation measurements.

The errors in the elevation measurement are a combination of errors in the reconstruction of the satellite orbit radius, errors in the atmospheric corrections and errors in the association of a surface elevation with the measured radar echo. Generally, the relative importance of these errors is not well known. The models of orbit radius are poorest in the Southern Hemisphere, making the behaviour of the ionosphere most variable.

It has been known for some time that the radar waves penetrate the ice surface to depths of about 10 metres. The penetration can bias elevation measurements derived from altimeter echoes. There is some evidence that the penetration is time dependent, particularly over areas of Greenland where higher mean temperatures exist.

The measurement of the change in elevation of ice shelves with time provides the mass balance of the shelves. Combined with accumulation observations, the change data can support calculations of the melting from the ice shelves, which has an important impact on the deep circulation of the Southern Ocean.

The errors in a volume change measurement are due to time-variant parts of the measurement, unaccounted for in the measurement method or corrections. Principal among these are changes in the instrument parameters, time-variant biases in the radial component of the orbit, changes resulting from the variation in the pattern of the orbit tracks, drifts between the modelled and actual ionospheric corrections and changes in the surface state of the ice sheet, leading to varying degrees of penetration. Presently, the only way to deal with ionospheric and surface variations is by ground measurement.

The RA-2 altimeter will have the capability to repeat measurements made by the ERS series of altimeters. Moreover, as already mentioned in section 2.2.1, the altimeter on Envisat also has two features that are new. In addition to the dual frequency which allows the effect of rapid spatial changes in ionospheric propagation to be corrected for, it is equipped with a more sophisticated tracking system that will permit greater continuity of coverage over the margins of the ice sheets.

4. Science Objectives

With the launch of the dual frequency RA-2 altimeter on Envisat, combined with the MWR for atmospheric correction and the DORIS/LRR system for accurate orbit precision, the Agency will not only ensure continuity of the altimeter observations provided by ERS-1/2, but also take a major step forward in ensuring provision of radar altimeter data with high quality.

The supply of RA-2/MWR observations will ensure that the user community is provided with continuous altimeter observations into the next century. The length of the altimeter record will exceed 15 years and, through inter-calibration with previous altimeter missions, and by combining data and models it will be possible, for the first time, to start to examine changes, on interannual to decadal timescales, of:

- global and regional sea level
- dynamic ocean circulation pattern
- significant waveheight climatology
- ice sheet elevation

The Envisat sun-synchronous orbit covers high latitude ocean, ice sheet and land surface areas not covered by TOPEX/POSEIDON, GFO or Jason, whilst its 35 day repeat cycle allows for denser cross-track spacing. As such, it will offer optimum synergetic combinations with the simultaneously operating Jason/GFO altimetric missions for a wide range of different applications. The advantage in exploiting simultaneous altimeter missions with such widely different spatial and temporal sampling and inclination has clearly been demonstrated by the current ERS missions, together with data from TOPEX/POSEIDON (*Le Traon and Ogor, 1998*).

Taking into account what has been presented in the previous chapters, in particular Chapter 2 on the altimetric system and mission definition, this Chapter describes how the observations and mission requirements for the RA-2/MWR are derived from the needs of scientists working in different disciplines. Following this, a complementary discussion of operational applications is included in Chapter 5.

4.1. Ocean Circulation

While the ocean's central role in modifying climate, through its large heat capacity and transport properties, coupled with its complex interactions with the atmosphere and cryosphere, is well known, our knowledge is not yet sufficient for the accurate prediction of climate change resulting from fluctuations in natural or anthropogenic forcing. For example, it is known qualitatively that a large part of the excess energy input (the incoming solar radiation minus the infrared radiation to space) in tropical areas is carried by the oceans

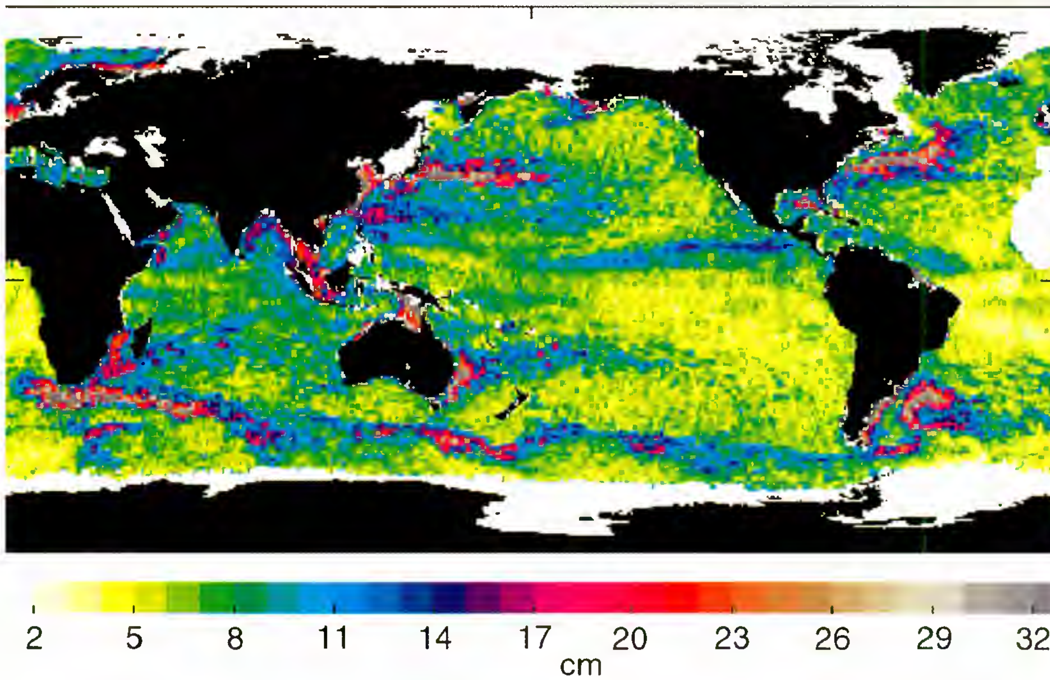

Figure 4.1: Sea surface topography from ERS-1 after correction using TOPEX/POSEIDON precise orbit.

towards the poles, the remainder being transported by the atmosphere. Quantitative estimates are coarse, however, and predictions of how such fluxes would be modified by 'enhanced greenhouse forcing' are even more uncertain. Such uncertainties resulted in the formation of the World Climate Research Programme (WCRP) by the World Meteorological Organisation and the International Council of Scientific Unions. They have been and are being addressed through very large oceanographic research programmes like WOCE and CLIVAR.

These programmes rely heavily on the availability of satellite altimetry data, such as provided by the TOPEX/POSEIDON and ERS-1/ERS-2 missions; operating simultaneously, these satellites allow the measurement of very precise, regular and quasi-global sea surface heights. As most changes in ocean surface currents (on timescales of a few days or longer) result in geostrophic balance, gradients of the sea surface pressure (or 'dynamic topography', the sea level above the geoid) as derived from radar altimetry can be employed almost directly as proxies for surface current information.

Unlike *in-situ* measurements, they are global, synoptic and can be repeated for many years. They are related to ocean processes and currents within the whole water column and can be assimilated directly into ocean and climate models (*Cheney et al, 1997, de Mey, 1998*).

Measurements of sea level are made from space via satellite radar altimetry and from in-situ devices such as coastal tide gauges, bottom pressure recorders and GPS-buoy systems. During the last decade, the technique of radar altimetry has become fully developed, enabling routine and precise quasi-global measurements of mean sea level to be obtained. Analyses of almost four years of TOPEX/POSEIDON altimetric data have provided observations of the ocean dynamic topography to an absolute accuracy of 3-4 cm. In comparison, the ERS-1 orbits are typically accurate to within 15 cm. However, since TOPEX/POSEIDON and ERS-1 were flying simultaneously, the more precise TOPEX/POSEIDON data can be used to correct the ERS-1 orbit error, as shown in Figure 4.1. The same is possible for ERS-2, but with the improved orbit determination from

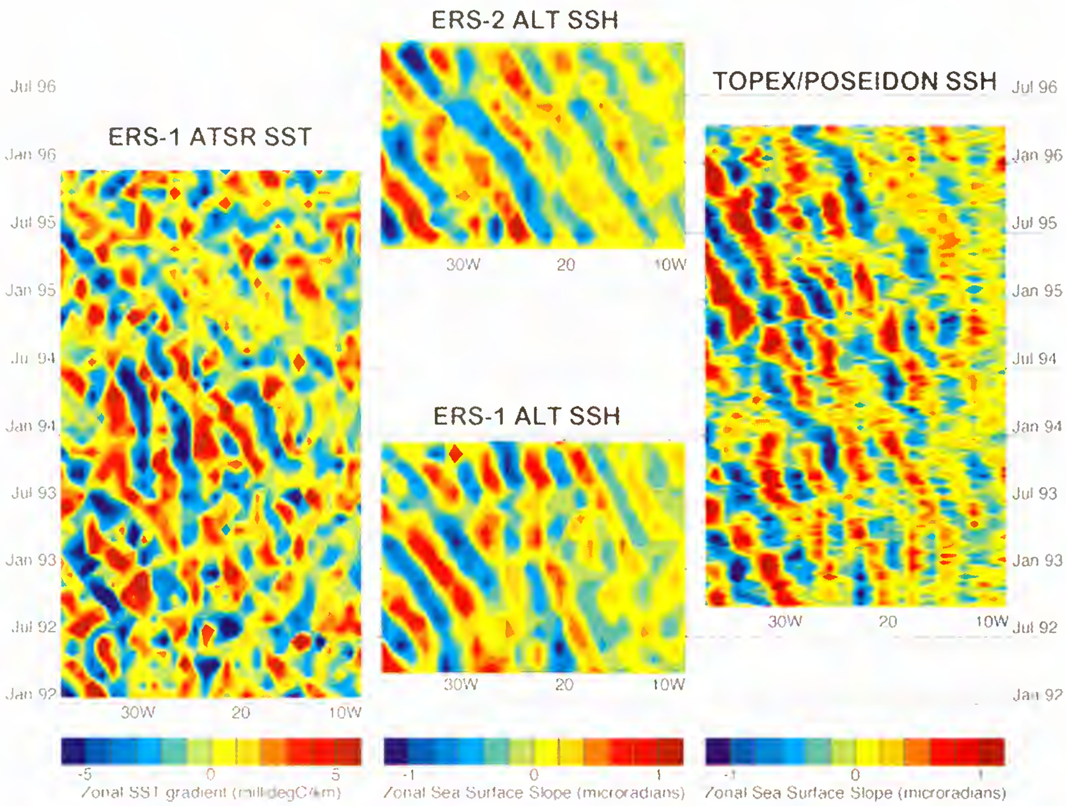

Figure 4.2: Westward propagating Rossby waves derived from ERS-ATSR (left), ERS radar altimeter (centre) and TOPEX/POSEIDON (right). (Courtesy of P.Cippolini)

the PRARE (Precise Range and Range-Rate Equipment) the differences are smaller (*Le Traon and Ogor, 1998*).

It is clear that a more detailed understanding of the ocean circulation is required to refine the global average sea level increase of between 13 and 111 cm predicted in the next century. Values at the low end of the range would have virtually no general impact, but high-end values would have significant impacts for low-lying countries. For example, a 50 cm increase implies an order of magnitude increase in the frequency of storm surge over-topping on the east coast of England. Most of the uncertainty can be assigned to a lack of knowledge of ocean circulation and its transports, especially of heat fluxes. Improvements in the accuracy of estimates are urgently required to enable effective coastal planning.

To advance our knowledge and prediction capabilities of the world climate on seasonal, interannual, and longer time scales, it is essential that ocean circulation processes be well observed, understood and simulated. Ocean thermodynamics has a stabilising role on climate. The ocean and atmosphere together are responsible for the meridional heat transfers. Mechanical energy, mass and heat are exchanged at their interface and couple the two systems together. Therefore global, repeated, observations of the ocean topography are a critical element of the research into climate dynamics and on the perturbations to the coupled atmosphere/ocean system.
In Figure 4.2 this is illustrated with the altimeter observations of westward propagating Rossby waves. The practical applications of this research, through improved ocean circulation prediction, include the economic effects on agriculture and fishing (El Niño and North Atlantic Oscillation-NAO for example) and the consequences of sea-level changes on coastal, populated lowlands such as most of the coasts of Europe.

As far as data assimilation is concerned, model error statistics are essential in order to carry out reliable predictions. In order to assess these errors, models must be run for long times (i.e. 10 years or more) with a continuous data flow. It is therefore essential that continuity of the high-precision altimeter systems is ensured. Envisat will satisfy this need until about 2004-2005.

It is not possible to optimise the sampling of any single satellite mission to observe all oceanic processes and regions. The sampling problem must therefore be thought of in terms of complementarity. The overlapping of ERS-1/2 on a 35-day orbit and the 10-day orbit of TOPEX/POSEIDON in 1993 and from 1995 onwards, illustrates such a complementarity: the fast-varying tropics, large scale disturbances and western boundary currents require the latter, while the mesoscale and high latitudes are being observed by the former (*Le Traon & Dibarboure, 1998*).

The main requirement for future altimeter missions is to have at least two (and preferably three) missions with one very precise long-term altimeter system (such as TOPEX/POSEIDON and JASON). The very precise system is needed to constrain the large scale signal estimation and to provide a long-term reference. This is critical for climate studies (e.g. El Niño monitoring and prediction). Only the combination of several altimeter missions has the ability to resolve the main space and time scales of the ocean circulation, in particular of the mesoscale ocean circulation. There is a large improvement in sampling characteristics when going from one satellite to two satellites. Compared to ERS, the combination of TOPEX/POSEIDON and ERS has, for example, a sea level mean mapping error reduced by a factor larger than two. The improvement is not as large when going from two to three satellites (except for velocity field mapping) (*Le Traon and Dibarboure, 1998*).

There are a number of plans for ocean observation programmes (see section 4.10). Planned or recently launched altimetry missions including, in addition to Envisat RA-2, the GEOSAT Follow-On (launched in February 1998), the high-accuracy TOPEX/POSEIDON Follow-On (Jason) series and the altimetric mission planned under NPOESS, play a vital role in this context.

The GEOSAT Follow-On (GFO) series of the US Navy started with the launch of the single frequency altimeter onboard GFO-1 on 10 February 1998. This mission is planned to last 8 years. The continuation of the series beyond 2006 is not yet decided. Currently, the GFO series has the same 17-day repeat orbit and ground tracks as GEOSAT, which has a maximum latitude of 72°.

The Jason series will start with a first launch in 2000. The sampling and other satellite characteristics will be almost identical to those of TOPEX/POSEIDON. It has been shown that such a sampling provides an adequate coverage of the tropical areas and general circulation variability; in addition its excellent error budget has given access to precise measurements of sea level, including seasonal steric height changes and interannual sea-level drift. TOPEX/POSEIDON also revealed a large interannual variability both in the tropics and in the subtropics, which also justifies a requirement for 'long' time series. However the Jason orbit will not cover latitudes above 66°, and its 10-day-repeat ground track network will be too wide-spaced to resolve the mid-latitude mesoscale eddies.

The effects of high-latitude ocean circulation and its interaction with sea ice, on seasonal to interannual climate predictability, are only now being studied, thanks to the coverage of the ERS altimeter missions and the approved Envisat altimeter mission. These studies should complement the active ongoing research on ENSO (El Niño/Southern Oscillation) and predictability in the tropics. Since the coverage and characteristics of sea-ice change seasonally, large intra-annual and sometimes interannual variations in the energy, heat and freshwater budgets of the upper ocean are observed; these processes impact on the large-scale thermohaline circulation as a whole. Ice transport southward from the Arctic provides an important source of fresh water to the Greenland and Norwegian seas, impacting the deep convective overturning and bottom water formation in this region. This process may influence the global-scale thermohaline circulation. Mesoscale high-latitude eddies and currents move heat around, and significantly modify the sea ice distribution, which has an important effect on climate through changes in albedo.

The high-latitude circulation of the ocean is composed of a relatively weak mean circulation, constrained by the coasts, and of a relatively small-scale variability linked to fronts, eddies, and the meandering of mean currents. The Rossby radius at high-latitudes is small, on the order of 5 km. Typical spatial scales associated with the mesoscale variability are in the range 50-200 km at mid-latitudes and reduce to 5-50 km at high latitudes. Typical temporal scales at mid- and high latitudes are weeks to months. Expected amplitudes for mesoscale eddies and meanders are in the range 5-30 cm, down to a few centimetres for high-latitude fronts.

Coastal and shelf processes typically follow the geometry of the continental margins, with extended length scales parallel to the coast and shorter (1-10 km) scales perpendicular to the coast. The dynamics of coastal regions are complicated, and many of the details of the coupling between the tides, storm surges, coastal currents and the deeper ocean have yet to be worked out. Temporal scales are, typically, considerably shorter than those of the open ocean, of order days to weeks.

The sampling is determined by the need to sample the high latitude mesoscale and, if possible, the processes occuring at the continental margins. For this, a cross-track distance of 15 km (or better) at ±75° latitude is required. This value is acceptable for high-latitude mesoscale processes, provided that space-time interpolation methods are applied to the data. Coastal and shelf processes may have time scales of a few days or a week, coupled with shorter scales perpendicular to the coasts. The latter cannot be surveyed by a single satellite. A sun-synchronous 35-day repeat-cycle provides the spatial sampling required at high latitudes and the temporal sampling required for the ocean mesoscale. The measurements are made by calculating height anomolies along track profiles. These differences will contain changes in ocean topography, and differences in the geoid, due to any across-track variation in the geoid. The satellite ground tracks must repeat, because the geoid spectrum stays "red" up to the ocean synoptic scales (50-100 km). Given a sampling strategy, the ground track repeatability should be better than ±1 km in the cross-track direction at the equator (*Minster et al, 1995*).

4.2. Ice Sheet and Glacier

Scales of time-invariant topography.
For ice sheets in dynamic equilibrium, the topography is an expression of the force required for the ice flow to overcome internal shear stresses and stresses of friction at its bed. At the large scale, a change in elevation generates a hydrostatic pressure gradient within the ice, which, when integrated through the ice column, balances the shear forces within and at the base of sheet. Over much of the ice sheet the topography is distinctly two scale. At the regional scale, slopes range from 0 to 1 degree, and at smaller scales variations of a few metres in the vertical, at length scales of tens of kilometres, are found, connected with the surface expression of bedrock topography.

This situation alters considerably when basal shear stresses become very small or non-existent, as is the case with the Antarctic ice streams and ice shelves. In these cases, longitudinal stresses may become important (the ice pulls or pushes itself along), the force balance of the ice is much more complicated and topographic variations may be more subtle. In the case of ice streams, where the flow is channelled, the horizontal scale of variation may become shorter, perhaps one km or less, and variations of 10 cm may be dynamically significant. Over ice shelves, variations of this magnitude are also significant, but have greatly increased horizontal scales, typically 10 km or greater.

The interior topography of the Antarctic and Greenland Ice Sheets has been well-defined by the ERS-1 geodetic mission phase (Figures 4.3 a,b) but the present uncertainty in ice sheet thickness is considerably larger and there is limited value in repeated observations of the topography. The Ronne Flichner, Ross and Amery Ice Shelves are also well mapped to 82° S, and again uncertainties in the gravity field are considerable larger than those in elevation. Here, too, further pulse-limited observations are of limited value. Elevation of the ice sheet margins and of the ice streams, remains of considerable importance, although many of the most important Antarctic streams lie south of 82° S, and the topography in the ice sheet margins may vary too rapidly for useful, pulse-limited measurements.

Scales of time-variant topography.
Time-variations in ice sheet mass and elevation are known to occur, but the spatial and temporal scales are very poorly known. At the continental scale and over the course of this century, the variation of the Greenland and Antarctic Ice Sheets is thought to have been limited to within 0.2 of the mean accumulation rate (MAR). At point locations, it is reasonably established that a short term variation of 0.15 MAR root-mean-square (rms) is typical of the mass accumulation rate, although the temporal correlation interval is not well-established and may span inter-annual to interdecadal scales. This century these variations have been poorly correlated at the 1000 km scale, and it seems reasonable to assume that the short-term variability in the continent-wide accumulation rate is considerable smaller than 0.15 MAR rms, although there are some data to the contrary.

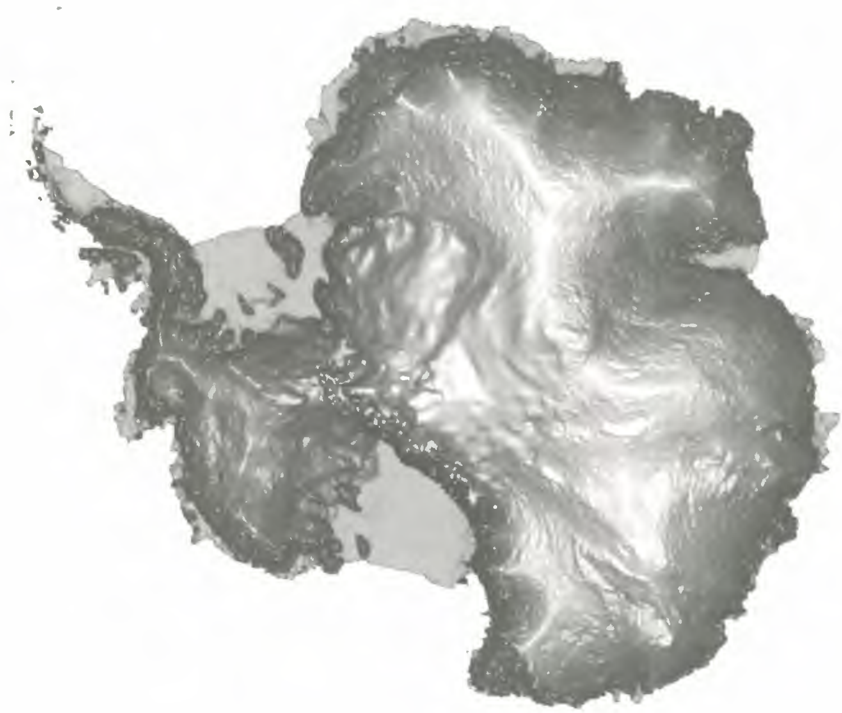

Figure 4.3a: Topography map of Antarctica derived from the ERS altimeter with data filled in from other sources south of 82° S (Courtesy of J. Bamber)

Figure 4.3b: Topographic map of Greenland derived from the ERS altimeter (Courtesy of J. Bamber)

For the cold, dry Antarctic interior and northern Greenland Ice Sheet, short-term variability will occur and reflect variations in the density of snow. For accumulation rates of 10 cm/year ice equivalent, the short term variability in elevation is 3.5 cm/year. This requires resolution at scales of 1 year and 50 km if the present uncertainty of the scale of this fluctuation is to be resolved. At ice sheet margins, where accumulation rates of 1 m/year ice equivalent occur, the short term variability is 35 cm/year. The longer-term, continent scale uncertainty corresponds to 5 cm/year ice equivalent and the measurement accuracy must be considerably better than this to be useful.

With the ERS missions, achieving an accuracy of 1 cm/year at the large scale has easily been achieved. At shorter scales, an elevation precision of 2 cm/year at 50 km has been achieved, but rather poorer precision at the ice sheet margins where the cross-over density is smaller. The accuracy, however, is limited by residual error in the surface-to-volume scattering ratio correction, which may introduce point errors of up to 10 cm. Although these are associated with variations of layering and grain-size, which are highly variable in space, little is known about their mean variation, and this error cannot be excluded from observations of the data alone. Over a five-year interval, this corresponds to 2 cm/year. Thus, the spatial scale of variation in the altimeter observations at 50 to 250 km remains ambiguous.

It is worthwhile emphasising that the uncertainty in the temporal and spatial scale of the accumulation rate variations has an important implication for mass balance studies. The ground observations are too few to determine the large-scale variability, and in consequence it is not possible to connect, with any certainty, elevation rates based on short time intervals (5-10 year) and longer (century) imbalances. A very much better understanding of the spatial scale of elevation rate fluctuations would greatly increase the relevance of the altimetric time-series.

Recently, *Wingham et al, (1998)* provide evidence that the ERS satellite radar altimeter measurements (4 million ice-mode cross-over points) show that the average elevation of the Antarctic Ice Sheet interior (63% of the grounded ice sheet) fell by 0.9 ± 0.5 cm/year from 1992 to 1996. Moreover, when they account for the variability of snowfall observed in Antarctic ice cores, they conclude that the mass imbalance of the interior this century is only -0.06 ± 0.08 of the mean MAR. Hence, the interior of the Antarctic Ice Sheet has been at most only a modest source or sink of sea level mass this century. The continuation and improved accuracy of such elevation change data to be expected by the RA-2/MWR will further enhance the value and importance of monitoring ice sheet elevation change.

4.3. Lakes and Inland Waters

Satellite altimetry can provide global water level information over large wetlands, lakes and rivers. Such information is valuable, both to hydrologists and climatologists, since only a small percentage of inland water bodies are gauged, and even for those that are it is often difficult to obtain the data.

Globally there are over 1400 lakes with surface areas exceeding 100 km^2 (the limit above which altimeter data can be analysed simply as for the ocean). Of these, ~300 are "closed" lakes, i.e. lakes without outlets and hence very sensitive to changes in local climate. Approximately 70% of the global distribution of these lakes is observed by an altimeter in a

35-day repeat cycle compared with 50% for a 17-day repeat cycle, and 10-20% for a 10-day repeat cycle.

The altimeter data processing requirements become more complex for water bodies with dimensions smaller than the measurement footprint. The latter is a strong function of surface roughness, varying from the first Fresnel zone for a smooth surface, to the maximum pulse limited footprint (~10 km diameter) for waves of 20 m significant waveheight which is unrealistic for lakes. Thus, the ability to make measurements of water bodies less than about 100 km^2 depends on the surface state.

The water level may be used to generate height maps, which reveal the geoid if no significant water flow or wind set-up is taking place (as is the case in most lakes). If the geoid is known independently and the water is in motion, flow directions and possibly flow rates may be deduced. This can be especially valuable in wetlands, where the surface slopes are very small and are extremely difficult to map from the ground. Repeated measurements provide time series which reveal seasonal and longer-term variations.

All the familiar altimetric corrections are required in order to maximise the accuracy of the water level measurements, including satellite orbit corrections, instrument corrections, refraction corrections and surface corrections. Tides, wind set up, and freeze periods must also be taken into account, although these may provide interesting signals in their own right. Apart from the instrument corrections, the techniques to address all of these are much less well developed than for the open ocean. For example, except in the case of very large water bodies, land contamination obviates the use of passive microwave sounder data to estimate the tropospheric water vapour correction. Further research is required to establish methodologies to address this and other difficulties. The goal is to achieve sub-decimetre accuracy and precision. Note though, that in many cases the amplitude of seasonal variations is several metres so less accurate level estimates can still be useful.

The historical data sets from Seasat and GEOSAT, and those currently being acquired from the ERS and TOPEX-Poseidon missions, are being used in a series of pilot projects to develop the data processing techniques and to evaluate the usefulness and range of applications of the results.

The science issues to be addressed by the RA-2 over inland water include the detection and measurement of water flows, the monitoring of water level variations and the study of their links to climate change.

The RA-2 is designed with an adaptive range window and robust tracker. It should therefore obtain more continuous coverage than has been possible in the past, providing improved coverage of lakes already monitored and an increase in the number of lakes that can be monitored.

4.4. Land

Pulse-limited altimeters are fundamentally unsuited for observations of the land surface owing to the complex effect on the echo waveforms of topography and spatially variable backscatter. Nevertheless, approximately 10% of the Earth's land surface is sufficiently flat and uniform that useful height estimates can be obtained. In general, this restricts land topographic mapping by altimetry to arid areas, especially sand deserts, and to grassland prairies.

Figure 4.4: Digital elevation map of South America derived from ERS altimetry (Courtesy of J. Bamber)

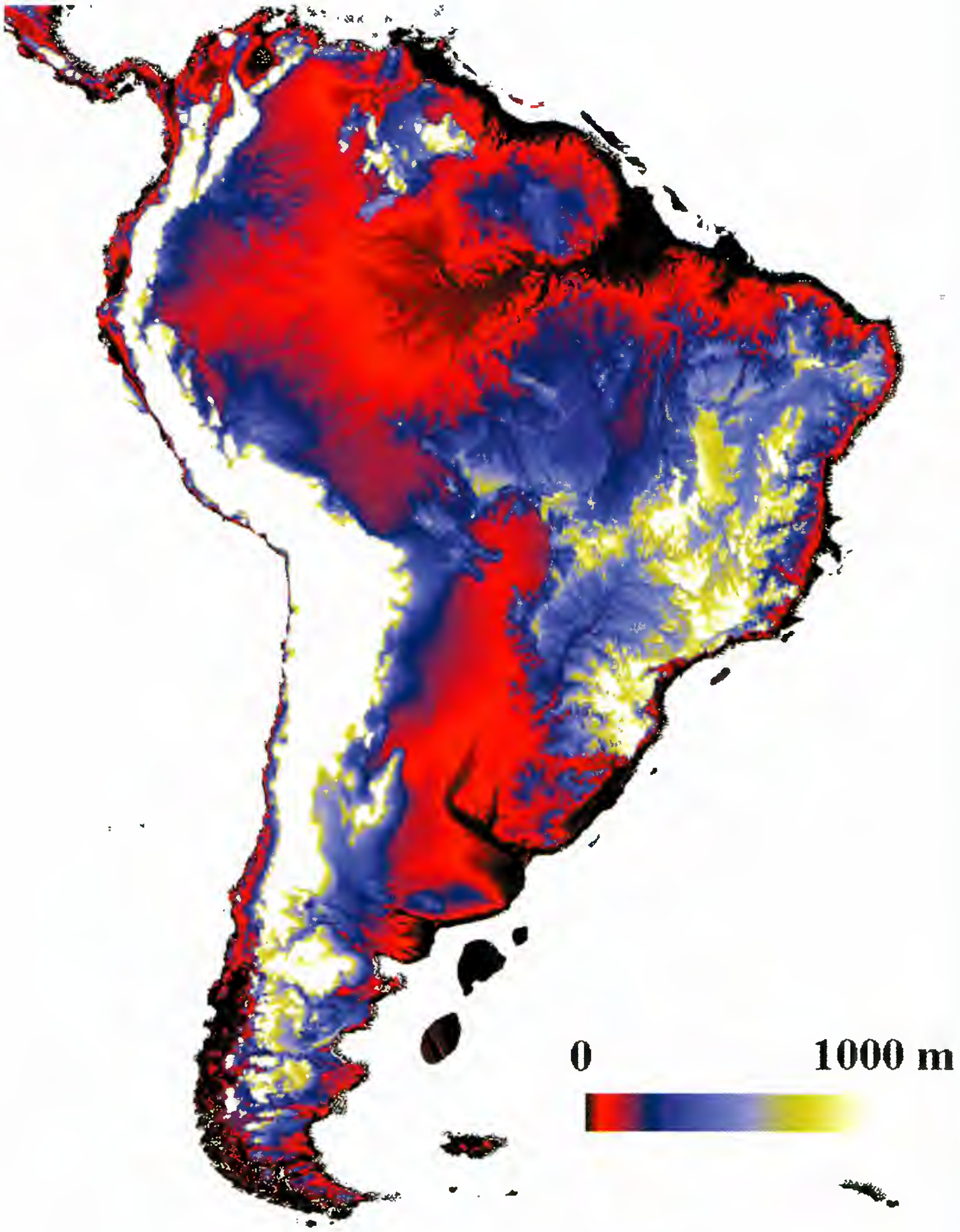

The use of the data for basic topographic mapping includes the validation/correction of Digital Elevation Models (since errors of several hundred metres have been demonstrated when using pulse-limited altimeter data to verify existing DEMs) and the delineation of drainage basins in remote areas with gentle topography (Figure 4.4). The height distribution of medium scale topographic relief, such as dunes, can be estimated, as can surface characteristics such as surface small-scale roughness and moisture content (in some circumstances). Attempts have been made to use land surfaces as references to evaluate orbit solutions and to estimate altimeter range bias, but closure is limited to the ~1 m level by difficulties associated with the complex nature of the relationship between the echo waveforms, the surface topography and the backscatter distribution.

The studies to be carried out using the RA-2 over land include the detection of temporal variations in radar backscatter coefficient (associated mainly with changes in moisture content and/or surface small-scale roughness) and height (at the cm level associated with isostatic rebound, and tectonic motions).

The adaptive range window and robust tracker of the RA-2 will ensure increased data coverage and quality relative to previous missions. However, the density of spatial coverage is a key issue for land height mapping and the 35 day repeat cycle will not be sufficient to provide dense enough global sampling.

4.5. Polar Oceans (Marine Geophysics)

The extension of altimetric measurements to latitudes of 82° by the ERS satellite has provided new coverage of the polar oceans including areas of seasonal and permanent sea ice cover. The development of techniques for the extraction of altimetric heights in sea ice areas has allowed the generation of marine gravity maps of the polar oceans leading to important results concerning the tectonic development of these regions. Since the gravity signal represents the zero order component in the altimetric height measurement the improvements expected from Envisat will provide the means to explore the potential of mapping the higher order components due to oceanographic and possibly glacial signals.

Marine gravity mapping using the ERS-1 satellite over sea ice areas has proved extremely fruitful leading to major geophysical discoveries in both the Antarctic and Arctic regions (Figures 4.5 a & b). Data from the ERS-1 geodetic mission were particularly useful in allowing high resolution gravity maps to be generated. Gravity anomalies are calculated from along track slopes so high accuracy measurements are required at short wavelengths (though this is not so critical at long wavelengths). Polar gravity fields would benefit most from a repeat of the ERS-1 geodetic mission. However, multiple 35 day repeat cycles from Envisat, combined with geodetic mission data, will allow more accurate fields to be generated.

Accurate marine geoids in the polar oceans are required for improvements to global gravity models, particularly at intermediate wavelengths. The improved accuracy and longer time series provided by Envisat will allow more accurate marine geoids to be developed. This task depends critically on the availability of accurate atmospheric corrections, orbits and tidal models in the polar regions. Crossover analysis in the polar regions will feedback into the improvement of Envisat orbits in these regions.

Temporal variability in sea surface height over areas covered in sea ice has the potential to greatly improve tidal models in the polar oceans. These measurements also have the potential to provide constraints to models of Arctic Ocean circulation which are now being developed. Both of these objectives will benefit greatly from the improved accuracy of Envisat and also from the extension of the time series provided by the ERS satellites.

Whilst the processing of waveform data from ERS-1/2 allows the correction of the gross tracking errors over sea ice, residual noise remains in the re-tracked height signal, some of which can be attributed to aspects of the instrument's design. The improvements in design of the Envisat RA-2 and the consequent impact on sea surface height measurements over sea ice include:

- Quantisation of the waveform echo bin samples - waveform samples on the ERS altimeter instruments were quantised to 5 bits prior to waveform averaging. The lack of a noise floor on ERS altimeter data leads to errors in interpolating to the correct tracking point on the leading edge of peaked altimeter returns.

- Pulse blurring - The majority of ERS altimeter data over sea ice has been gathered in the ocean mode. The SMLE tracker onboard the ERS satellite leads to large oscillations in the tracker position. Simulations reveal that blurring of the leading edge of the altimeter echo can contribute

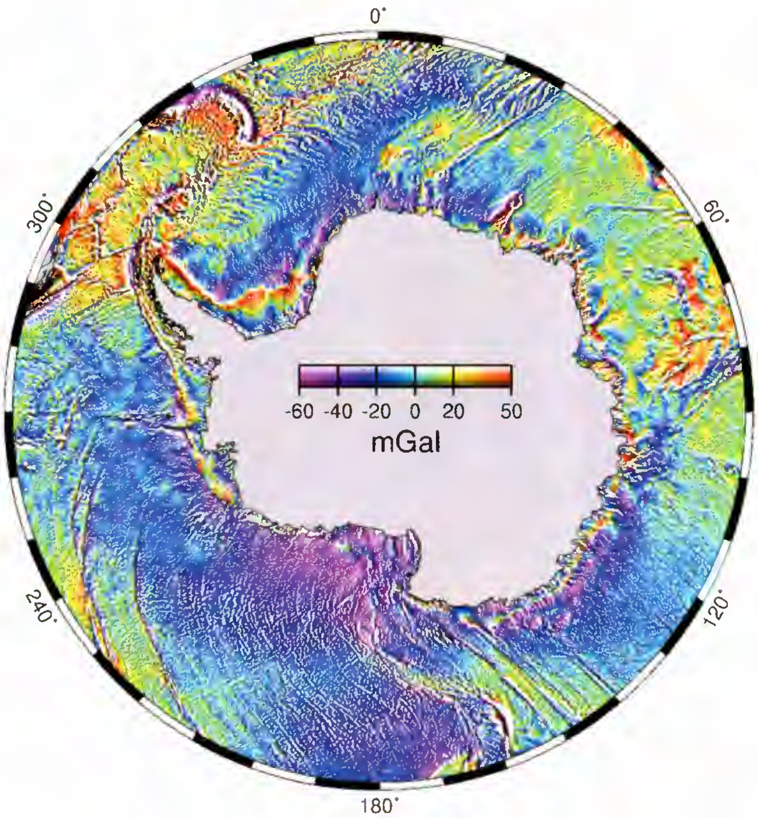

Figure 4.5 a: High resolution gravity map surrounding Antarctica.

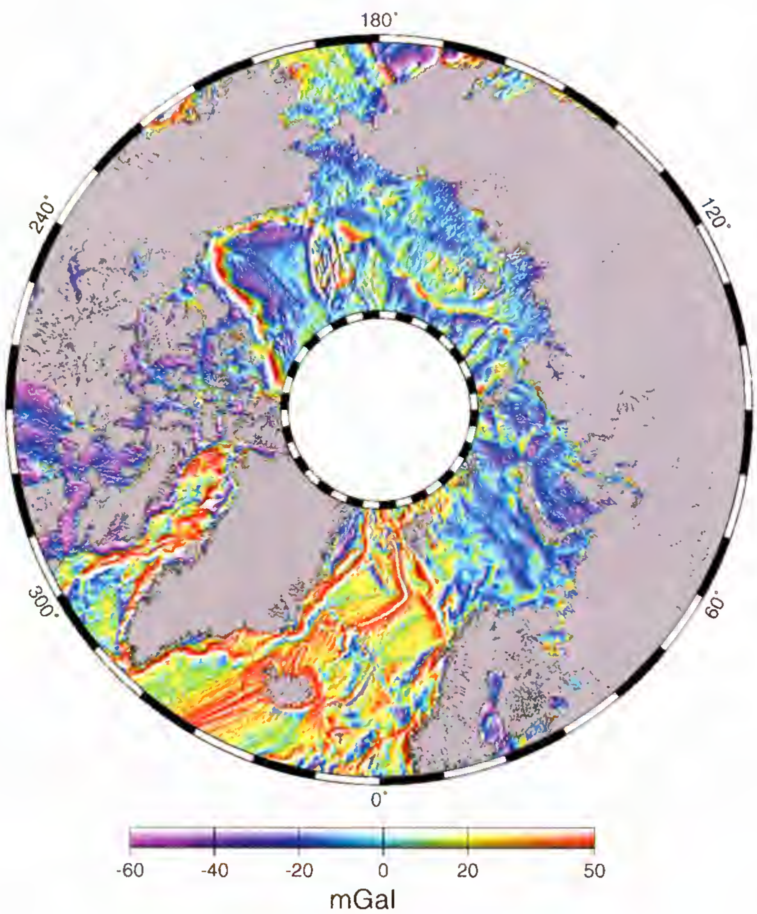

Figure 4.5 b: High resolution gravity field map of the Arctic.

significant errors to the retracked surface heights.

The Envisat altimeter's design will largely overcome these two major sources of systematic error in the ERS data. The Envisat waveforms are recorded with a dynamic range of 16 bits, thereby overcoming problems with the ERS quantisation. Also the Envisat altimeter employs an OCOG tracking algorithm which will result in a much more stable tracking window position for sea ice returns. Since the range window is relatively stationary the impact of pulse blurring will be significantly reduced.

The Envisat system also offers the opportunity to better understand the nature of return echoes over sea ice areas which currently remain poorly understood. Comparison of the dual frequency returns over sea ice will provide the means to better understand the scattering mechanisms responsible for the specular sea ice returns. Waveform data obtained during burst mode will allow investigation of the coherence phenomenon frequently observed over sea ice.

4.6. Water Vapour

Water vapour plays a major role in the troposphere, but is still poorly represented in global atmospheric models (climate or prediction meteorological models). The main cause of this deficiency is the high variability of humidity in space (horizontally and vertically) and time, due to the interactions with dynamic processes (e.g. convection) and to condensation - evaporation processes at the sea surface as well as at all levels in the troposphere. However, recent progress in assimilation techniques has lead to an improvement in the quality of the meteorological models by making possible the assimilation of SSM/I integrated water contents *(Filiberti et al, 1994, 1998; Phalippou and Gérard, 1996)*. However, these models still have too rough a grid resolution to be able to represent small and mesoscale water vapour features.

The effect of water vapour on electromagnetic waves is a delay, ranging from 3 to 20 cm, varying with the region of the Earth (mainly latitudinal variation over the oceans). The rapid changes of water vapour at small to mesoscale (passing of a meteorological front, in particular) induce variations of several centimetres, which must be known to correctly interpret the altimeter path length at the mesoscale.For these reasons, altimeters have been supported by microwave radiometers since ERS-1. These instruments are simple (nadir viewing, two or three channels in the band 18 - 22 - 37 GHz), and provide the integrated water vapour content (or the path delay, which is nearly proportional to it) and an estimate of the integrated content of cloud water. Although the ERS-1/2 MWR is a two channel radiometer, *Eymard et al (1996)* and *Gérard and Eymard (1998)* have shown that water vapour and cloud liquid water contents are derived with an accuracy similar to the one obtained with the TOPEX/TMR (three channels) by *Keihm et al (1995)* and (5 channels between 18 and 37 GHz) (*Alishouse et al, 1991*, among others), by using the altimeter surface wind as an additional channel.

The Microwave radiometer on-board Envisat will have the same channels as the ERS-1/2 instruments (23.8 and 36.5 GHz), so this conclusion will certainly be valid. However, the combination of the MWR and RA-2 measurements could be improved by directly using the radar sigma-0 at the two frequencies 3.2 and 13.6 GHz. These two frequencies have very different behaviours both in the atmosphere (attenuation by liquid water and path delay due to water vapour), and at the sea surface (reflectivity from capillarity waves). The passive microwave signal from the surface is related to its emissivity, which is directly linked to the reflectivity. The use of RA-2 measurements will therefore improve the accuracy of determination of atmospheric contents, and in turn, the use of MWR data could possibly improve the accuracy of the surface wind and surface wave height, due to its sensitivity to the foam cover. The MWR derived products are therefore coupled with those of the altimeter (surface wind, wave height). In the future they should be jointly assimilated in numerical weather prediction models.

4.7. Ionosphere

The absorption of solar radiation leads to ionisation occuring in the upper atmosphere with ion and electron concentration that is highly variable with respect to location, height, day time and season. The ionosphere is dispersive so the propagation of electromagnetic waves is delayed by an amount that is frequency dependent. That means that travel time differences between ranges observed at different frequencies allow some electron content to be inferred. For a typical magnitude of the total electron content (TEC) the range correction for a Ku-band altimeter can be as large as 10-15 cm. The two-frequency design of the RA-2 of Envisat, operating at 13.575 and 3.2 GHz, is therefore an essential system feature for determining ionospheric corrections to a precision well above that of the other error sources. TOPEX, the first dual-frequency altimeter, has clearly demonstrated that ionospheric corrections can be obtained to an accuracy at the subcentimetre level (*Imel, 1994*).

Altimeter satellites without dual-frequency capabilities must rely on empirical models to predict the TEC. The Bent model (*Bent and Llewellyn, 1973*) has been used for ERS-1/2. Recently, the International Reference Ionosphere (IRI) (*Bilitza et al. 1993*), with the latest version IRI95, has been used instead for the reprocessing of past missions such as GEOSAT. However, both the Bent and IRI are global models that are known to have errors as large as fifty percent of the signal, because they cannot account for the highly variable ionospheric conditions. Comparisons between the Bent model correction and the TOPEX dual-frequency correction exhibit systematic geographically-distributed patterns with up to 4 cm differences, changing their sign within a narrow band along the geomagnetic equator. These differences can be attributed to errors in the Bent model. If such errors cannot be removed they corrupt the sea level determination and its interpretation. In order to establish a long-term consistent time series of altimeter missions - a basic requirement for investigating the sea level rise - the ionospheric correction for single-frequency altimeters (GEOSAT, ERS-1, ERS-2, GFO) must be improved.

Other dual-frequency point positioning and orbit determination systems like GPS, GLONASS, DORIS and PRARE have been used in many investigations to demonstrate their capability for monitoring the highly variable ionosphere (even by means of slant measurements). DORIS (operating at 2.036 and 0.401 GHz) with its numerous and homogeneously distributed ground beacons was the first of these systems that were used to derive TEC estimates on a global scale (*Escudier et al, 1991*). With the launch of TOPEX/Poseidon the combined Bent/DORIS ionospheric corrections have been made operational and serve for TOPEX as a backup to the dual-frequency correction and as the primary source for the ionospheric correction to the Poseidon single-frequency altimeter. It also happens that the wavelength spectra of the DORIS and TOPEX derived corrections do not have the same content, which enriches knowledge of the correction itself. Also, an identified stable bias between the two corrections may prove very informative for in depth studies on the DORIS and TOPEX instruments themselves, especially in terms of TOPEX C-band calibration. Being more than just a backup to TOPEX, DORIS data have posed new questions which would not otherwise have been raised. The same configuration on Envisat (DORIS + dual frequency altimeter) holds the promise for the evaluation of both systems in terms of TEC recovery. Moreover, on a routine basis they can be compared with the hourly maps of the vertical TEC based on GPS measurements (performed at frequencies of 1.575 and 1.228 GHz) which are incorporated into regional or global services (*Jakowski, 1992, Melbourne, 1997, Mannucci et al, 1998*).

Although the second frequency of the Envisat altimeter was designed to serve the RA-2 sensor itself, it might be of specific interest to use the altimetric two-frequency measurements to complete or complement such a regular and systematic monitoring of the ionosphere. The space-time sampling of the altimeter alone is not sufficient for such monitoring. The particular advantages of the RA-2 estimates of TEC are, the fact that the two frequencies are well separated (which implies the capability for a precise recovery of TEC) and that, through the nadir looking altimeter there is no need to apply a mapping function to transform slant TEC observation to vertical estimates. The altimeter derived TEC values can thus contribute to a global tomography of the ionosphere with higher precision and without any assumption about the structure of ionospheric layers.

4.8. New Scientific Opportunities

Precipitation

Global oceanic precipitation is one of the most needed but least known geophysical parameters. This results from the fact that, on the one hand, rain plays a vital role in air-sea interaction via freshwater fluxes and in the general circulation of the atmosphere, as well as in the global hydrological and geochemical cycles; on the other hand, continuous and accurate measurement of rain over the global ocean is lacking, because of its complex nature in time, space and intensity.

A new field of altimetric application, to provide rain estimates over the ocean, has recently been suggested for the TOPEX/POSEIDON altimeter (*Chen et al., 1996*) in which the dual frequency radar altimeter, combined with the three-frequency microwave radiometers, offers the opportunity to detect oceanic rainfall. The presence of rain along the sub-satellite track can significantly degrade the altimeter measurements, causing an attenuation of the backscattered signals; a change in its path delay, and a change in the surface roughness (*Chapron and Tournadre, 1998*). Moreover, rain attenuation at Ku-band is an order of magnitude larger than at C-band. In the study, a joint TOPEX/TMR rain probability index is proposed derived from a one year data record. The index is based on a simple detection of simultaneous departure from the normal C-Ku band backscatter relationship, together with an account of liquid water vapor content as estimated from the TOPEX Microwave Radiometer (TMR).

The resulting rain frequency statistics show quantitative agreement with those obtained from COADS in the Intertropical Convergence Zone, while qualitative agreement is found for other regions of the world ocean. These results therefore suggest that coincident dual frequency radar altimeter and radiometer observations can complement the Special Sensor Microwave/Imager (SSM/I) and the joint Tropical Rainfall Measurement Mission (TRMM) in observing global oceanic precipitation. The relatively fine resolution of the combined altimeter/microwave observations also allows the rain cell characteristics (size, rain rate) to be examined and described from the waveform data under various weather conditions.

Although the dual-frequency Envisat RA-2 altimeter is slightly shifted in frequency from that of TOPEX (i.e. 13.75 GHz and 3.2 GHz compared with 13.6 GHz and 5.3 GHz) and the microwave radiometer only operates at two frequencies (23.8 GHz and 36.5 GHz), it is tempting to apply the same methodology for the Envisat RA-2/MWR to gain information on oceanic rainfall.

Sea Ice

Sea ice models form an important component of the coupled climate models which are being used for the investigation of large scale and long term climate problems. To properly represent the role of sea ice in the climate system these models must account for both thermodynamic and dynamic processes. The most important parameter for the discrimination between different dynamical parameterisations is sea ice thickness (OOSDP, 1995). Sea ice thickness is also a potentially important indicator of climate change, but the scarcity of thickness measurements, and high interannual variability [*McLaren et al., 1992*] leads to difficulty in identifying a trend [*Walsh, 1995*]. The measurement of sea ice thickness using satellite systems is frequently described as an unachievable goal. Current knowledge of sea ice thickness relies exclusively on surface or subsurface measurements and consequently our understanding of the regional, seasonal and interannual variation of ice thickness is extremely limited.

Recently developed techniques, using data from the ERS satellites, have demonstrated the potential of spaceborne radar altimetry to measure sea ice elevation and hence sea ice thickness [*Peacock et al., 1997*; *Peacock et al., 1998*]. The technique relies first on the accurate retrieval of sea surface elevation in ice covered seas, using complex procedures to deal with the unconventional radar echoes received when sea ice is present. Repeat measurements along the same ground track and consideration of radar backscatter theory indicate that the highly peaked returns normally observed over sea ice originate, for the most part, from areas of calm water or thin ice lying between ice floes. Hence such returns can be taken to represent measurements of instantaneous sea level in the polar oceans. A small fraction (~5%) of data are, however, diffuse in nature and comparisons with coincident imagery show that these occur when the altimeter footprint is entirely filled with consolidated ice. By differencing the ice and sea surface elevation measurements, an estimate of sea ice freeboard can be obtained. Ice thickness is then calculated using a ratio between freeboard and draft, obtained using both empirical measurements and theoretical models. Although some uncertainties still exist comparisons of monthly mean ice thickness in the Fram Strait with that from moored upward looking sonars show that the accuracy of altimeter estimates of ice thickness is in the region of ~0.5 m.

The Envisat RA-2 will provide an important role in extending the time series of sea ice thickness into the next century. This will provide a unique dataset, both for the sea ice modelling community and for studying the impact of global climate change on sea ice thickness. It is

Figure 4.6: Illustration of instrument coverage overlap for a descending track

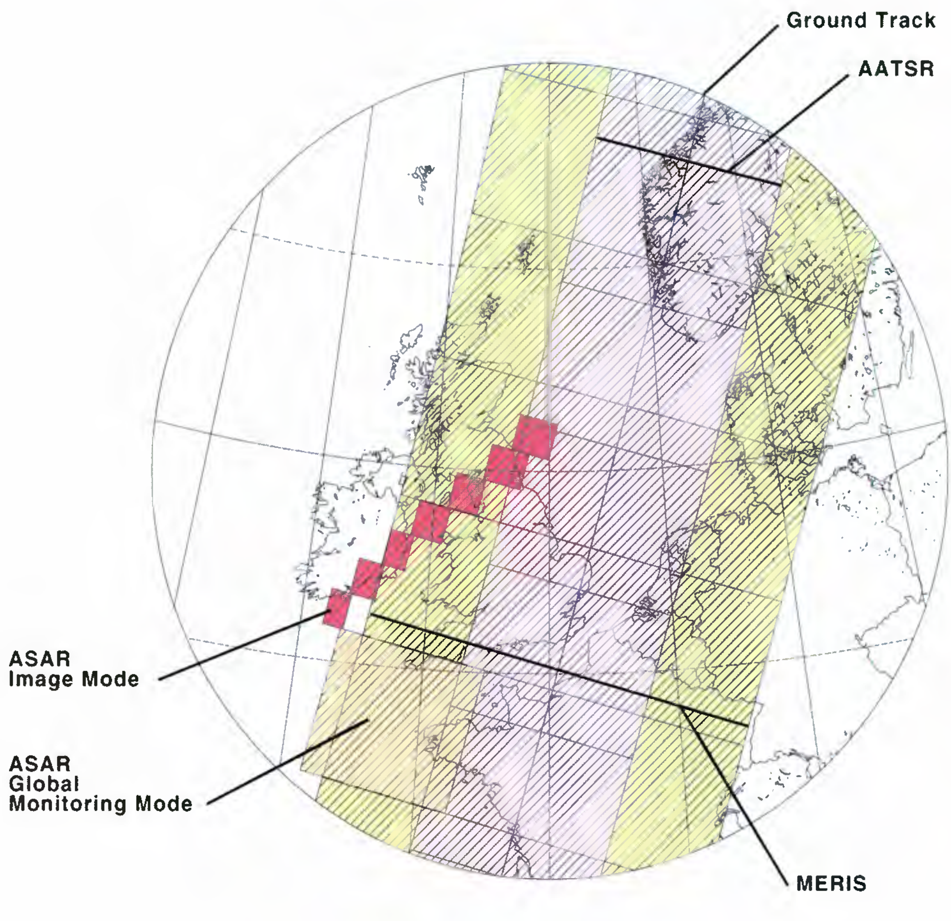

anticipated that the design of the RA-2 will provide significant improvements in sea ice freeboard determination over that provided by the ERS altimeters. The onboard tracking system will provide a much more stable record of the peaked echoes which dominate in ice covered seas. The improved SNR and two additional gates at the centre of the range window will enhance the accuracy of surface elevation determination. The provision of dual frequency data at high latitude and the opportunity to collect 'burst' mode data will provide important insights into the origin of radar echoes in ice covered seas. Finally the time scale of the Envisat mission (2000-2005) will provide a unique opportunity to compare its radar measurements with those from the spaceborne laser system (GLAS) due for launch in 2001.

4.9. Synergy

In view of the number of instruments on the Envisat platform, the opportunities for coincident and non-coincident synergy are very good because several different types of observation are available of the same place at the same or at different times (Figure 4.6). These include for example:

- coincident synergy such as from RA-2/MWR and AATSR, and RA-2/MWR and MERIS; this could for example be used to study phenomena with characteristic sea surface temperature, surface colour and surface topography signatures,
- synergy with a time-delay such as from RA-2/MWR and ASAR.

Disciplines	Geophysical Quantity	Contribution From Other Envisat Sensors	Contribution From RA-2/ MWR-2
Atmosphere	Clouds Water vapour content Radiative fluxes (TOA) Temperature Trace gases Aerosols Precipitation	MERIS GOMOS-MIPAS-SCIAMACHY (G-M-S) G-M-S MERIS	 MWR-2 RA-2/MWR-2
Land	Surface temperature Vegetation characteristics Surface elevation	AATSR ASAR, MERIS ASAR	 RA-2
Ocean	Colour Sea surface temperature Sea level topography Mean sea level Turbidity Waves Wind	MERIS AATSR MERIS (ASAR) ASAR ASAR	 RA-2 RA-2 RA-2 RA-2
Ice/Snow	Extent Snow cover Topography/elevation Surface temperature	ASAR ASAR ASAR AATSR	 RA-2
Gravity	Marine gravity anomalies		RA-2

Table 4.1: Relationship between Envisat mission objectives and geophysical parameters.

A more comprehensive overview of the Envisat mission objectives and the associated instrument contributions, including highlights of the RA-2/MWR-2 prime and secondary contributions, is given in Table 4.1.

Specifically, the coincident observations of ocean topography and sea surface temperature variation enhance the opportunity to derive precise descriptions of oceanic features such as mesoscale eddies, warm and cold Gulf Stream rings, and slowly propagating Rossby waves. With the combination of ocean colour studies, ocean topography and sea surface temperature, sea surface chlorophyll and biomass distribution can be undertaken.

Non-coincident, time-delay, synergy does appear feasible and attractive, with the possibility of combining interferometry from ASAR with topography and elevation maps derived from altimetry.

4.10. Relation to Other Programmes

The Intergovernmental Panel on Climate Change

The Intergovernmental Panel on Climate Change (IPCC) was established under the auspices of the United Nations to advise governments on the state of knowledge on climate change and its implications. It has prepared several assessment reports but here specific mention is made of the need for further work in the following areas:

- estimation of future emissions and biogeochemical cycling (including sources and sinks) of greenhouse gases, aerosols and aerosol precursors, and projections of future concentrations and radiative properties

- representation of climate processes in models, especially feedback associated with clouds, oceans, sea ice and vegetation, in order to improve projections of rates and regional patterns of climate change

- systematic collection of long-term instrumental and proxy observations of climate system variables (e.g. solar output, atmospheric energy balance components, hydrological cycles, ocean characteristics and ecosystem changes) for the purpose of model testing, assessment of temporal and regional variability and for detection and attribution studies.

The World Climate Research Programme

The World Climate Research Programme (WCRP) forms part of the World Climate Programme (WCP) and was established to provide a mechanism for the international coordination of global climate research. Its overall goal is to develop a fundamental understanding of the global climate system in order to determine the extent to which climate may be predicted on all scales of space and time and to determine the nature of those climate changes due to human activities.

The WCRP's programmes are concerned with research into the behaviour of the atmosphere, ocean, sea-ice and land-surface as interacting components of the physical climate system. The present WCRP projects comprise the Global Energy and Water Cycle Experiment (GEWEX), the World Ocean Circulation Experiment (WOCE), the Arctic Climate System Study (ACSYS), the study of Stratospheric Processes and their Role in Climate (SPARC) and the Climate Variability and Predictability (CLIVAR) Study.

The International Geosphere Biosphere Programme

The International Geosphere Biosphere Programme (IGBP) is intended to advance understanding of the interacting physical, chemical and biological processes regulating the Earth system and the environment it provides for life, as well as to monitor and study the changes that are occurring in this system - including the effects of human activities. Emphasis is placed on global change processes, occurring on timescales from a decade to a century, which are sensitive to human perturbations. The programme has close links with the Human Dimensions of Global Change Programme (HDP).

Some critical gaps have been identified in the understanding of global biogeochemical cycles and life support processes. To address these, seven Core Projects have been established, namely the International Atmospheric Chemistry Project (IGAC), the Global Change and Terrestrial Ecosystems (GCTE), the Biospheric Aspects of the Hydrological Cycle (BAHC), the Land-Ocean Interactions in the Coastal Zone (LOICZ), the Joint Global Ocean Flux Study (JGOFS), the Past Global Changes (PAGES) and the Land Use and Land Cover Change (LUCC) project.

It is also relevant to note that in support of these seven Core Projects there are three additional activities of an integrative nature, namely the Task Force on Global Analysis, Interpretation and Modelling (GAIM), the Global Change System for Analysis, Research and Training (START) and the Data and Information System (IGBP-DIS). The last illustrates the importance the IGBP attaches to effective data acquisition and management.

Sources of Data
All the international programmes considered above assume the provision of data from many sources. They accept that in many instances, in addition to the data provided by space-based systems, data from ground-based systems or the outputs of numerical models will have a vital role to play, partly in providing complementary sources of data and partly in helping to validate the performance of other systems.

International Observing Systems. The most well established of the operating observing systems is without doubt the World Weather Watch (WWW). Another prominent, though less established, system is the Global Oceans Observing System (GOOS). These systems address the need for the regular provision of key meteorological and oceanographic data for operational purposes.

Closely linked to GOOS is the Global Climate Observing System (GCOS) which was established to meet the needs for climate monitoring and climate change detection. These data are intended to find application to national economic development planning as well as contributing to research towards improvements in the understanding, modelling and prediction of the climate system. In the GCOS space plan, seven GCOS 'missions' are identified of which two are directly relevant to the ocean and the Envisat mission, namely ocean characteristics and the ocean-atmosphere boundary.

Numerical Models. The other source of data which is assuming increasing importance is the output of numerical models. These can assimilate data from a multiple of sources (space- as well as ground-based), optimising the synergistic use of these data, and providing a systematic means for data handling and quality control. The latter includes, not only the intercomparison of data from different sources, but also the validation of data against model predictions. Conversely the satellite observations such as those from Envisat RA-2 can help validate and improve the modelling of Earth system processes, leading to improvements in model performance.

Future Gravity Field Missions. In the absence of a sufficiently accurate geoid, altimetry measurements will refer to an unknown mean reference surface. However we are at the dawn of a new era in satellite gravity field missions, in which three missions, i.e. CHAMP (German satellite mission), GRACE (joint US-German satellite mission) and GOCE (ESA Earth Explorer mission) will possibly be realised within the next 5-8 years.

CHAMP is based on a satellite to satellite (high-low) tracking concept and aims at improving our knowledge of the global gravity field in a homogeneous way, by factors of two in resolution and of 5 to 10 in precision (depending on the resolution). It will fullfill an intermediate goal of the geodetic and geophysical community in a relatively simple manner at low cost (*Reigber et al, 1996*). It is scheduled to be launched in mid 1999.

GRACE is based on a satellite to satellite (low-low combined with high-low) tracking concept and aims at monitoring time variations, from monthly to annual (even interannual) of the long wavelength part of the gravity field up to spherical harmonics degree and order 90 (i.e. a half wavelength of 450 km) (*NRC, 1997*). If it completes its planned four to five year mission lifetime it should also yield a very good stationary gravity field up to this scale. It is tentatively scheduled for launch in 2001.

The GOCE mission is based on an electrostatic gradiometer instrument, combined with high-low satellite-to satellite tracking system. It aims to measure and provide the most accurate, global and high resolution snapshot of the gravity field and its corresponding geoid surface, up to degree and order 200 (i.e. half wavelength of 100 km) from an altitude of about 250 km (*ESA SP-1196/1, Balmino et al, 1998*). Its mission lifetime will be about 20 months, with two operating windows of 7 months. If selected its launch is foreseen for 2003-2004.

5. Operational Applications

The ground segment of the Envisat mission has been designed to accommodate real-time operational monitoring. There are a variety of operational applications which can utilise measurements from the RA-2 system. Significant wave height and wind speed are routinely used by international weather centres. These data are made available within a few hours of satellite acquisition and are mostly independent of the quality of the satellite orbit determination. Sea level estimates from altimetry, on the other hand, are directly tied to the accuracy of the satellite orbit. Ocean mesoscale monitoring, covering spatial scales of hundreds of km and less, can be conducted in near real-time (1-2 days) with preliminary orbits accurate to within tens of cm. Large scale monitoring, on 1000 km spatial scales and seasonal to inter-annual time scales, requires precise orbits with less than 10 cm orbit error. These applications require the near-final quality data sets, expected to be available several weeks after the data are acquired. The suite of altimeter products (discussed in Chapter 2), has been designed with this hierarchy of timeliness and precision demands in mind. The following sections discuss the operational applications for wind and wave, ocean mesoscale and ocean large-scale monitoring and forecasting.

5.1. Sea State (Wind and Waves)

In addition to information on the sea levels, the radar altimeter provides a measure of wind speed through the backscattered energy and a measure of the significant wave height through the distortion of the mean shape of the return pulse. The earlier return from the wave crests and the delayed return from the wave troughs lead to a broadening of the return pulse which can be directly related to the significant wave height. In order to determine the mean pulse shape, several hundred pulses need to be averaged, giving one wave height measurement about every 7 km along the satellite track. For a Gaussian sea surface, the relation between pulse shape and the rms sea surface displacement can be computed theoretically. This model, which ignores deviations from Gaussianity, has been confirmed by numerous comparisons with *in-situ* measurements, although large wave heights tend to be underestimated by the altimeter by as much as 10% (*Goodberlet et al, 1992, Günther et al, 1993, Carter et al, 1992*).

The availability of wave height data from the radar altimeter has provided a strong influence on wave modelling and has also stimulated the development of wave height assimilation techniques. One of the principal motivations for developing the third generation wave model WAM (*Komen et al, 1994*) was to provide a

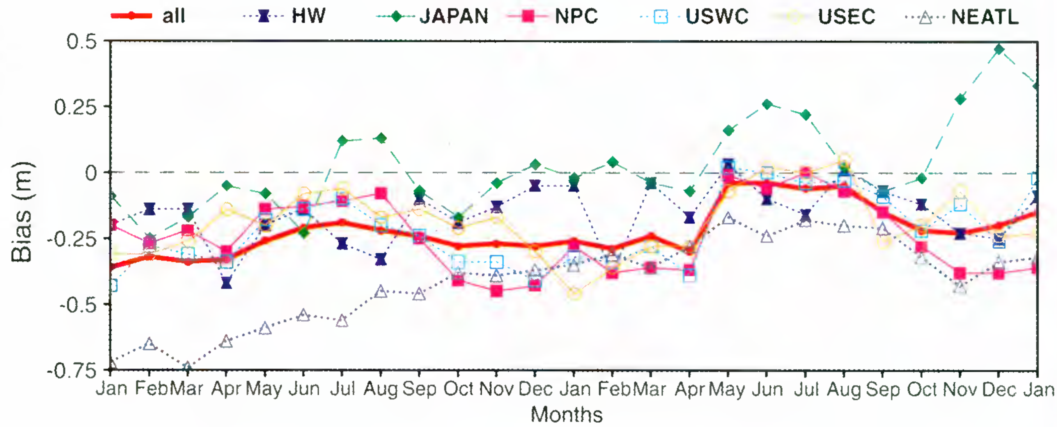

Figure 5.1: Plots of the mean difference between waveheight bias (ECMWF analysis) and buoy wave height at different locations as a function of time.

state-of-the art model for the assimilation of global wind and wave data from satellites for improved wind and wave field analysis and forecasting. Presently, the WAM model is in use at a number of forecasting centres (e.g. NCEP, FNMOC, BMRC, and ECMWF) and altimeter wave height data are assimilated at MeteoFrance, KNMI, DNMI, UKMO and ECMWF.

Since the quality of the wave analysis nowadays depends to a certain extent on the altimeter data, it is important to have high quality altimeter wave height data. By doubling the pulse power the quality of the ERS-2 altimeter data has been improved compared to the ERS-1 wave height data. This follows from verification of the altimeter product against buoy data. The improved quality of the ERS-2 altimeter data has resulted in a better wave analysis. This follows from a comparison of the wave analysis with buoy data. Figure 5.1 shows the mean difference between ECMWF analysed wave height and buoy wave height at different locations as a function of time. Before May 1996 there was a bias in wave height of about 25 cm, but when in April 1996 ECMWF switched from ERS-1 to ERS-2 data the bias reduced markedly. A similar improvement was noted in the UKMO wave product. The improved altimeter product from ERS-2 also resulted in better wave forecasts. This is shown in Figure 5.2 which contains plots of Day 1, Day 3, Day 5, Day 7 and Day 10 forecast error as functions of time over the period May 1995 to July 1996, for the tropics. Over the chosen period, a clear reduction in forecast error is seen at the end of January 1996 and the end of

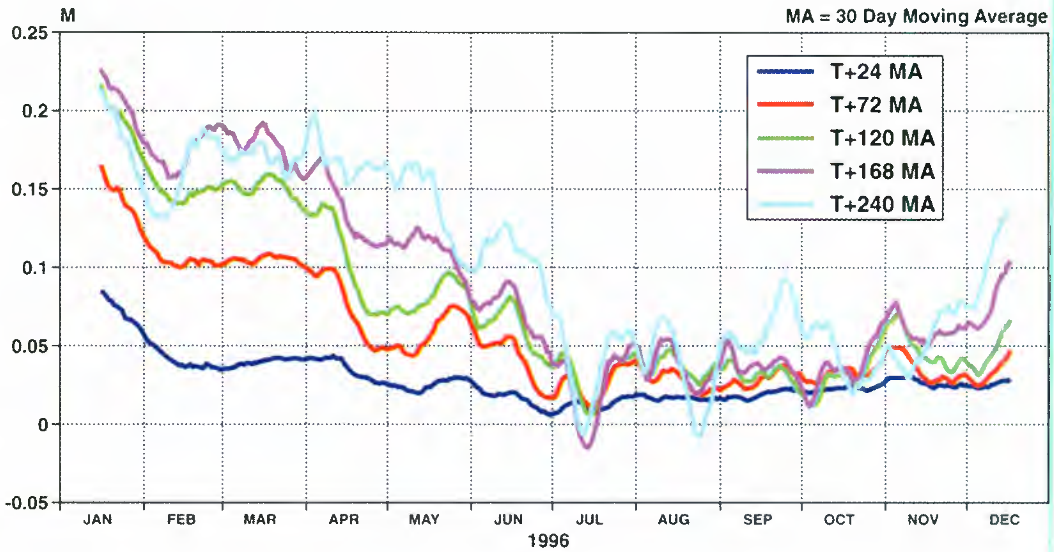

Figure 5.2: Plots of day 1, day 3, day 5, day 7 and day 10 forecast errors as function of time over the period May 1995 to July 1996 for the Tropics.

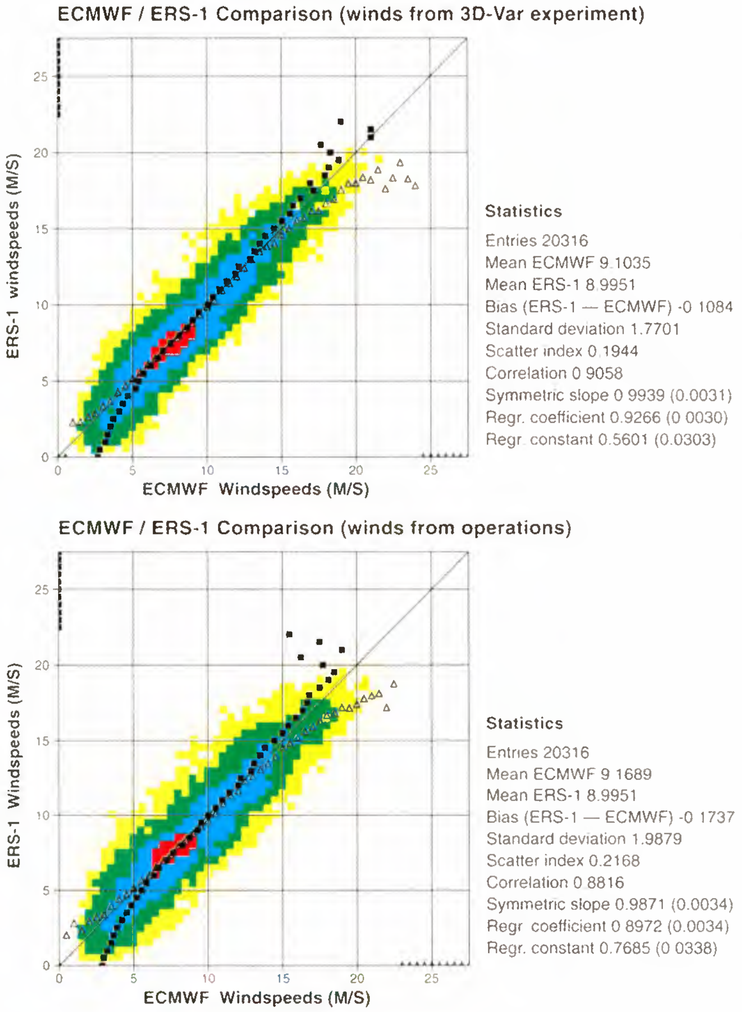

Figure 5.3: Scatterplots regarding the usefulness of scatterometer data in ECMWF's analysis system. The positive impact of the use of scatterometer data in data assimilation is shown on the southern hemisphere wind fields, resulting in a reduction in the standard deviation of error from 1.99 to 1.77 m/s.

April 1996. The later date corresponds to the introduction of ERS-2 data in the wave assimilation system, while the earlier date corresponds to a switch at ECMWF from the optimal interpolation (OI) assimilation scheme to the Variational approach when ECMWF started using ERS-1 scatterometer data.

The need for accurate altimeter products is evident, and the dual frequency radar altimeter onboard Envisat is expected to give further improvements, so that a more accurate determination of the waveform will be possible. This allows deviations from a Gaussian distribution of the 2-dimensional surface wave field to be inferred, which are important for young wind seas. In turn a more accurate determination of wave height is to be expected.

As already pointed out, a measure of wind speed may be derived from the backscattered energy. At UKMO the altimeter wind speeds are used in the wave data assimilation scheme, while at ECMWF this is not done because wave heights depend in a sensitive manner on wind speed (a 10% error in wind speed would give rise to a 20% error in wind sea wave height). One could also consider the direct assimilation of wind speed data in an atmospheric model, but so far this has not been done. Rather than pursuing this approach, ECMWF uses the altimeter wind speed data to monitor the quality of the analysed surface wind speed. This is very useful in particular when the impacts of changes in the assimilation scheme or the model have to be assessed. An example is given in Figure 5.3 which is derived from extensive investigations at ECMWF regarding the usefulness of scatterometer data in ECMWF's analysis system. The positive impact of the use of scatterometer data in data assimilation is shown on the southern hemisphere wind fields, resulting in a reduction in the standard deviation of error from 1.99 to 1.77 m/s. The importance of the radar altimeter wind speeds is therefore also quite evident in this case.

The radar altimeter wind and wave data are also potentially useful in the context of monitoring changes in the wind and wave climate. In particular the wave height field depends in a sensitive manner on the forcing wind field, and changes in the wave climate therefore provide an indicator for changes in the atmospheric climate. The long time series recorded in the northern Atlantic by the Seven Stones light vessel allowed the determination of a statistically significant increase of the wave height of about 30% over a 30 year period (*Bacon and Carter 1991*). These valuable but very expensive measurements were not continued, partly due to the cost and partly because of the possibility of satellites providing the same data.

The altimeter data provided by Geosat, TOPEX-POSEIDON, ERS-1, ERS-2 and GFO as well as Envisat and Jason will make valuable contributions to the monitoring of these wave climate changes. However, it is then of considerable importance to ensure a continuous and uniform data set. As well as cross calibration between successive satellites during periods of overlap, this can be achieved either by using buoy observations as a "go-between", as is done at the James Rennell Centre by comparison with long term running wave model products, as is done at ECMWF.

5.2. Ocean Forecasting

5.2.1 Mesoscale

The oceanographic mesoscale is comprised of highly energetic features, including western boundary currents and their eddy fields. Routine monitoring of strong current features provides extremely valuable information to fishermen, pleasure sailors, merchant ship crews and oil-platform operators. To satisfy these users needs, the timeliness of data delivery is paramount; daily updates are essential. Radar altimetry is able to meet this need by utilising either predicted orbits (as is now done with ERS-2), or on-board generated orbits. The DORIS "DIODE" orbit determination system on-board Envisat will provide sufficiently accurate orbits, in real time, to satisfy mesoscale monitoring requirements. Even if orbit errors reach the one metre level, short-arc error removal techniques can be used when processing the height data for mesoscale analyses.

Mesoscale monitoring has been successfully demonstrated with ERS-2 data in the Gulf of Mexico and Gulf Stream current system, and in the North Atlantic Azores front region. Figure 5.4 shows an example of sea surface topography in the Gulf of Mexico, overlaid on a map of sea surface temperature. The Gulf of Mexico Loop current, which flows into the Gulf from the Caribbean and exits into the Gulf Stream south of Florida, appears as a high temperature jet in the southeast. A large cyclonic eddy which has just pinched off the current is seen to the northwest of the main current. The contours of surface topography correlate very well with the temperature field. The high-gradient regions in the contours, indicating large geostrophic currents, follow the path of the current observed in the surface temperature field. The benefit of real-time monitoring from altimetry is that the radar is an all-weather, all-season instrument. By contrast, images of

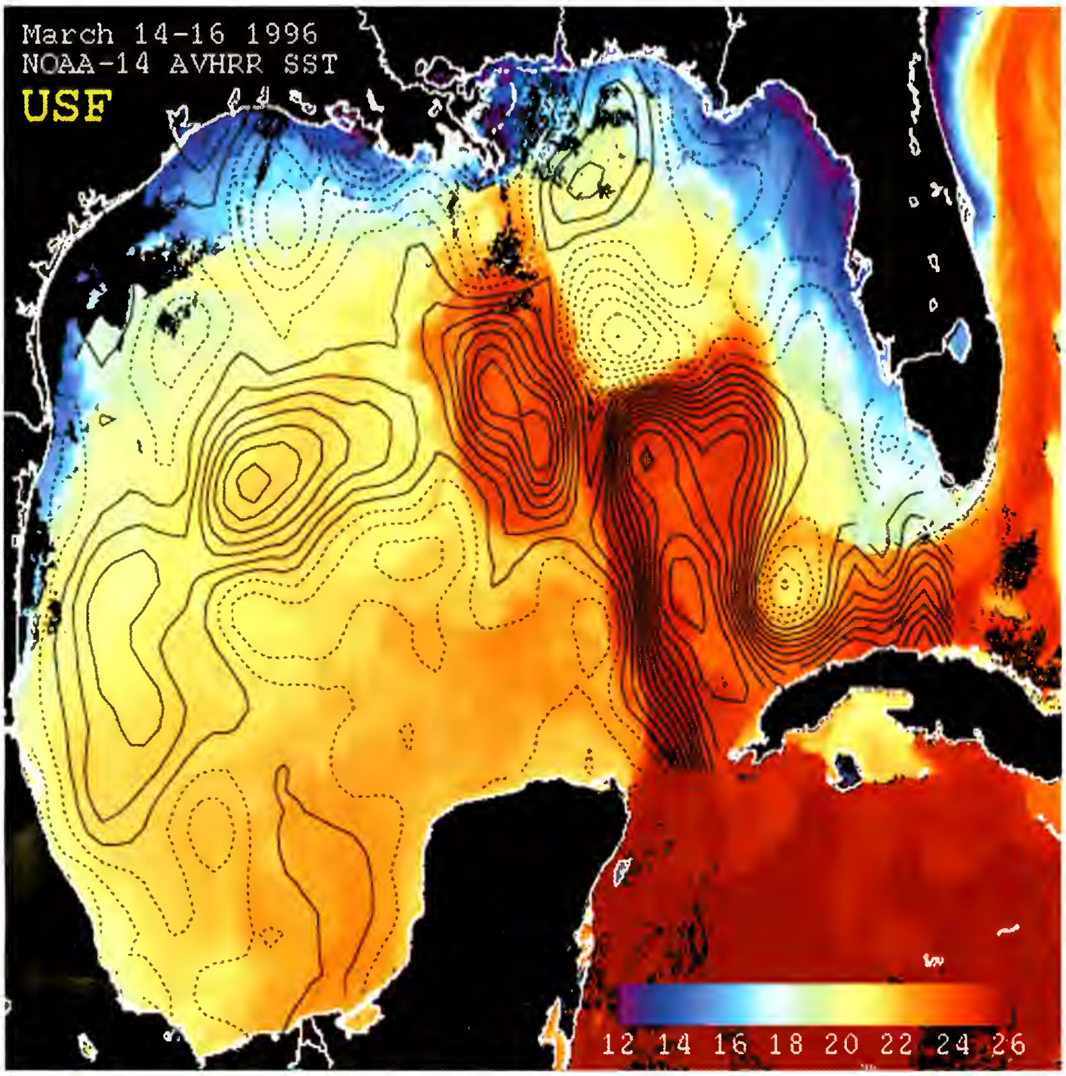

Figure 5.4: Example of sea surface topography in the Gulf of Mexico (contours) derived from the ERS altimeter overlaid on a map of sea surface temperature from the NOAA AVHRR. Colour scale is indicated in lower right corner. (Courtesy of Univ. of Colorado/Univ. of South Florida).

sea surface temperature in the Gulf are often hampered by cloud cover. Furthermore, in summer a warm surface layer develops which hides the underlying temperature structure, making it difficult to identify the strength and location of the Loop current and its eddies.

Since 1991, the Service Hydrographique et Océanographique de la Marine (SHOM) (French Navy) has been conducting a long-term program - called SOAP - aiming at developing Operational Oceanography for mesoscale applications. The program started in 1991 with the SOAP93 project, taking advantage of the availability of TOPEX/POSEIDON and ERS-1 altimeter data for the following years. SOAP93 was a demonstration system, implemented near the Azores front region. The model was a 1/8° quasi-geostrophic, open boundary, regional model assimilating altimetry with an optimal interpolation scheme. SOAP93 was operated for the first time in October 1993 during the Semaphore experiment, and then continuously from 1994 to 1997 under near real time conditions (*Dombrowky et al., 1995*). The system was extremely useful for providing monitoring and prediction of the Azores front and its associated mesoscale variability. Comparison with *in-situ* data gathered during the Semaphore experiment demonstrated the quality of the system. The follow-on system, called SOPRANE, is implemented over a larger area (North-East Atlantic) and is currently assimilating TOPEX/POSEIDON and ERS-2 data.

Coastal models could also utilise altimetry to provide oceanic "boundary conditions" on the open ocean side of the model domain. Altimetry does not give highly accurate data near land, but the combination of a suitable model incorporating the altimetry would enhance coastal forecasting.

5.2.2 Large-scale

On basin to global scales, the primary operational application is climate monitoring and forecasting. This includes phenomena such as the El Niño/Southern Oscillation which is manifested in sea surface temperature and sea surface topography anomalies (Figures 5.5 a & b) which occur on seasonal to inter-annual time scales. For monitoring such large scales, the timeliness of the altimetric analyses can be relaxed to a few weeks. It is critical to have the most accurate orbit available in that time-frame. An accuracy of a few cm, in estimates of large-scale sea level change, is required for assimilation into coupled ocean/atmosphere models.

Until recently, operational models such as those run by the National Centres for Environmental Prediction (NCEP, formerly NMC) only assimilated thermal oceanographic data. Sea surface temperatures from satellites and buoys, plus subsurface temperatures from XBTs and moorings, were used in the ocean model. At the end of 1996, NCEP began assimilating TOPEX altimeter data into their model on an operational basis. The sea level heights from altimetry have been shown to increase the forecasting skill of the model, particularly when salinity changes (in contrast to temperature) effect a large-scale change in sea level. When

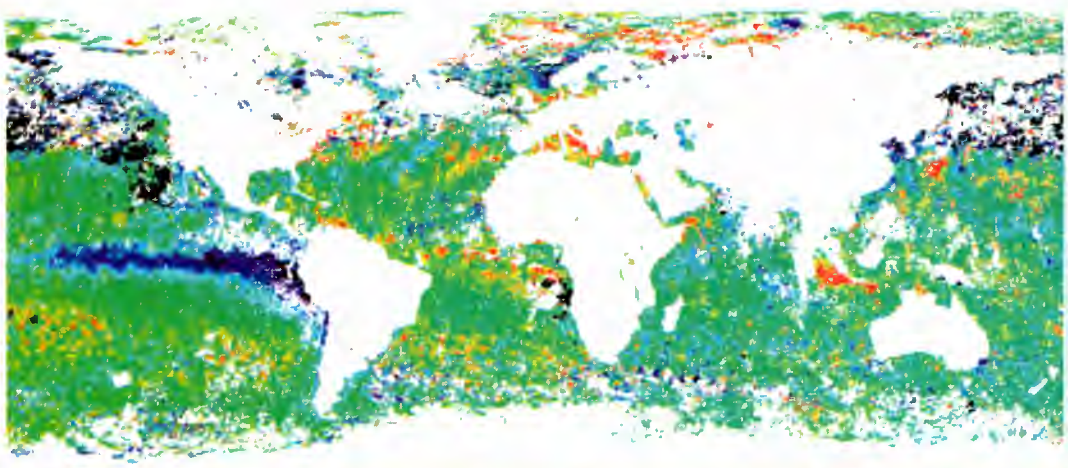

Figure 5.5 a: Sea surface temperature anomaly (> 4° C in blue colour) of the 1997 El Niño derived from the monthly mean ERS Along Track Scanning Radiometer (ATSR) observations of July 1995 subtracted from July 1997 (Acknowledgement ESA-ESRIN)

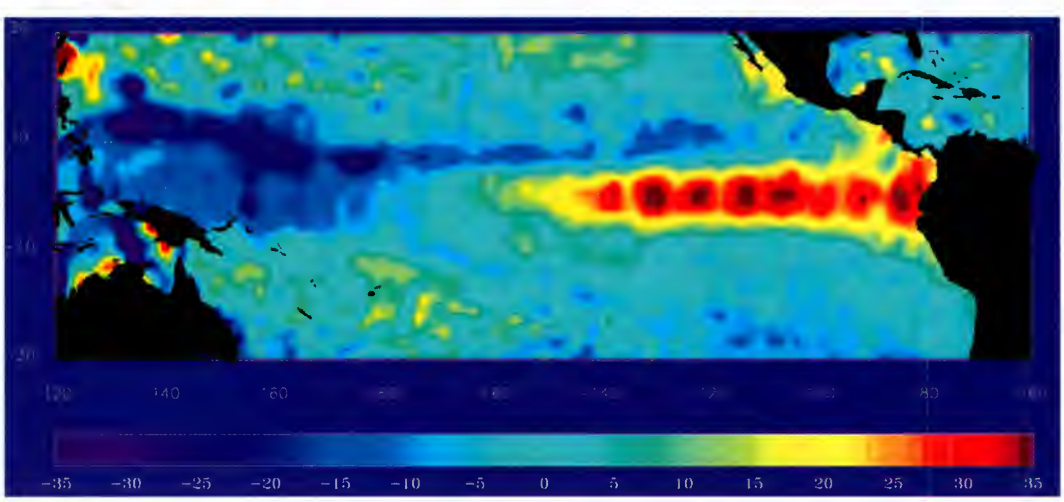

Figure 5.5 b: Sea surface topography anomaly (red-to-yellow colours) of the 1997 El Niño derived from the ERS Radar Altimeter (RA) (Acknowledgement: Delft Univ. of Technology/ ESA-ESRIN)

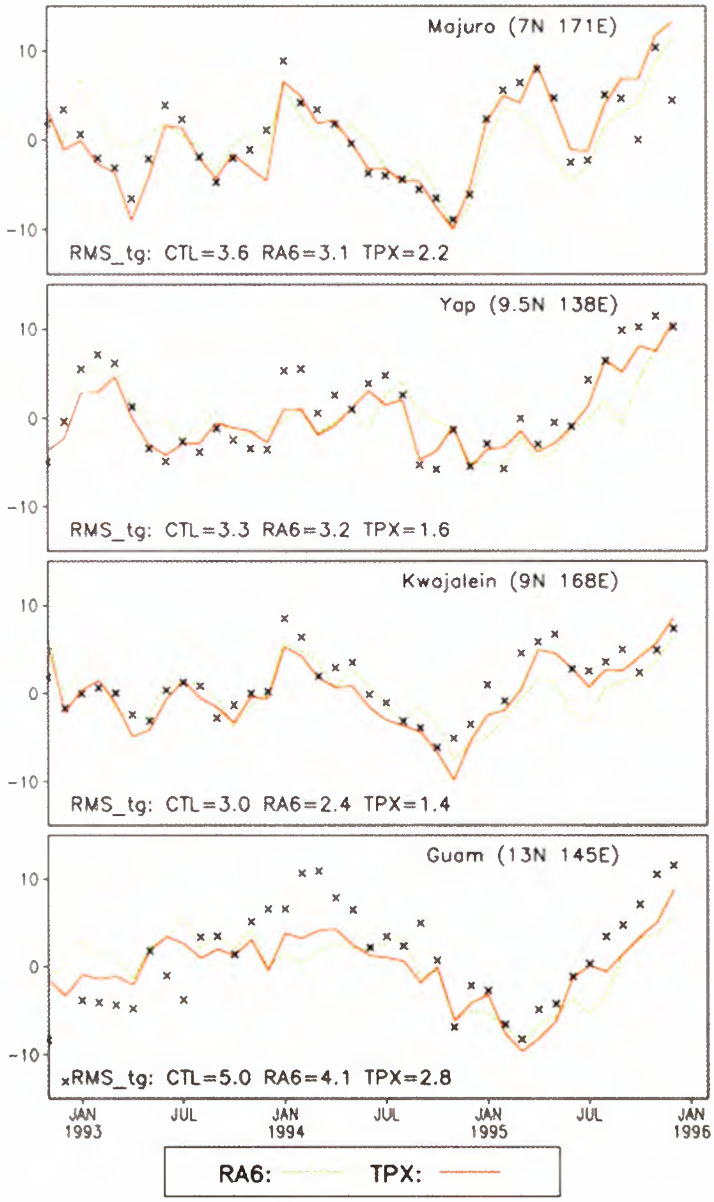

Figure 5.6: Example of the improvement in predicted sea level from the NCEP model. Model run "RA6" is without altimetry, while run "TPX" includes altimetric heights. RMS of fits between the tide gauge and model sea levels drop from 4.1 to 2.8 cm.

assimilating only thermal data, the model is not aware of the dynamical changes associated with these salinity variations (*Vossepoel et al., 1998*). An example of the improvement in predicted sea level from the NCEP model is show in Figure 5.6. The sea levels measured by four tropical Pacific tide gauges are shown by the crosses. The dashed lines represent the coupled model prediction without altimetry, and the solid lines show the model output after assimilating the altimetry. At all locations the rms difference between the tide gauge and model sea level is reduced by about one cm (in 2-4 cm) by including the altimeter data.

Several other meteorological organisations, such as the European Centre for Medium-range Weather Forecasts (ECMWF) have plans to run coupled ocean/atmosphere models to monitor climatic variations such as El Niño. They too will ultimately assimilate altimetric sea level to improve their forecasting ability. Assimilation of ERS-2 and Geosat Follow-On data is planned for the NCEP model, with the hope of improving the models through the enhanced spatial resolution compared to the TOPEX data.

5.2.3 Global Data Assimilation

In the future, mesoscale and large scale monitoring could be extended to the global scale by assimilation of real time altimetry into high resolution ocean models. The goal of the MERCATOR project (*Courtier, 1997*) is to implement (within 5 to 7 years) a system which simulates the global ocean with a primitive equation high resolution (1/12 degree) model , which assimilates altimeter data, sea surface temperature (SST) data and *in-situ* data. The system will be used for scientific, military and commercial applications of oceanography. It will also contribute to the development of a climatic prediction system relying on a coupled ocean atmosphere model. MERCATOR is a contribution to the Global Ocean Data Assimilation Experiment (GODAE) which plans a pilot demonstration phase during the years 2003 - 2005 *(Smith and Lefebvre, 1997*). GODAE's objective is to demonstrate the practicality and feasibility of routine, real-time global ocean data assimilation and prediction. GODAE will emphasise integration of the remote (in particular altimetry) and in-situ data streams, and the use of models and data assimilation to draw maximum benefit from the observations.

5.3. Other Potential Applications

The operational applications of altimetry described above are perhaps the most obvious, but in the future other possible uses for the data will be explored. Some possibilities include:

- Estimates of "rain rate" on synoptic (atmospheric) scales by utilising Envisat's dual frequency altimeter measurements, in conjunction with the dual-frequency radiometer.
- Ice-edge detection based on waveform analysis from the radar pulse returns.
- Exploring the synergy of ocean current / surface wave interactions and their manifestation in the fundamental altimetric measurements of return backscatter power and waveform shape.
- Storm surge and tsunami "flood warning" forecasts, perhaps via assimilation of real time altimetry into barotropic ocean models. This interesting possibility is further addressed below.

Tsunamis are generated by submarine earthquakes. The sudden lift or drop of a part of the ocean bottom causes a corresponding modification, a bump or a trough respectively, at the ocean surface, that spreads around in the form of one or more tsunami waves. They are manifested as very long waves, the first one being the highest and most dangerous. Enhanced by the shoaling effect when reaching shallow water areas, they are a tremendous hazard for coastal regions.

Assuming an ocean depth of 4000 metres, tsunamis move with a speed of about 200 m/s, i.e. 720 km/h. With a period of ten minutes or more, this corresponds to wavelengths in excess of 100 km. The ERS-2 altimeter will provide one measurement per second at about 7 km intervals. Therefore a tsunami is characterised by more than 16 sequential data. The problem with the detectability of a tsunami is their limited height, less than 20 cm, often less than 10 cm far from the source as well as from the satellite coverage. This puts them within the range of the noise of the signal.

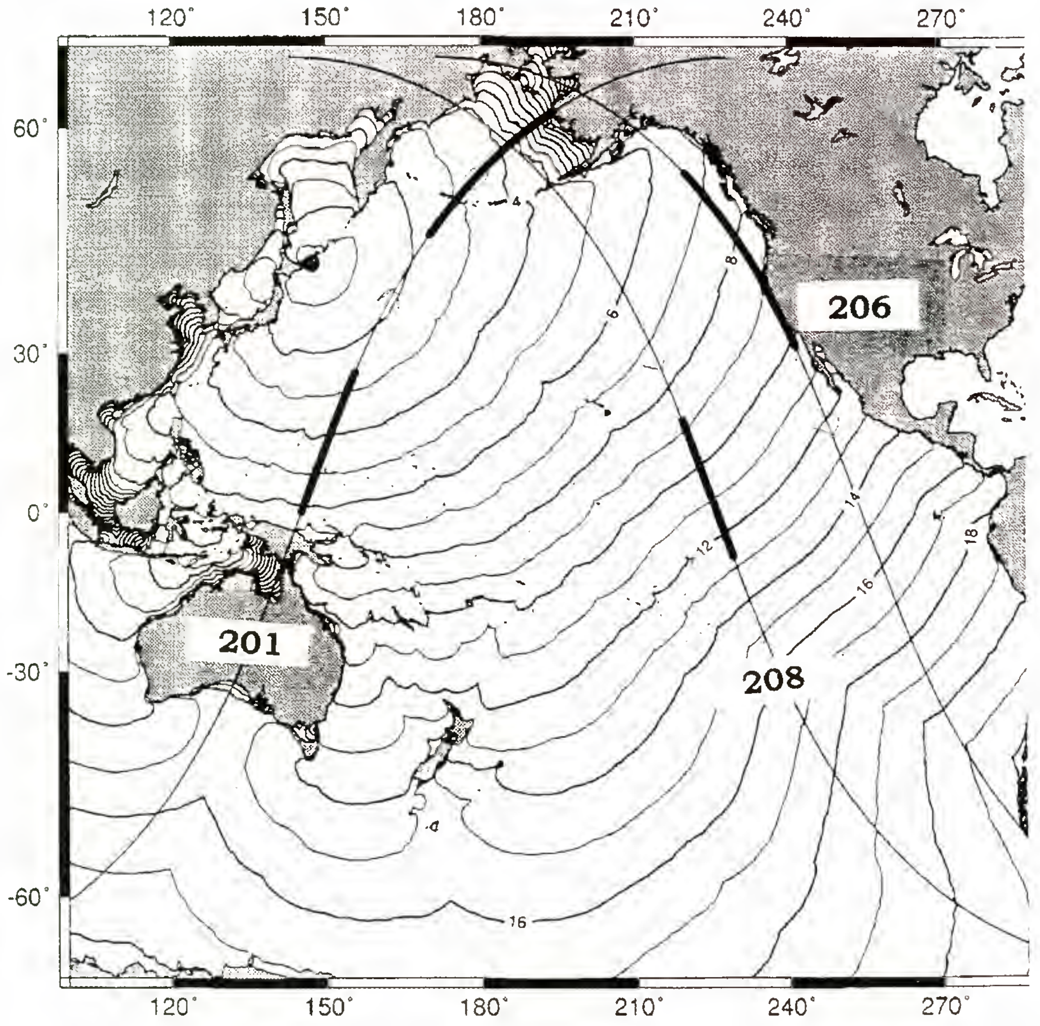

Figure 5.7: The propagation of a tsunami wave in the Pacific Ocean. The isolines show location at different times. The thickened part of the TOPEX/POSEIDON trajectories show where the ground tracks crossed the tsunami (after *Callahan and Daffer, 1994*).

Visual inspection of altimeter signals in correspondence to known earthquake events does not immediately reveal the presence of a tsunami, also because the wavelengths we are looking for are characteristic of other oceanographic phenomena. One way to bypass this problem is to rely on the different time scale of the tsunami (short) with respect to that (long) of the alternative possibilities. So, rather than studying the actual signal, it is convenient to analyse its difference with respect to the previous passes. Nevertheless, clear separation from the background noise requires special filtering techniques. Direct tests on synthetic data show that single waves are detectable in a background noise which has the same or even double the rms amplitude.

Figure 5.7 (from *Callaghan and Daffer, 1994*) shows the propagation in the Pacific Ocean of a tsunami wave which originated in the Kurili Islands at 13.23 UTC on 4 October. The isolines show its position at different times (hours elapsed from the earthquake). The three trajectories show the ground track of three passes of TOPEX/POSEIDON, crossing the tsunami at the thickened segments. The altimeter signal has been cleaned of the average of the previous six

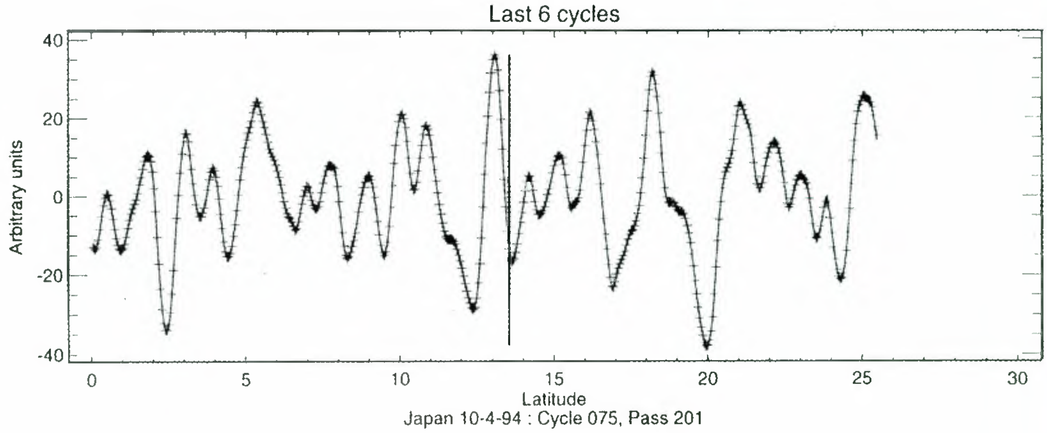

Figure 5.8: Correlation between the altimeter signal and a single sine wave of 150 km wavelength. The vertical line shows where track number 201 is expected to cross the tsunami. The peak close to it indicates the likely direction

passes and correlated with pure sine waves of different length. The best results, shown in Figure 5.8 for the segment north of Australia, have been obtained with the 150 km long sine wave, suggesting that a tsunami of similar length was in fact present there at the time of the overpass.

In general, the detection of a tsunami can be obscured by the presence of other signals of comparable magnitude, associated with various circulation phenomena. A detailed circulation model of the oceans, run in real time and making full use of the information derived from the previous passes, would provide full information on the expected surface profile. Starting from this, it could be possible to detect the presence of a tsunami wave on the ocean surface.

6. Concluding Remarks

This report has detailed the scientific research and applications based on the RA-2/MWR instrument system which will fly on the Envisat satellite, scheduled to be launched in the first half of 2000.

The principal team of scientists behind the report are the members of the RA-2/MWR science advisory group, complemented with Agency staff. The team has consulted widely in the science and user communities.

First, the end-to-end description of the dual frequency RA-2 system and its mission elements highlights the new features of RA-2 (compared to the ERS altimeter) which are intended to enable better correction of errors introduced by ionospheric fluctuations and to measure echoes from the ocean, ice and land surfaces with improved accuracy and without interruption. This is followed by a thorough review of the main altimeter errors, their correction and corresponding measurement accuracies.

Subsequently the foundations for the multidisciplinary scientific objectives and the operational applications are described. These two sections build on the experience with current operating radar altimeter systems such as those on ERS, TOPEX/POSEIDON and Geosat-Follow-On, with a projection towards the future utilisation of the dual frequency RA-2 on Envisat.

RA-2/MWR guarantees the continuity of the ERS altimeter data, thereby ensuring a long-term data set. It will also complement the data provided by the TOPEX/POSEIDON mission, the GFO mission and Jason, by filling in many gaps in surface coverage. Practically all disciplines of interest within the Earth system, including the ocean, the cryosphere, the land, the atmosphere and the Earth gravity field are addressed in the context of scientific research, climate monitoring and operational marine sea state and ocean forecasting.

These multidisciplinary observations from the Envisat RA-2/MWR mission will, moreover, make a timely and fundamental contribution in the context of international research programmes such as the World Climate Research Programme (WCRP) and the International Geosphere Biosphere Programme (IGBP). These international programmes assume the provision of data from many sources, which in addition to the data provided by space-based systems, include data from ground-based systems or the outputs of numerical models.

The numerical models can furthermore assimilate data from multiple sources (space- as well as ground-based), optimising the synergistic use of the data, and providing a systematic means for data handling and quality control. The latter includes, not only the comparison of data from different sources, but also the validation of data against model predictions. Conversely the satellite observations, such as those from Envisat RA-2, can help validate and improve the modelling of Earth system processes and provide better intial fields and thus more reliable forecasts. During the Global Ocean Data Assimilation Experiment (GODAE) which will operate from 2003 to 2005, this will be fully demonstrated.

References

Alishouse J.C, S.A. Snyder, J. Vongsathorn and R.R. Ferraro, *Determination of oceanic total precipitable water from the SSM/I.* IEEE Trans. Geosci. Remote Sensing, 28, 811-816, 1990.

Bacon S. and D.J.T. Carter, *Wave climate changes in the North Atlantic and North Sea*, International Journal of Rem. Sens., 11, 545-558, 1991.

Balmino G, F. Perosanz, R. Rummel, N. Sneeuw, H. Sünkel and P. Woodworth, *European Views on dedicated Gravity Field Missions: GRACE and GOCE*, Earth Sciences Division Report Contract, No. 001, May, 1998.

Bent R.B and S.K. Llewellyn, *Documentation and Description of the Bent Ionospheric Model, AFCRL-TR-73-0657*, Space & Missiles Organization, Los Angeles, California, 1973.

Bilitza D, *International reference ionosphere - status 1995/96*. Adv. Space Res., accepted, 1997.

Brunje A.J.T, R. Haagmans and E.J. de Min, *A preliminary North sea geoid model GEONZ97*. MD-rap., MDGAP-9735, Delft, 1997.

Callahan P.S and W.H. Daffer, *Search for Earthquake Effects in Topex/Poseidon Data*, AGU, 1994.

Carter D.J.T, P.G. Challenor and M.A. Srokosz, *An assessment of Geosat wave height and wind speed measurements*, Journal of Geophys. Res., 97, 11383 - 11392, 1992.

Cartwright D.E. and A.C. Edden, *Corrected tables of tidal harmonics*, Geophys. J. of the Roy. Soc., 23 , 253-264, 1973.

Chapron B. and J. Tournadre, *Use of dual-frequency altimeter measurements*, AVISO Altimetry Newsletter, No. 6, p. 31, April, 1998.

Chen G, B. Chapron, J. Tournadre, K. Katsaros and D. Vandemark, *Global oceanic precipitation: A joint view by TOPEX and TMR data*, J. Geophys. Res. (Ocean), vol. 102, No. C5, pp. 10457-10471, 1997.

Cheney B, L. Miller, C.K. Tai, J. Lillibridge, J. Kuhn, M. Ji and D. Behringer, *Operational altimeter data processing and assimilation for El Niño forecasts*, Proceedings of International Symposium on Monitoring of the Oceans in the 2000s: An integrated approach, Biarritz, France, 15-17 October, 1997.

Courtier P, *The MERCATOR project and the future of operational oceanography*, Proceedings of International Symposium on Monitoring of the Oceans in the 2000s: An integrated approach, Biarritz, France, 15-17 October, 1997.

De Mey P, *The SATCHMO Project: Assimilation of satellite altimeter data in ocean models*, AVISO Altimetry Newsletter, No. 6, p. 41, April, 1998.

Denker H, D. Behrend and W. Torge, *The European Gravimetric Quasigeoid EGG96*. IAG Symp., Proc. GraGeoMar96, Springer Verlag, 1997.

Dombrowsky E, P. Bahurel, P. De Mey, H. Dolou and V. Cassé, *SOAP93 Real time assimilation of altimeter data in the Azores current from 1992 to 1995 - oceanographic results*, Proceedings 2nd ERS Applications Workshop, London, ESA Publications Division, Noordwijk, December 1995.

Eanes R. and S. Bettadpur, *The CSR 3.0 global ocean tide model.* Center for Space Research, Univ. of Texas, Tech. Mem. CSR-TM-95-06, Austin, TX, 1995.

Escudier P, N. Picot and O.Z. Zanife, *Altimetric Ionospheric Correction Using DORIS Doppler Data*, Proc. IUGG Vienna, 1991.

ESA SP-359, *Proceedings of First ERS-1 Symposium, Space at the service of our environment*, ESA Publications Division, Noordwijk, vols. I and II, March, 1993.

ESA SP-361, *Proceedings of Second ERS-1 Symposium, Space at the service of our environment*, ESA Publications Division, Noordwijk, vols. I and II, January, 1994.

ESA SP-1196/1, *GOCE: Gravity Field and Steady-State Circulation Mission, Report for Assessment, The Nine Candidate Earth Explorer Missions*, ESA Publications Division, Noordwijk, 1996.

ESA SP-414, *Proceedings of Third ERS-1 Symposium, Space at the service of our environment*, ESA Publications Division, Noordwijk, vols. I, II and III, March, 1997.

ESA SP-1221, *Envisat Mission Product Summary Overview*, ESA Publications Division, Noordwijk, March 1998.

Eymard L, L. Tabary, E. Gérard, A. Le Cornec and S.A. Boukabara, *The microwave radiometer aboard ERS-1, Part 2 : Validation of the geophysical products*, IEEE Trans. Geosci. Remote Sensing, 34, 291-303, 1996.

Filiberti M.A, F. Rabier, J.N. Thépaut, L. Eymard and P. Courtier, *Four-dimensional variational SSM/I water vapour data assimilation in the ECMWF model*, IFS, Quarterly J. Royal Meteor. Soc., 124, 1743-1770, 1998.

Filiberti M.A, L. Eymard and B. Urban, *Assimilation of satellite precipitable water in a meteorological forecast model*, Mon. Wea. Rev., 122, 3, 486 - 506, 1994

Francis R. and M. Roca, *RA-2 In-orbit Calibration Plan: Range*, ESA -ESTEC, Noordwijk, The Netherlands, August, 1998.

Fu L-L and G. Pihos, *Determining the response of sea level to atmospheric forcing using TOPEX/POSEIDON data*, Journal of Geophys. Res., vol. 99, 24633-24642, 1994.

Gaspar P, and F. Ogor, *Estimation and analysis of the sea state bias of the ERS-1 altimeter*. Report of task B1-B2 of IFREMER contract no: 94/2.426 016/C, 1994.

Gaspar P, F. Ogor, P.Y. Le Traon and O.Z. Zanife, *Estimating the sea state bias of the TOPEX and POSEIDON altimeters from crossover differences.* J. Geophys. Res. (Oceans), 99, 24981-24 994, 1994.

Gaspar P. and R.M. Ponte, *Relation between sea level and barometric pressure determined from altimeter data and model simulations*, J. Geophys. Res. (Ocean), vol. 102, pp. 961-971, 1997.

Gaspar P, and J.P. Florens, *Estimation of the sea state bias in radar altimeter measurements of sea level: Results from a new non-parametric method.* J. Geophys. Res. (Oceans) , vol.103, No. C8, pp. 15803-15814, 1998.

Gérard E. and L. Eymard, *Remote Sensing of integrated cloud liquid water:development of algorithms and quality control*, Radio Science, 33, 433-447, 1998.

Peacock N.R, S.W. Laxon, R. Scharoo and W. Maslowski, *Improving the Signal to Noise Ratio of Altimetric Measurements in Ice Covered Seas* (Abstract), EOS (Supl.), 78, (46), F140, 1997.

Peacock N.R, S.W. Laxon, R. Scharoo, W. Maslowski and D.P. Winebrenner, *Geophysical signature from precise altimetric height measurements in the Arctic Ocean,* IGARRS' 98, Seattle, Washington, 1998.

Ponte R.M, D.A. Salstein and R.D. Rosen. *Sea level response to pressure forcing in a barotropic numerical model.* J. Phys. Oceanogr., 21, 1043-1057, 1991.

Quartly G, *Retrieving Rainfall rates from ERS altimeter data,* ESA SP-414, Proceedings of Third ERS Symposium, Space at the service of our environment, ESA Publications Division, Noordwijk, vol I, II and III, Florence 14-21 March, 1997.

Reigber Ch, R. Bock, Ch. Forste, L. Grunwaldt, N. Jakowski, H. Lühr, P. Schwintzer and C. Tilgner, CHAMP Phase-B, Executive Summary, G.F.Z., STR96/13, 1996.

Saastamoinen J, *Atmospheric correction for the troposphere and stratosphere in radio ranging of satellites*, Geophys. Monog., 15, American Geophysical Union, Washington, DC, 1972.

Smith N. and M. Lefebvre, *The Global Data Assimilation Experiment (GODAE),* Proceedings of International Symposium on Monitoring of the Oceans in the 2000s: An integrated approach, Biarritz, France, 15-17 October, 1997.

Schwintzer P, C. Reigber, A. Bode, Z. Kang, S.Y. Zhu, F-H. Massmann, J.C. Raimondo, R. Biancale, G. Balmino, J.M. Lemoine, B. Moynot, J.C. Marty, F. Barlier and Y. Boudon, *Long-wavelength global gravity field models: GRIM4-S4, GRIM4-C4*, Journal of Geodesy, 71, pp. 189-208, 1997.

Srokosz M.A, *On the joint distribution of surface elevations and slopes for a nonlinear random sea, with an application to radar altimetry.* J. Geophys. Res., 91, 995-1006, 1986.

Tapley B.D, J.B. Lundberg, and G. H. Born, *The Seasat altimeter wet tropospheric range correction,* J. Geophys. Res., 87, 2313-3220, 1982.

Tapley B.D. et al. *The Joint Gravity Model 3*, J.Geophys Res., Vol. 101, 25779-25811, 1996.

Tscherning C.C, *Evaluation of the EGM96, the EGG97 and the GEONZ97 (gravimetric) geoids in the North Sea Area.* Bulletin of the IGeS, Vol. 7, pp.24-29, Milano, 1998.

Van Dam T.M. and J. Wahr, *The atmospheric load response of the ocean determined using Geosat altimeter data,* Geophys. J. Int., 113, pp. 1-16, 1993.

Vossepoel F.C, R.W. Reynolds and L. Miller, *Use of sea level observations to estimate salinity variability in the tropical Pacific,* Submitted to J. Atmospheric and Oceanic Technology, 1998.

Walsh J.E, *Long-term observations for monitoring of the cryosphere,* Climatic Change, 31 , 369-394, 1995.

Wingham D.J, A.J. Ridout, R. Scharroo, R.J. Arthern and C.K. Shum, *Antarctic Elevation Change from 1992 to 1996*, Science, vol. 0, 16 October 1998.

Yi Yuchan, *Determination of Gridded mean Sea Surface from TOPEX, ERS-1 and GEOSAT Altimeter data,* Department Geodetic Science and Surveying, The Ohio State University, Rep. No. 434, Columbus 9363-9368, 1995.

Goodberlet M.A, C.T. Swift and J.C. Wilkerson, *Validation of ocean surface wind fields and wave height measurements derived from data of the ERS-1 scatterometer and radar altimeter (early results)*, In Proceedings of the workshop on ERS-1 Geophysical Validation, ESA WPP-36, pp. 61-64, Penhors, France, 27-30 April, 1992.

Günther H, P. Lionello and B. Hansen, *The impact of the ERS-1 altimeter on the wave analysis and forecast*. Report no. GKSS 93/E/44, GKSS, Geesthacht, Germany, 56 pages, 1993.

Imel D.A, *Evaluation of the Topex/Poseidon dual-frequency ionosphere - correction*, J. Geophys. Res., Vol. 99(C12), 24895-24906, 1994.

Keihm S, M. Janssen and C. Ruf, *Topex-Poseidon microwave radiometer (TMR), part iii: wet troposphere range correction algorithm and pre-launch error budget*. IEEE Trans. Geosci. Remote Sensing, 33, 2, 147-161, 1995.

Komen G.J, L. Cavaleri, M. Donelan, K. Hasselmann, S. Hasselmann and P.A.E.M. Janssen, *Dynamics and Modelling of Ocean Waves*, Cambridge University Press, Cambridge, 532 pp., 1994.

Lambeck K, *Geophysical geodesy*, Oxford University Press Publications, New York, 718 pp, 1988.

Lemoine F.G, D.Smith, R.Smith, L.Kunz, E.Pavlis, N.Pavlis, S.Klosko, D.Chinn, M. Torrence, R. Williamson, C. Cox, K. Rachlin, Y. Wang, S. Kenyon, R. Salman, R.Trimmer, R.Rapp and S.Nerem, *The development of the NASA GSFC and DMA joint geopotential model*. Proc. Symp. on Gravity, Geoid and Marine Geodesy, Tokyo, 1996.

Le Traon P-Y and F. Ogor, *ERS-1 orbit improvement using TOPEX/POSEIDON: The 2 cm challenge*, J. Geophys. Res. (Ocean), vol. 103, No. C4, April 15, 1998.

Le Traon P-Y and G. Dibarboure, *Mapping capabilities of multiple altimeter missions*, Submitted to Journal of Atmospheric and Oceanic Technology, 1998.

Mannucci A.J, B.D.Wilson, D.N. Yuan, C.M. Ho, U.J. Lindqwister and T.F. Runge, *A global mapping technique for GPS-derived ionospheric TEC measurements*, Radio Sci., 33, 565, 1998.

McLaren A.S, J.E. Walsh, R.H. Bourke, R.L. Weaver and W. Wittmann, *Variability in sea ice thickness over the North Pole from 1977-1990*, Nature, 358, (16 July 1992), 224-226, 1992.

Melbourne W.G., *Sounding the Earth's Atmosphere and Ionosphere with GPS*, EOS 76(46), 465-466, 1995.

Minster J-F, C. Brossier and P. Rogel, *Variations of the mean sea level from Topex/Poseidon data*, Journal of Geophys. Res., 100, 25153-25162, 1995.

NRC - National research Council: *Satellite Gravity and the Geosphere*, National Academy Press, Washington DC, 1997.

Pavlis N.K, *Development and Applications of Geopotential Models*, Lecture Notes, Escola de Geoide, Rio de Janeiro, Sept. 1997.

Phalippou L. and E. Gerard, *Use of precise microwave imagery in Numerical Weather Prediction*. Study report to the European Space Agency, 70 pp (available from ECMWF), 1996.

European Space Agency
Agence spatiale européenne

Contact: ESA Publications Division
c/o ESTEC, PO Box 299, 2200 AG Noordwijk, The Netherlands
Tel. (31) 71 565 3400 - Fax (31) 71 565 5433